Reactive nitrogen species in normal and inflamed synovium

Klocke, Rainer

Award date:
2005

Awarding institution:
University of Bath

Reactive nitrogen species in normal and inflamed synovium

Submitted by Rainer Klocke
For the degree of Doctor of Philosophy

University of Bath
Department of Pharmacy & Pharmacology
October 2005

ProQuest LLC
789 East Eisenhower Parkway
P.O. Box 1346
Ann Arbor, MI 48106-1346

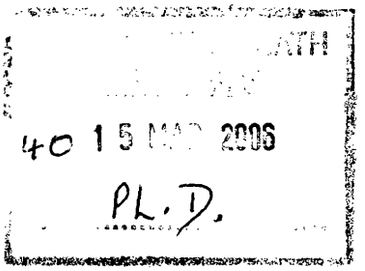
40 15 MAR 2006
PL.D.

Table of Contents

Peer-reviewed publications based on this thesis.....[183]

Mapp PI, **Klocke R**, Walsh DA, Chana JK, Stevens CR, Gallagher PJ, Blake DR. Localization of 3-nitrotyrosine to rheumatoid and normal synovium. Arthritis Rheum 2001;44:1534-1539.

Klocke R, Mani AR, Moore KP, Morris CJ, Blake DR, Mapp PI. Inactivation of xanthine oxidoreductase is associated with increased joint swelling and nitrotyrosine formation in acute antigen-induced arthritis. Clin Exp Rheumatol 2005;23:345-350.

List of figures and tables

Acknowledgements

I am grateful to Drs Paul I. Mapp and Clifford R. Stevens for their help and support as my supervisors during the early and final parts of this project, respectively. I am indebted to Prof David R. Blake and his team at the University of Bath and the Royal National Hospital for Rheumatic Diseases in Bath for all the inspiration, support and encouragement during this work. In particular, I am grateful to Dr Caren Peters for her helpful instruction on histological technique, to Dr Timothy Millar for the introduction to XOR activity assays and to Dr Vivienne Winrow for teaching me electrophoretic and immunoblotting techniques, as well as providing very helpful support and feed back on drafts of this thesis. I wish to thank Mrs Louise Anderson and her team at the University of Bath for her support with the animal work. This work benefited greatly from the collaboration with Drs Alireza Mani and Kevin P. Moore from the Centre for Hepatology, Royal Free Hospital Medical School in London, UK, and I am grateful for their gas chromatographic-mass spectrometric nitrotyrosine measurements.
The Arthritis Research Campaign, UK deserves particular thanks for funding me as a Clinical Research Fellow for most of the duration of this work.

I owe thanks to my wonderful wife and children for their patience, loving support and distraction over the years. Finally, I thank my parents for enabling and allowing me to venture this far.

Summary

Nitric oxide (NO) and superoxide ($O_2^{\bullet-}$) react rapidly with each other to form peroxynitrite ($ONOO^-$), a highly reactive species, implicated in tissue injury of numerous diseases. $ONOO^-$ causes nitration of tyrosine leading to 3-nitrotyrosine (3-NT), which is considered a marker of formation of $ONOO^-$ and other reactive nitrogen species (RNS) *in situ*. Unexpectedly, 3-NT was recently identified in blood vessels of structurally *normal* human synovium, suggesting a physiological role for $ONOO^-$ in joints. Xanthine oxidoreductase (XOR) may contribute to this $ONOO^-$ formation, since it can generate both NO and $O_2^{\bullet-}$ during xanthine metabolism, is expressed in human synovium and shares anti-microbial properties with $ONOO^-$.

The aim of this present work was to confirm and characterize 3-NT in normal joint tissue in non-primate species and to determine the enzymatic origin of NO, preceding 3-NT formation. A major hypothesis to be tested was that XOR contributes to articular 3-NT formation in normal and inflamed joints.

Using immunohistochemical and mass-spectrometric techniques on synovial tissue from rats, mice and cattle, 3-NT was detected in the normal synovial vasculature and hyaline cartilage chondrocytes, developing soon after birth. Mice lacking nitric oxide synthase 1, 2 or 3 had unchanged 3-NT immunoreactivity. Rat joints displayed biochemical and histochemical XOR activity which was substantially suppressed by tungsten diet. However, in tungsten-fed rats, articular 3-NT immunoreactivity and content was unaltered. Wistar rats on a tungsten or control diet underwent antigen-induced knee arthritis. Contrary to expectation, tungsten-fed animals showed higher articular 3-NT content and more severe acute joint swelling than control animals.

This work suggests that cartilage and synovium of normal joints contain relatively high amounts of 3-NT/RNS in several mammalian species, ensured by multiple enzymatic sources of NO. XOR is not a significant source of RNS during antigen-induced arthritis, rather it may protect against RNS formation and acute antigen-induced joint inflammation.

List of abbreviations and acronyms

AIA	antigen-induced arthritis
AMPS	ammonium persulfate
ANOVA	analysis of variance
CFA	complete Freund's adjuvant
CO_2	carbon dioxide
COX	cyclooxygenase
conc.	concentrated
DAPI	4'-6-diamidino-2-phenylindole
DPI	diphenyleneiodonium
DTH	delayed-type hypersensitivity
ESR	electron spin resonance
ECL	enhanced chemiluminescence
ECM	extra-cellular matrix
FAD	flavin adenine dinucleotide
FITC	fluorescein isothiocyanate
GC/ MS	gas chromatography / mass spectrometry
GSH	glutathione
GSNO	S-nitrosoglutathione
H&E	haematoxylin-eosin
H_2O/dd	double-distilled water
H_2O/Q	ultra-pure water (milli-Q filtered)
HRP	horse radish peroxidase
i.a.	*intra-articular*
ICC	intra-class correlation coefficient
IHC	immunohistochemistry
IL	interleukin
IR	immunoreactivity
i.p.	*intra-peritoneal*

IXPt	isoxanthopterin
LOD	limit of detection
LPS	lipopolysaccharide
MPMS	1-methoxyphenazine methosulfate
MPO	myeloperoxidase
MW	molecular weight
NAD^+	nicotinamide adenine dinucleotide (oxidized)
NADPH	nicotinamide adenine dinucleotide phosphate (hydrogenated)
NC	nitrocellulose
NO	nitric oxide
NO_2^-	nitrite
NO_3^-	nitrate
NO_2	nitrogen dioxide
NOS	nitric oxide synthase
3-NT	3-nitrotyrosine
OA	osteoarthritis
OCT	optimum cryo-temperature
O_2	dioxygen
$O_2^{\bullet-}$	superoxide
$^{\bullet}OH$	hydroxyl radical
$ONOO^-$	peroxynitrite
PAGE	polyacrylamide gel electrophoresis
PB	sodium phosphate buffer
PBS	phosphate-buffered saline
PG	prostaglandin
PMSF	phenylmethylsulfonylfluoride
PVA	polyvinyl alcohol
RA	rheumatoid arthritis
RNS	reactive nitrogen species
rpm	revolutions per minute
RT	room temperature

3-NT	3-nitrotyrosine
SDS	sodium dodecyl sulfate
SOD	superoxide dismutase
SEM	standard error of the mean
TBS	Tris-buffered saline
TNBT	tetranitro blue tetrazolium
TNF	tumor necrosis factor
Triton X-100	iso-octylphenoxypolyethoxyethanol
UA	uric acid
XO	xanthine oxidase
XOR	xanthine oxidoreductase
XDH	xanthine dehydrogenase

Chapter 1: General Introduction

Reactive chemical species, derived from nitrogen and oxygen, are increased in biological fluids and joint tissue from individuals suffering from joint diseases such as rheumatoid arthritis or osteoarthritis. While mostly thought of as mediators of damage, it is increasingly recognised that such reactive nitrogen and oxygen species may also be beneficial. However, their precise role during normal joint function and joint inflammation remains to be established. This thesis is concerned with 3-nitrotyrosine, a marker of reactive nitrogen species formation, in relationship to normal and inflamed joints.

In this section, the chemical nature and origins of reactive nitrogen and oxygen species will be explained, as far as relevant to this thesis.

1.1 Reactive nitrogen and oxygen species

Chemically, free radicals are molecules capable of independent existence that contain unpaired orbital electrons (Halliwell B and Gutteridge JMC, 1999) They possess an unstable electromagnetic balance and therefore they avidly react with other atoms/molecules to achieve complete orbital electron pairs, either by attracting electron(s), *i.e.* being reduced, or by discarding electron(s), *i.e.* being oxidized. Other highly reactive intermediates (*e.g.* hydrogen peroxide, peroxynitrite) are not free radicals and the term reactive nitrogen or oxygen species (RNS/ROS) is usually preferred, when referring to reactive metabolites derived from nitric oxide or superoxide (Halliwell B and Gutteridge JMC, 1999).

1.1.1 Superoxide

Superoxide ($O_2^{\bullet-}$) originates from single-electron transfer onto molecular (di-)oxygen (O_2). All aerobic life forms employ the step-wise enzymatic reduction of molecular oxygen and, as such, the production of $O_2^{\bullet-}$ during normal metabolism is inevitable. Mitochondrial respiratory enzymes are probably the main source of this physiological $O_2^{\bullet-}$ leak (Halliwell B and Gutteridge JMC, 1999). When stimulated, cells such as neutrophils and macrophages can produce high amounts of $O_2^{\bullet-}$ from a membrane-bound NADPH oxidase that forms the basis of an effective antimicrobial killing mechanism (Babior BM, 1978). Many non-phagocytic cells have been shown to have a similar cytosolic NADPH oxidase and produce $O_2^{\bullet-}$ under stimulation *in vitro*: *e.g.* endothelial cells, vascular smooth muscle cells (Griendling KK, *et al.*, 1994) fibroblasts, chondrocytes and osteoclasts (Jones OTG and Hancock JT, 2000). A further important enzymatic source of $O_2^{\bullet-}$ is xanthine oxidoreductase (XOR), best known for its role in the metabolism of purines. Because of its relevance to this thesis, XOR will be described in more detail below. It has also been reported that all nitric oxide synthase isoenzymes (see below) are able to reduce O_2 to $O_2^{\bullet-}$ *in vitro* via a reductase subunit (Miller RT, *et al.*, 1997; Xia Y, *et al.*, 1998a; Xia Y, *et al.*, 1998b) .

1.1.1.1 Basic reactions of superoxide

In aqueous solution at a physiological pH of 7.4, $O_2^{\bullet-}$ is generally not very reactive with biomolecules, such as lipids, proteins or DNA (Halliwell B and Gutteridge JMC, 1999). It is thought that most damage caused by $O_2^{\bullet-}$ requires reactions with other free radicals, most notably nitric oxide, and iron ions in iron-sulfur proteins. Since $O_2^{\bullet-}$ is not very stable, its fate will depend on a number of factors, that include proximity and concentration of potential reactants, their thermodynamic properties (*i.e.* willingness to be reduced/oxidized) and pH. Below, the basic reactions, relevant to $O_2^{\bullet-}$-mediated tissue damage, are briefly explained. The important reaction with nitric oxide ($NO^{\bullet}$) will be discussed section 1.1.3.

$O_2^{\bullet-}$ will dismutate in aqueous solutions to form hydrogen peroxide (H_2O_2) [1];

$$\mathbf{O_2^{\bullet-} + O_2^{\bullet-} + 2\ H^+ \rightarrow H_2O_2 + O_2} \qquad [1]$$

H_2O_2 is toxic to most cells in the 10 – 100 μM range leading to lipid, protein and DNA oxidation, yet no such damage is observed when isolated biomolecules are incubated with H_2O_2 at millimolar concentrations. This implies that further reactions are required to mediate H_2O_2 cytotoxicity and there is evidence that the highly reactive hydroxyl radical ($^{\bullet}OH$) is this mediator.

$^{\bullet}OH$ may be formed from H_2O_2 in the **Haber-Weiss reaction** [2].

$$\mathbf{O_2^{\bullet-} + H_2O_2 \rightarrow {}^{\bullet}OH + OH^- + O_2.} \qquad [2]$$

$^{\bullet}OH$ is one of the most reactive free radical, but it is not known to what extent $^{\bullet}OH$ formation occurs *in vivo*. The Haber-Weiss reaction is unlikely to occur to any relevant extent *in vivo*, due to the much higher rate reaction of $O_2^{\bullet-}$ dismutation that is catalysed by a group of superoxide dismutase (SOD) enzymes.

More likely to occur *in vivo* is the formation of $^{\bullet}OH$ from the reaction of H_2O_2 with ferrous iron or other reduced transition metals in the **Fenton reaction** [3]:

$$Fe^{2+} + H_2O_2 \rightarrow {}^{\bullet}OH + OH^- + Fe^{3+} \qquad [3]$$

1.1.1.2 XOR as a source of superoxide

XOR activity was first described in milk a century ago (Schardinger F, 1902), as a factor in uncooked milk that decolourised methylene blue (as the final electron acceptor) upon addition of formaldehyde (as the electron-donating substrate). XOR is part of the molybdo-enzyme family, which also includes aldehyde oxidase (AO) and sulfite oxidase (SO). XOR protein exists as a dimer of two identical 150 kDa protein subunits, each consisting of one molybdopterin-binding site (Mo-Co), two non-identical iron-sulfur centres and a flavin adenine dinucleotide (FAD)-binding site (***Fig. 1.1.1.2***) (Enroth C, *et al.*, 2000). The gene encoding human XOR is located on the short arm of chromosome 2 (locus 2p23-p22) and the amino acid sequence is >90% homologous with rat and mouse enzyme (Ichida K, *et al.*, 1993), indicating the highly conserved nature of this enzyme. In humans, basal activity of the XOR promoter is much lower compared to rodents (Xu P, *et al.*, 2000). Gene expression is enhanced by pro-inflammatory cytokines and other mediators of an acute inflammatory response. Both transcriptional and post-translational XOR activity are increased by hypoxia and reduced by hyperoxia (Terada LS, *et al.*, 1997).

The enzyme exists in two interconvertible forms: xanthine dehydrogenase (XDH; EC 1.1.1.204) and xanthine oxidase (XO; EC 1.1.3.22) (Stirpe F and Della Corte E, 1969), that differ in their substrate specificity. Both will oxidise hypoxanthine to xanthine and xanthine to uric acid as part of purine metabolism. However, XO will reduce O_2 only [4], whereas XDH will reduce O_2 and NAD^+, but with greater affinity for the latter [5] (Waud WR and Rajagopalan KV, 1976).

xanthine (hypoxanthine) + 2 O_2 + H_2O → uric acid (xanthine) + 2 $O_2^{\bullet-}$ + 2 H^+ [4]

xanthine (hypoxanthine) + NAD^+ + H_2O → uric acid (xanthine) + NADH + H^+ [5]

Aspects of the mechanisms of these reactions remain uncertain (Hille R and Nishino T, 1995). Simplified, the reduction of XOR takes place at the Mo-Co centre by accepting two electrons from the purine substrate (***Fig. 1.1.1.2***).

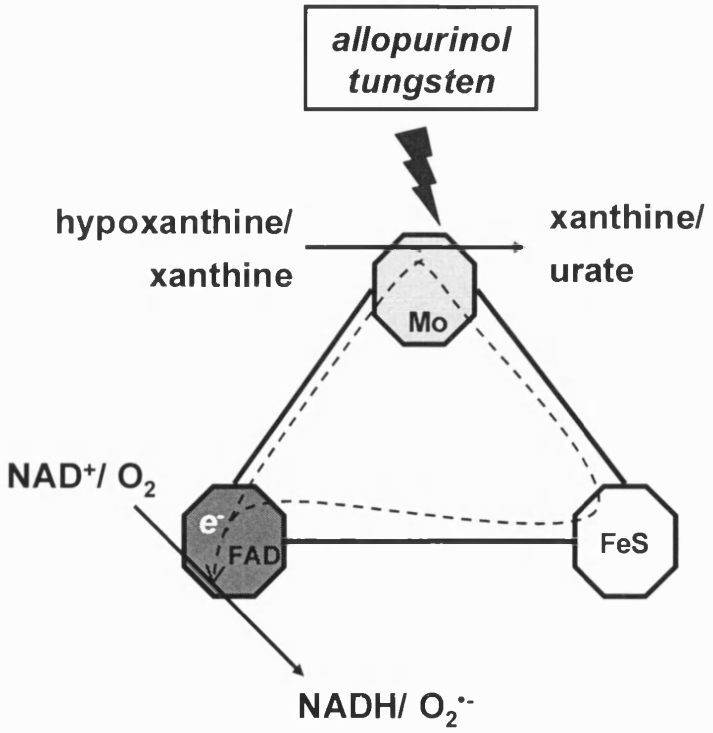

Fig. 1.1.1.2: Schematic structure and basic reactions of xanthine oxidoreductase.

While the iron-sulfur centres serve as an electron reservoir, the electrons are ultimately transferred to O_2/NAD^+at the FAD-site. The hypoxanthine analogue ***allopurinol*** has been used in clinical practice for many years to inhibit uric acid production in purine overload states, such as gout or during cancer chemotherapy. It is oxidized by XOR at

the Mo-Co site yielding alloxanthine (a.k.a. oxypurinol) which then binds tightly to the reduced Mo-Co site, disabling further enzyme action (Massey V, *et al.*, 1970). Interestingly, XDH in breast milk was found to have a significant NADH oxidase activity when NAD^+ levels are low, by directly transferring electrons to O_2 to generate $O_2^{\bullet-}$ at the FAD site (Sanders SA, *et al.*, 1997) [6].

$$\mathbf{2\ O_2 + NADH \rightarrow 2\ O_2^{\bullet-} + NAD^+ + H^+} \qquad [6]$$

This form of superoxide generation is noteworthy, since it does not involve the Mo-Co site and hence is not inhibited by allopurinol. The ability of XOR to reduce nitrite to nitric oxide will be discussed in section 1.1.2.2.2.

Alternative inhibition of XOR in animals has been quantitatively achieved using dietary supplementation with sodium ***tungstate*** (Johnson JL, *et al.*, 1974; Suzuki H, *et al.*, 1998). Tungstate will replace active-centre molybdenum from XOR, thus rendering the enzyme inactive. Therefore all three known molybdo-enzyme (XOR, AO and SO) will be inactivated, and this occurs without any obvious signs of ill health in the animals (Johnson JL, *et al.*, 1974), even when exposure starts *in utero* (Pitt RM, *et al.*, 1991). This observation is contrasted by the very shortened life expectancy of molybdenum-cofactor gene 'knock-out' mice and the severe neurological deficits in the human disease (McKusick VA, 2004).

In both humans and rats most XOR activity exists as XDH *in vivo* (Della Corte E, *et al.*, 1969; Waud WR and Rajagopalan KV, 1976). Via two principle mechanisms XDH can be converted to XO *in vitro*. Limited proteolysis by proteases, such as trypsin, leads to *irreversible* conversion. Oxidation of specific thiol groups of the enzyme, *e.g.* by storage at -20°C, incubation at 37°C or anaerobic conditions (Della Corte E, *et al.*, 1969), causes *reversible* conversion to XO.

In humans and primates, XOR activity levels may be 100x lower than in other mammals including rats and mice (Abadeh S, *et al.*, 1992). This is not sufficiently explained by the reduced human XOR promoter activity, since the difference remains even when

equal enzyme amounts are considered. XOR variants lacking active centre molybdenum or sulphur are thought to be responsible for this observation, but it is uncertain whether these variants represent a physiological post-translational mechanism of regulation (Abadeh S, *et al.*, 1992).

1.1.1.3 Tissue localisation of XOR

The tissue localisation of XOR has in part produced conflicting results. In general, this is due to the different methods used for localisation of XOR. Antibody-based immunochemistry will detect XOR protein, irrespective of whether it represents active enzyme or not. Biochemical activity assays in homogenates or tissue sections rely on the presence of active enzyme, but are generally considered less sensitive than immuno-chemical assays. The interpretation for human tissue is particularly difficult due to the generally lower activity, described earlier (Abadeh S, *et al.*, 1992).

Table 1.1.1.3 summarizes the data from the literature for human and rat tissue. There is agreement that XOR protein and activity is expressed in liver cells and intestinal epithelium of both species. In humans, XOR protein can be demonstrated in lactating mammary tissue. For other parenchymal organs, such as the heart, the evidence of XOR expression is less certain, although endothelial cells within these organs have been more consistently shown to express XOR using a sensitive radio-immunoassay (Jarasch ED, *et al.*, 1986). Blotting studies for XOR gene transcripts suggest that human heart, brain, kidney and skeletal muscle do express XOR (Xu P, *et al.*, 1994), but for reasons explained earlier this does not imply that there is active protein.

In joint tissue, XOR activity has been found in normal and inflamed (i.e. rheumatoid) human synovium by means of a radiochemical assay (Allen RE, *et al.*, 1987). Immunohistochemistry has suggested that this activity localises predominantly to the capillary endothelium (Stevens CR, *et al.*, 1991a). Importantly, there are no reports in the literature about XOR in cartilage or rat synovium.

Table 1.1.1.3: **XOR localisation in normal human and rat tissue.**

Tissue Type	**Human**	**Rat**
Liver	+ (IB[1]; IHC[2,3]; HC[4]; RIA[5])	+ (IHC[10]; HC[11,12])
Intestine	+ (IB[1]; IHC[2,3]; HC[4]; RIA[5])	+ (IHC[10]; HC[11,12])
Mammary tissue	+ (IHC[2]; RIA[5])†	**NA**
Heart	+ (IB[6], IHC[3*,7]; RIA[5]) - (IB[1]; IHC[2])	+ (HC[11*]) - (HC[12])
Kidney	+ (IHC[3*]; IB[1]) - (IHC[2]; HC[4])	+ (IHC[10]; HC[12])
Brain	+ (IHC[3*]) - (IB[1]; IHC[2])	+ (IHC[10])
Skeletal muscle	+ (IHC[2,7]) - (IB[1])	+ (IHC[10]) - (HC[12])
Synovium	+ (IHC[8]; RC[9])	**NA**
Cartilage	**NA**	**NA**

+, reported as present; -, reported as absent; NA, no reports available.

The method of XOR detection/reference is shown in brackets; IB, immunoblotting; IHC, immunohistochemistry; HC, histochemistry; RIA, radio-immuno assay; RC, radiochemistry; † Esp. marked in lactating tissue; * XOR confined to endothelial cells of the tissue.

[1](Sarnesto A, *et al.*, 1996); [2](Linder N, *et al.*, 1999); [3](Moriwaki Y, *et al.*, 1993) ; [4](Kooij A, *et al.*, 1992b); [5](Jarasch ED, *et al.*, 1986); [6](Abadeh S, *et al.*, 1993); [7](Hellsten-Westing Y, 1993); [8](Stevens CR, *et al.*, 1991a); [9](Allen RE, *et al.*, 1987); [10](Moriwaki Y, *et al.*, 1996); [11](Kooij A, *et al.*, 1992a); [12](Moriwaki Y, *et al.*, 1998).

1.1.1.4 Biological role of superoxide from XOR

The biological role of XOR can be categorized into physiological *vs.* patho-physiological effects. Furthermore one can distinguish effects according to the XOR reaction product exerting a biological effect, *i.e.* $O_2^{\bullet-}$/ROS, nitric oxide/RNS and uric acid. The biological effects relating to RNS originating from XOR will be described in section 1.1.2.2.2.

Physiologically XOR is best known for its role in dealing with the waste products of purine metabolism. Purine metabolism in humans and primates produces ***uric acid*** (UA) as the end product. This is due to an inactivated gene for urate oxidase, an enzyme which is active in most other vertebrates to convert poorly soluble uric acid into the more soluble allantoin. As a consequence, serum uric acid levels are about ten times higher in humans than *e.g.* rodents (Xu P, *et al.*, 1996). This explains, in part, the predisposition of humans to develop gout, a disease characterised by UA crystal deposition in joint and renal tissue. It has been proposed that the evolutionary gain of this urate oxidase deficiency in man is enhanced longevity due to the anti-oxidant properties of UA (Ames BN, *et al.*, 1981). Interestingly, uric acid has been found to be a potent inhibitor of the tyrosine-nitrating action of peroxynitrite *in vitro* (Whiteman M and Halliwell B, 1996), although it may be less potent in the presence of physiological concentrations of bicarbonate (Whiteman M, *et al.*, 2002). There is now *in vivo* evidence, albeit in rodents, that treatment with uric acid ameliorates the course of experimental arthritis (Bezerra MM, *et al.*, 2004) and experimental allergic encephelomyelitis, an animal model of multiple sclerosis (Hooper DC, *et al.*, 1998). In humans, there is no evidence that XOR fulfils essential physiological function, since subjects with hereditary classical xanthinuria type I and a non-sense mutation of the XOR gene are asymptomatic (Ichida K, *et al.*, 1997). This is different from mice, where targeted gene XOR deletion produced runted homozygous animals with very short live expectancy, and heterozygous female animals with defective lactation (Vorbach C, *et al.*, 2002) .

Pathophysiologically, there is a plethora of evidence linking XOR-derived ROS to tissue injury that occurs upon reperfusion following a period of ischaemia/anoxia in a variety of tissues, such as intestine and heart [reviewed in (Berry CE and Hare JM, 2004; McCord JM, 1985)], liver, brain and skeletal muscle. It is thought that ischemia leads to a) conversion of XDH to XOR, b) accumulation of hypoxanthine from ATP depletion and c) release of chelated transition metals. Upon reperfusion XOR will then generate $O_2^{\bullet-}$, H_2O_2 and $^{\bullet}OH$ to cause tissue damage [reviewed in (Halliwell B and Gutteridge JMC, 1999)]. This observation has potential relevance to many aspects of vascular

disease and organ transplantation, although its significance remains to be established for human disease. More recently XOR-derived ROS has also been implicated in the development of hypertension, endothelial dysfunction and heart failure (Berry CE and Hare JM, 2004). The strength of pre-clinical evidence for a beneficial effect of XOR inhibition in myocardial dysfunction is such, that currently, a randomised, double-blind and placebo-controlled clinical trial is underway, testing the effects of oxypurinol in cardiac failure (Freudenberger RS, *et al.*, 2004).

1.1.2 Nitric oxide

Mammals excrete more nitrate than they ingest, and the suggestion that this is due to endogenous nitrate synthesis goes back over 80 years (Mitchell HH, *et al.*, 1916). Only fairly recently it was realized that this excess urinary nitrate is due to synthesis of nitric oxide (NO) [reviewed in (Nathan C, 1992)] , a free radical with numerous biological effects that have had a huge impact on the understanding of vascular and inflammatory disease mechanisms.

NO is a colourless gas with good solubility in organic solvents (Koppenol WH, 1998). It therefore readily diffuses within and across cells. One of the first biological roles identified for NO was that as a physiological vaso-relaxing factor, derived from endothelium (Palmer RM, *et al.*, 1988). Practically every cell type can express NO upon stimulation with pro-inflammatory cytokines or bacterial lipo-polysaccharides (LPS), *i.e.* under pathological circumstances, and many do so constitutively under physiological conditions.

1.1.2.1 Basic and physiological chemistry of NO

On exposure to air NO will react with O_2 to form the more reactive, brown nitrogen dioxide (NO_2) gas. In aqueous solutions NO will react with O_2 to yield mainly nitrite. Both these reactions follow a third-order rate law, *i.e.* the rate of NO oxidation will decline with increasing NO dilution (Halliwell B and Gutteridge JMC, 1999). At

physiological concentration of NO and O_2 (10 nM and 10 μM, respectively) this would result in a half-life of NO of many hours (10^6 s) (Koppenol WH, 1998). This, of course, ignores the presence of numerous other reactants present in biological systems. *In vivo* the most significant of these reactants will be haemoglobin, which will shorten the half-life of NO to a few seconds, but still leaving enough time for $NO^{\bullet}$ to diffuse across several cell diameters.

Like $O_2^{\bullet-}$, NO is only a relatively weak reactant with non-radical biomolecules. *In vivo* it seems likely that the one-electron reduction to nitroxyl anion (NO^-, a.k.a oxonitrate(1-)) is favoured over oxidation to nitrosonium cation (NO^+) for thermodynamic reasons (Koppenol WH, 1998). However, as already mentioned for $O_2^{\bullet-}$, the likelihood of a reaction will also depend on concentration (and with it the generation and decay) of NO and potential reactants, their spatial proximity, pH, oxygen tension, *etc.* The potential reactions of NO are numerous, and a useful starting point is to distinguish *direct* effects of NO on biomolecules from *indirect* ones, *i.e.* those that result from reactions of NO with $O_2^{\bullet-}$ or O_2 (***Figure 1.1.2.1***) (Grisham MB, *et al.*, 1999).

In vitro direct chemical reactions can be observed at relatively low flux of NO and it is postulated that constitutive, low-output generation of NO mediates these reactions *in vivo*. A direct effect is the formation of stable Fe^{2+}- NO complexes in haem moieties of enzymes, such as guanylate cyclase. The resultant increase in cellular cyclic guanine monophosphate can lead to vasodilatation, inhibition of platelet aggregation and neurotransmission [reviewed in (Ignarro LJ, 1991)]. The rapid reaction of NO with Fe^{2+}-oxy-haemoblobin and subsequent oxidation to nitrite is thought to be the main mechanism of NO breadown *in vivo* under aerobic conditions (Kelm M, 1999). Direct reactions of NO with other free radicals, such as lipid alkoxyl and –alkyl hydroperoxyl radicals, have been shown to inhibit lipid peroxidation and the generation of pro-inflammatory lipids (Rubbo H, *et al.*, 1994).

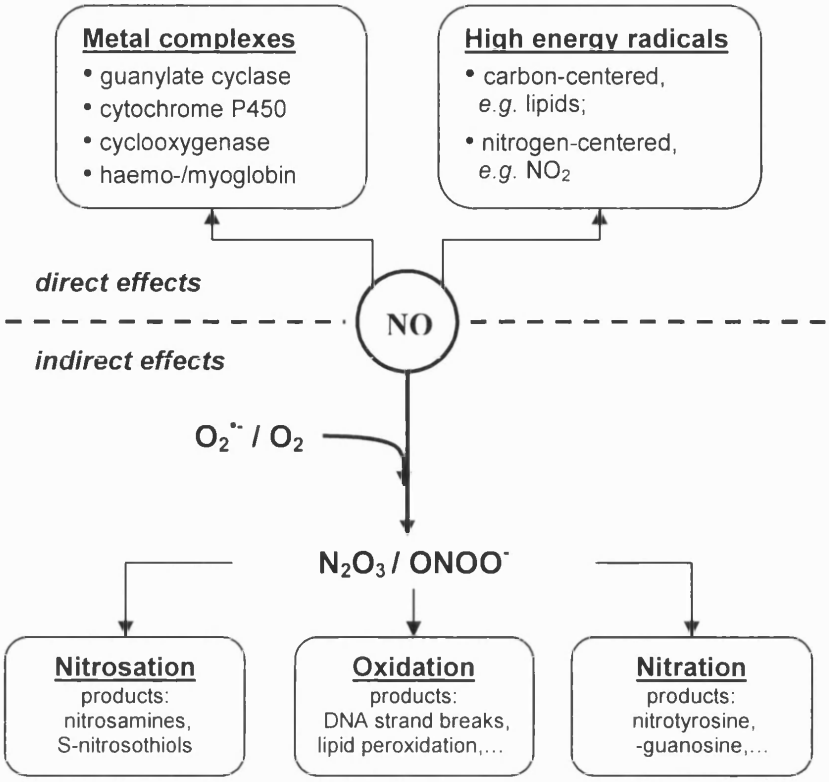

Figure 1.1.2.1: **Principal chemical reaction pathways of NO**, thought to occur *in vivo* [modified from (Grisham MB, *et al.*, 1999)].

The *indirect* effects of NO occur in general at higher fluxes of NO and in the presence of $O_2^{\bullet-}$ or O_2. Dinitro-trioxide (N_2O_3) occurs during the autoxidation of NO in aqueous solutions and is a strong nitrosative reactant to form *e.g.* putatively carcinogenic nitrosamines (R-N-N=O) and/or S-nitrosothiols (R-S-N=O) (Wink DA, *et al.*, 1997). The biological role of S-nitrosothiols is complex and not entirely clear, but includes functions as a 'slow-release' form of NO, a 'buffer' for peak NO production and pro-inflammatory actions [reviewed in (Gaston B, 1999)]. The reaction of NO with $O_2^{\bullet-}$ to yield the strong oxidising and nitrating reactant peroxynitrite ($ONOO^-$) is of particular importance to this thesis and will be discussed separately below.

Via the oxy-haemoglobin-mediated oxidation to nitrite and then further to nitrate (NO_3^-), the great majority of endogenously synthesised NO is thought to be excreted as NO_3^- in the urine. In the absence of excess dietary NO_2^-/ NO_3^-, the estimation of NO_2^-/ NO_3^- in biological fluids is generally accepted as a measure of endogenous NO synthesis (Kelm

M, 1999) and much of the evidence of increased NO production *in vivo* and *in vitro* is based on this assumption.

1.1.2.2 Sources of NO

1.1.2.2.1 Nitric oxide synthases

Soon after the recognition of NO as the vasodilating endothelial factor, it was found that NO originates from *L*-arginine (Palmer RM, *et al.*, 1988). At least three distinct enzymes are now known to generate NO from *L*-arginine in mammals and have been isolated, cloned and characterized (Förstermann U, *et al.*, 1994).

They all catalyse the same 5-electron oxidation of a guanidino nitrogen of *L*-arginine to yield NO and *L*-citrulline. Co-substrates for this reaction are molecular oxygen and NADPH, implying that NOS enzymes are unable to produce NO under anoxia. Furthermore they share tetrahydrobiopterin, flavin adenine dinucleotide (FAD), flavin mononucleotide (FMN) and haem as co-factors. There are two calcium-dependent forms: neuronal(n) and endothelial(e) nitric oxide synthase (nNOS or NOS I; eNOS or NOS III), that are mainly expressed in a constitutive way in selected cell types to yield low local concentrations of NO. The third form is a largely inducible, calcium-independent enzyme (iNOS or NOS II), that is expressed by almost all cell types in response to LPS or pro-inflammatory cytokines.

The genes of human nNOS, iNOS and eNOS are have been mapped to chromosomes 12 q24, 17 q11 and 7 q36, respectively and encode 130-160 kDa proteins that function as homo-dimers. The amino acid sequence identity between the human iso-enzymes is less than 59%, but the homology for each enzyme across species is high (> 90% for nNOS and eNOS; > 80% for iNOS).

The terms 'constitutive/inducible', 'neuronal' and 'endothelial' have survived in the nomenclature of NOS enzymes, but (as true for most biomolecules) they soon no longer accurately described the biology of these isoenzymes. It was soon recognized that the constitutive NOS enzymes are subject to complex pre-and post-translational regulation, and that iNOS is expressed constitutively in some tissues (Nathan C and Xie QW, 1994).

While, with very few exceptions, eNOS appears confined to the vascular endothelium, nNOS has been reported in central and peripheral neurons, adrenal tissue, skeletal muscle cells, testes and fertile oocytes (Förstermann U and Dun N, 1996; McKusick VA, 2005b).

1.1.2.2.2 XOR as source of NO

The possibility of NOS-independent NO generation was first raised when it was shown that ischemic rat heart muscle produced NO in a manner dependent on nitrite and independent of NOS (Zweier JL, *et al.*, 1995). The previously known ability of XOR to reduce nitrate to nitrite under low oxygen tension (Fridovich I and Hansert B, 1962) and the structural similarity of XOR to known microbial and plant nitrate-/nitrite reductases (Campbell WH and Kinghorn KR, 1990), led to investigations as to whether XOR could generate NO. It was demonstrated that under conditions of hypoxia ($\leq$1% O_2) and in the presence of NADH as the reducing agent XOR can generate NO from nitrite ($\geq$1 mM) (Zhang Z, *et al.*, 1998) and inorganic and organic nitrates (such as the therapeutic glycerol trinitrate) (Millar TM, *et al.*, 1998), as measured by ozone chemiluminescence. Inhibition of NO generation occurred in the presence of the molybdenum-site inhibitor allopurinol and the non-specific flavo-enzyme inhibitor diphenyleneiodonium (DPI), but not with nitro-*L*-arginine. This has led to the hypothesis that the reductive half-reaction of XOR occurs at the FAD-site and the oxidative half-reaction at the Mo-Co site of the enzyme. Godber *et al.* found that xanthine could be an alternative reducing agent, although it led to progressive inactivation of XOR over time due conversion of the enzyme to its desulfo-form (Godber BJL, *et al.*, 2000). They also showed that both XDH and XO can reduce nitrite to NO, and that NADH-mediated nitrite reduction can occur under normoxia in the presence of SOD. This suggests that XOR does reduce nitrite to NO under normoxia, which escapes detection by its fast reaction with simultaneously produced $O_2^{\bullet-}$. Li *et al.* (Li H, *et al.*, 2001) independently confirmed the capacity of XO as a nitrite reductase with electron spin resonance (ESR) and electrochemical methods of NO detection. They found that low micro-molar xanthine (K_m 1.5 μM) yielded 4-fold higher rates of NO generation than NADH under hypoxia, whereas higher xanthine levels diminished NO output. DPI had no effect on NO

generation with xanthine as substrate, suggesting that both xanthine oxidation and nitrite reduction takes place at the Mo-Co site of XOR. It was concluded that under conditions of no-flow ischemia the required substrate and XOR concentrations, pH and oxygen tension are achieved to make XOR-mediated NO generation a significant reaction *in vivo* (Li H, *et al.*, 2001). There are no studies to date to show that XOR generates NO *in vivo*. However, there is circumstantial evidence to suggest that XOR, as a source of NO and $O_2^{\bullet-}$, is the key principle behind the anti-microbial properties in human breast milk (Stevens CR, *et al.*, 2000).

1.1.2.2.3 Non-enzymatic sources of NO

Under acidic conditions nitrite can be reduced to NO without any enzyme involvement via disproportionation of nitrous acid [reviewed in (Weitzberg E and Lundberg JON, 1998)], *e.g.* under experimental conditions of cardiac ischemia (Samouilov A, *et al.*, 1998). However, it has been suggested that under these conditions the XOR-mediated NO generation would exceed the disproportionation of nitrite by a factor of 25 (Li H, *et al.*, 2001).

1.1.2.3 Biological effects of NO

Considering the diverse nature of potential reactions and sources of NO, it is not surprising to see a diversity of regulatory, protective and deleterious biological effects mediated by NO (***Figure 1.1.2.3***). In general, deleterious biological effects are mediated through indirect chemical reactions of NO, *i.e.* those involving prior reaction with $O_2^{\bullet-}$ or O_2. Conversely, most, but not all, physiological effects will result from direct reactions of NO. One important exemption to this rule is the anti-microbial action which is a lot higher for peroxynitrite, the reaction product of NO and $O_2^{\bullet-}$, than for NO (Brunelli L, *et al.*, 1995). The role of NO in joint health and disease will be discussed in section 1.3.

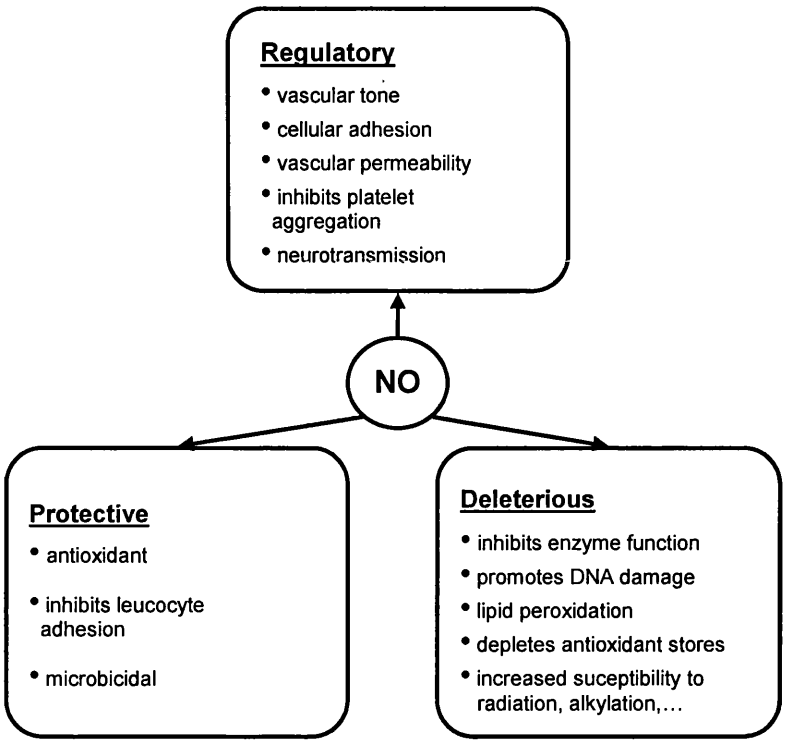

Figure 1.1.2.3: **The diverse biological effects of NO** [modified from (Grisham MB, *et al.*, 1999)].

1.1.3 Peroxynitrite

As mentioned earlier, the majority of deleterious actions of NO are a consequence of its reaction with co-existent $O_2^{\bullet-}$ or O_2.

The reaction of NO with $O_2^{\bullet-}$ can form peroxynitrite ($ONOO^-$) [7] (Pryor WA and Squadrito GL, 1995).

$$O{=}O^{\bullet-} + {}^{\bullet}N{=}O \rightarrow {}^{-}O\text{-}O\text{-}N{=}O \qquad [7]$$

Since this reaction allows NO with $O_2^{\bullet-}$ to share their unpaired electrons, it is highly favoured energetically, indicated by rate constant of up to 1.9×10^{10} $M^{-1}s^{-1}$ in acellular systems (Kissner R, *et al.*, 1998). This means that this reaction is mainly limited by diffusion only. This rate constant surpasses that of dismutation of $O_2^{\bullet-}$ by SOD enzymes,

the main competing physiological reaction, by about two orders of magnitude (Koppenol WH, 1998). Nevertheless the production of $ONOO^-$ *in vivo* can be expected to be confined to selected areas for a number of reasons. Firstly, the rate of $ONOO^-$-mediated oxidative and nitrating reactions decline when the flux of either $O_2^{\bullet-}$ or NO are in excess *in vitro* (Goldstein S, *et al.*, 2000; Miles AM, *et al.*, 1996). With estimated physiological cellular concentration of $O_2^{\bullet-}$ and NO of 0.1 – 1 nM and 0.1-1 μM, respectively (Grisham MB, *et al.*, 1999), generation of $O_2^{\bullet-}$ becomes the more important determinant of $ONOO^-$ generation *in vivo*. Furthermore the estimated physiological concentration of SOD is relatively high (4 - 20 μM), dismutating most of the emerging $O_2^{\bullet-}$ under physiological conditions.

1.1.3.1 Basic and physiological chemistry of peroxynitrite

The chemistry of $ONOO^-$ and its formation has been reviewed by Koppenol (Koppenol WH, 1998). With a $pK_a = 6.8$ (in 0.1 M phosphate buffer), $ONOO^-$ is a weak acid in aqueous solution. At physiological pH and body temperature, the protonated $ONOO^-$ (*i.e.* peroxynitrous acid) will undergo decomposition and isomerisation within seconds to yield the stable end products nitrate and di-oxygen. During this process, nitration and high-energy oxidation reactions have been observed *in vitro*, even though the precise nature of the chemical intermediates remain unclear (Koppenol WH, 1998). *In vitro* exposure to $ONOO^-$ has been shown to affect many biomolecules (*e.g.* proteins, DNA and lipids). Oxidative change has been described in lipids and DNA, leading to lipid peroxidation (Rubbo H, *et al.*, 1994) and 8-oxo-guanine/ DNA strand breaks, respectively (reviewed in (Szabo C and Oshima H, 1997)). $ONOO^-$ can lead to nitration of *e.g.* phenolic compounds, such as free and protein-bound tyrosine (Beckman JS, *et al.*, 1994a), and purines, such as guanine (Yermilov V, *et al.*, 1995). Many, in particular mitochondrial, enzymes have been shown to be modified by $ONOO^-$-mediated nitration of tyrosine residues [reviewed in (Greenacre SA and Ischiropoulos H, 2001)], with implications for enzyme function and signal transduction.

In vivo the effects of $ONOO^-$ are probably strongly influenced by its high reaction rate constant with the ubiquitous CO_2/HCO_3^- to form a nitrosoperoxycarbonate adduct. *In*

vitro studies have suggested that the presence of CO_2/HCO_3^- increases the nitration, but reduces the oxidation of biomolecules by $ONOO^-$ (Denicola A, *et al.*, 1996; Yermilov V, *et al.*, 1996).

It is worth noting, however, that the reported biological effects mediated by $ONOO^-$ have been based on the exposure to synthetically derived $ONOO^-$. This is problematic since all methods of $ONOO^-$ generation have certain limitations including the contamination with other nitrogen and oxygen species and difficulties in controlling the final $ONOO^-$ concentration (Uppu RM, *et al.*, 1996). Similarly, the detection of such $ONOO^-$ generation in biological tissues is fraught with problems. Since $ONOO^-$ is not a free radical, more direct methods such as electron spin resonance (ESR) are not possible. The detection has therefore largely been based on the demonstration of substrate modifications by synthetic $ONOO^-$ (*e.g.* nitrotyrosine, oxidised dihydrorhodamine, chemiluminescence) which, used in isolation, have limited specificity (Tarpey MM and Fridovich I, 2001).

In an elegant study on *ex vivo* perfused rat hearts, Wang and Zweier were able to show a concurrent peak of NO *and* $O_2^{\bullet-}$ production (by ESR) during early reperfusion after ischaemia (Wang P and Zweier JL, 1996). This was associated with increased $ONOO^-$ (by luminal chemiluminescence, blocked by NOS inhibition or $O_2^{\bullet-}$ scavenging with SOD) and histological nitro-tyrosine immunostaining in post-ischaemic hearts. This study suggests that endogenous NO and $O_2^{\bullet-}$ formation leads to tyrosine nitration via $ONOO^-$ *in vivo*.

1.1.3.2 Biological effects of peroxynitrite

The above chemical effects of $ONOO^-$ on the various bio-molecules are of adverse biological consequence in nearly all cell, tissue and animal models that have been examined. Via enzyme modification, DNA breaks and lipid peroxidation, the main consequences range from cellular dysfunction and membrane leakage to cell death,

apoptosis and mutagenesis [reviewed in (Groves JT, 1999; Szabo C and Oshima H, 1997)].

Localised $ONOO^-$ formation *in situ* has been described in relevant tissues from very diverse disease states [reviewed in (Greenacre SA and Ischiropoulos H, 2001)], such as atherosclerosis, septic shock, respiratory distress syndrome, allogenic kidney transplant rejection, carbon monoxide poisoning, arthritis and neuro-degenerative diseases, mostly by way of demonstrating the presence of 3-nitrotyrosine (further explained below). *In vitro,* studies using chemiluminescence and/or various antagonists/scavengers to demonstrate that both NO and $O_2^{\bullet-}$ are involved, detected $ONOO^-$ production in cytokine-stimulated rat macrophages (Ischiropoulos H, *et al.*, 1992a), human neutrophils (Carreras MC, *et al.*, 1994), bovine endothelial cells (Kooy NW and Royall JA, 1994), rat pulmonary vascular smooth muscle cells (Boota A, *et al.*, 1996) and motor neurone cells (Estevez AG, *et al.*, 1998).

From the above, one would not expect any beneficial roles for $ONOO^-$. However, there are examples of $ONOO^-$ effects that will be of benefit to the host (***Table 1.1.3.2***). $ONOO^-$ is more bactericidal compared to NO *in vitro* (Brunelli L, *et al.*, 1995), and this has implications *in vivo* (Umezawa K, *et al.*, 1997). Apart from direct bactericidal effects, $ONOO^-$ could also enhance host defense to infection via priming of $O_2^{\bullet-}$ production in neutrophils (Rohn TT, *et al.*, 1999). Physiologically achievable $ONOO^-$ concentrations in reperfusion following cardiac ischaemia in rats and cats reduced the amount of myocardial necrosis and neutrophil-endothelium adhesion with improved endothelial function (Lefer DJ, *et al.*, 1997; Nossuli TO, *et al.*, 1998). This effect seemed mediated via S-nitrosothiol formation, which is supported by independent *in vitro* data (Mayer B, *et al.*, 1995). $ONOO^-$ may also be responsible for the protective effect of brief, non-injurious periods of ischaemia (so called preconditioning) against subsequent ischaemia-reperfusion injury of the heart (Laude K, *et al.*, 2002).

***Table 1.1.3.2*: Beneficial effects of peroxynitrite.**

Function	*System*	*Experimental Effect*	*Reference*
Microbial host-defense	*E.coli* (*in vitro*)	Equimolar $ONOO^-$ far more bactericidal than NO	(Brunelli L, *et al.*, 1995)
Microbial host-defense	*S.typhimurium* Septicaemia (mice)	NO (from iNOS) *and* $O_2^{\bullet-}$ (from XOR) are both required for maximum tissue protection	(Umezawa K, *et al.*, 1997)
Ischaemia-Reperfusion Injury	Mesenteric arteries and heart (rat, *ex vivo*)	0.1 – 1 μM $ONOO^-$ during reperfusion: diminished P-selectin expression, neutrophil-endothelium adherence and reversed cardiac contractile dysfunction	(Lefer DJ, *et al.*, 1997)
Ischaemia-Reperfusion Injury	Heart (cat, *ex vivo*)	2μM $ONOO^-$ during reperfusion: diminished P-selectin expression, neutrophil-endothelium adherence and reversed cardiac contractile dysfunction	(Nossuli TO, *et al.*, 1998)
Ischaemia-Reperfusion Injury	Coronary arteries (rat, *in vivo/vitro*)	$ONOO^-$ mediates protection of endothelial function following ischaemic preconditioning	(Laude K, *et al.*, 2002)

1.1.4 3-Nitrotyrosine

The nitration of *L*-tyrosine by $ONOO^-$ at the *ortho*-position leads to 3-nitro-*L*-tyrosine (3-NT) *in vitro* (Ischiropoulos H, *et al.*, 1992b). This can occur both in free tyrosine and, more importantly, in protein-bound tyrosine. This post-translational modification of tyrosine residues has gained considerable importance over recent years due to its selective nature and association with altered enzyme function and a wide range of diseases.

1.1.4.1 Mechanisms of tyrosine nitration

It was questioned whether $ONOO^-$, generated from NO and $O_2^{\bullet-}$, is able to nitrate tyrosine under physiological conditions (Pfeiffer S and Mayer B, 1998). However, other investigators were able to show that simultaneously generated NO and $O_2^{\bullet-}$ can form 3-NT (Reiter CD, *et al.*, 2000; Sawa T, *et al.*, 2000), provided hypoxanthine is avoided as substrate for XOR-mediated $O_2^{\bullet-}$-generation as the uric acid product will rapidly scavenge $ONOO^-$ (Kooy NW, *et al.*, 1994). Nevertheless, a number of other pathways of tyrosine nitration have been described *in vitro*, which are independent of $ONOO^-$. 3-NT formation can occur non-enzymatically *in vitro* at physiological pH in the presence of NO_2^- and hypochlorous acid (HOCl), a powerful agent used in the killing mechanism of neutrophils (Eiserich JP, *et al.*, 1996). HOCl is produced by myeloperoxidase (MPO) and other haem-containing peroxidases, such as horseradish, lacto- and eosinophil-peroxidase. Accordingly, it was shown that such peroxidases are equally able to nitrate tyrosine in the presence of NO_2^- (van der Vliet A, *et al.*, 1997). It would appear that the main mechanism of this reaction involves a one-electron oxidation of NO_2^- to yield $^{\bullet}NO_2$ (Brennan ML, *et al.*, 2002). Details of the MPO-dependent reaction to yield 3-NT has been reviewed recently by Radi (Radi R, 2004). It is also recognised that tyrosine nitration occurs non-enzymatically in the presence of NO_2^- under acidic conditions (Oldreive C, *et al.*, 1998), which can pose a problem for some analytical methods of 3-NT detection.

There is now evidence from MPO-deficient mice to suggest that MPO is required for tyrosine nitration during inflammation *in vivo* (Brennan ML, *et al.*, 2002; Gaut JP, *et al.*, 2002). However, some inflammatory models and intracellular protein tyrosine nitration do not require MPO activity (Brennan ML, *et al.*, 2002). Furthermore, there is *ex vivo* evidence implicating $ONOO^-$ in LPS-mediated prostacyclin synthase nitration in bovine arteries (Zou MH, *et al.*, 1999). Therefore, $ONOO^-$ to form 3-NT *in vivo* remains very much a possibility (Radi R, 2004). Importantly, although *in vitro* evidence has shown that NO itself may nitrate tyrosine at physiological tyrosyl radical sites of prostaglandin H synthase (Gunther MR, *et al.*, 1997), there is no *in vivo* evidence to show that NO alone nitrates tyrosine residues. It would therefore seem that Halliwell's

conclusion remains valid that 3-NT in biological samples is best regarded as evidence for reactive nitrogen species formation in general, rather than a specifically $ONOO^-$ (Halliwell B, 1997).

1.1.4.2 Methods of 3-NT detection

A range of immune and physico-chemical methods have been developed to detect 3-NT in biological samples with increasing sensitivity [reviewed in (Herce-Pagliai C, *et al.*, 1998)].

Initially, immunohistochemical studies were carried out with a rabbit polyclonal antibody directed against $ONOO^-$-treated keyhole limpet haemocyanin (Beckman JS, *et al.*, 1994b). These demonstrated strong immunoreactivity in cellular inflammatory infiltrates of formalin-fixed, paraffin-embedded human atherosclerotic tissue that was abolished by pre-incubation with 3-NT or pre-treatment of sections with dithionite (which reduces nitro-tyrosine to amino-tyrosine). By immunoaffinity purification against 3-NT and with appropriate specificity controls (see section 3.3.3.4), these antibodies became a cornerstone of demonstrating 3-NT in tissue sections from a wide variety of disease states (Viera L, *et al.*, 1999). The antibody is commercially available and recognizes 3-NT across a range of species (Product information sheet, TCS Biologicals, UK, #06-284). This antibody has also been applied in an indirect competitive enzyme-linked immunosorbent assay (ELISA), allowing some quantitation of 3-NT in samples. 3-NT in samples was measured against known standards in their ability to compete with $ONOO^-$-treated bovine serum albumin, as the immobilized antigen (Khan J, *et al.*, 1998). Several commercially available, mono- and polyclonal anti-3-NT antibodies have recently been characterized for use in competitive solid-phase ELISAs (Franze T, *et al.*, 2004). Compared to immunochemical methods, physico-chemical methods are less sensitive, but more specific. Sensitivity rises from high-performance liquid chromatography with UV-detection of 3-NT (limit of detection (LOD): approx. 0.2 µM (Kaur H and Halliwell B, 1994)) to combined gas chromatographic- mass spectrometric methods (LOD 400 attomol) (Crowley JR, *et al.*, 1998). Common to all these methods is the need for hydrolysis of proteins into individual amino acids. Since this has

conventionally been done under acidic conditions, there is scope for artefactual 3-NT formation (Oldreive C, *et al.*, 1998). This problem has been circumvented by employing an alkaline method of hydrolysis (Frost MT, *et al.*, 2000), which was used for the studies presented here.

During the completion of my studies, the analysis of nitrated proteins in tissue homogenates has been taken one step further. Digests of 3-NT immuno-positive protein gel spots have been analysed by a mass spectrometric method (*i.e.* matrix-assisted laser desorption ionization/ time-of-flight mass spectrometry), providing a highly accurate measure of peptide molecular mass that allows identification of protein identity from protein databases (Aulak KS, *et al.*, 2001). This proteomic approach allows the identification of a larger number of nitrated proteins in a given biological system.

1.1.4.3 Biological significance of 3-NT

Since its original description as an exposure marker for $ONOO^-$ over 10 years ago (Ischiropoulos H, *et al.*, 1992b), 3-NT formation in proteins is emerging as a post-translational modification mechanism to regulate enzyme function and signal transduction under pathological and probably physiological conditons [reviewed in (Ischiropoulos H, 2003)].

This role of tyrosine nitration in proteins is suggested by the following findings:

a) Tyrosine nitration in proteins is selective

Biological nitration yields of tyrosine under inflammatory conditions are low with only one to five in 10,000 tyrosine residues (10-50 μmol/mol) detected as 3-NT (Brennan ML, *et al.*, 2002). Furthermore, there is good evidence that tyrosine nitration is not a random, but very selective process. An increasing number of examples show that nitration of a small number of proteins and tyrosine sites associates with altered enzyme function and pathological anatomy or physiology. For instance, the mitochondrial anti-oxidant enzyme manganese SOD (MnSOD) in human rejected kidney allografts, was found to be the main nitrated protein at few specific tyrosine residues, mimicked by

$ONOO^-$ exposure and associated with loss of enzyme function (MacMillan-Crow LA, *et al.*, 1996). Increased tyrosine nitration of MnSOD has also been reported in *aged* compared to young rat vascular tissue (van der Loo B, *et al.*, 2000d). Similarly, the vaso-relaxing prostacyclin (PGI_2) synthase in bovine artery walls is tyrosine-nitrated during atherosclerosis and endotoxin treatment, leading to enzyme inactivation and defective vasorelaxation (Bachschmid M, *et al.*, 2003; Zou MH, *et al.*, 1999). These effects could be mimicked *in vitro* by peroxynitrite and were found to be associated with selective nitration of tyrosine 430 (Schmidt P, *et al.*, 2003). It is worth noting however that, although specific tyrosine nitration may be exclusively responsible for the altered function of some enzymes [*e.g.* in glutathione reductase (Savvides SN, *et al.*, 2002)], in others, oxidative changes other than specific tyrosine nitration may determine enzyme function [*e.g.* in tyrosine hydroxylase (Kuhn DM, *et al.*, 2002)].

Specificity of tyrosine nitration is also suggested by the selective localisation of 3-NT in biological tissues. Electron-microscopic studies have confirmed this at the subcellular level. For instance, electron-microscopy showed 3-NT to immuno-localise in particular within mitochondria and the sub-endothelial space of aortic vessels of aged rats (van der Loo B, *et al.*, 2000c).

The observed specificity of tyrosine nitration in proteins is thought to depend on the concentration and proximity of the nitrating agent, the surface exposure of tyrosine residues and their proximity to active metal-enzyme complexes (Ischiropoulos H, 2003).

b) Tyrosine nitration can result in loss or gain of enzyme function

An indiscriminate pattern of protein tyrosine nitration could be expected to produce a uniform loss of enzyme function, but this is not what has been observed. There are a number of examples, where selective tyrosine nitration is associated with an increased biological signal. For instance, the mitochondrial respiratory chain enzyme cytochrome c (Cassina AM, *et al.*, 2000) and the membranous signalling enzyme protein kinase Cε (Balafanova Z, *et al.*, 2002) have been shown to undergo activation following $ONOO^-$-induced tyrosine nitration. In addition, nitration of tyrosine residues may interfere with tyrosine phosphorylation, a common mechanism of cell signalling. Both loss (Brito C, *et*

al., 1999; Gow AJ, *et al.*, 1996) and gain (Mallozzi C, *et al.*, 2001) in function have been described as a consequence.

c) Tyrosine nitration appears to be a reversible process

While immunoreactivity has long been recognised as a stable footprint marker of RNS, it has become clear that 3-NT proteins undergo selective 'denitrase' repair mechanisms. A soluble factor from rat spleen and lung was found to denitrate 3-NT bovine serum albumin (Kamisaki Y, *et al.*, 1998). Recently, it was demonstrated that a number of rat mitochondrial enzymes, including MnSOD, can undergo rapid de-nitration and nitration synchronous with ischemia-reperfusion cycles (Koeck T, *et al.*, 2004). There is also evidence that tyrosine nitration may cause accelerated degradation of enzymes *in vitro* (Grune T, *et al.*, 1998).

d) Tyrosine nitration is part of both physiological and pathophysiological pathways

Tyrosine nitration of proteins is not only a mechanism to mediate patho-physiological events, but also part of normal cellular and tissue physiology. $ONOO^-$-mediated tyrosine nitration has been shown to inhibit tyrosine phosphorylation and targets proteins for degradation *in vitro* (Gow AJ, *et al.*, 1996). $ONOO^-$-induced tyrosine nitration of normal T lymphocytes inhibits activation-induced tyrosine phosphorylation and thus lymphocyte proliferation (Brito C, *et al.*, 1999). Furthermore, it primes the cells to undergo apoptotic cell death. $ONOO^-$ was detectable from macrophages upon immune stimulation and the authors postulate that this mechanism serves as a physiological suppressor of immune stimulation. Naseem *et al.* showed that tyrosine nitration of specific proteins occurred within normal platelets upon physiological activation by collagen (Naseem KM, *et al.*, 2000). The tyrosine nitration was mimicked by $ONOO^-$ treatment. Finally, tyrosine nitration of the microtubule-associated protein τ is thought to be necessary for normal neural development (Capelletti G, *et al.*, 2004).

Although tyrosine nitration is a selective process, the number and nature of affected proteins reported in the literature is large and diverse. Since the start of the present studies, analysis of liver and lung tissue of LPS-treated rats and cardiac tissue of aged

rats revealed 40 and 48 putative tyrosine-nitrated enzymes, respectively (Aulak KS, *et al.*, 2001; Kanski J, *et al.*, 2004). The identified enzymes comprised mitochondrial and cytosolic enzymes, mostly of importance to energy production and cell structure, and less so to cell signalling and anti-oxidant defence.

1.2 Synovial joints

1.2.1 Histology and physiology of normal synovium and cartilage

Joints have evolved to allow bone ends to angle, slide and twist relative to each other for the purpose of smooth and easy, yet secure movement. Joints consist of hyaline cartilage, covering the bone ends, and a surrounding fibrous capsule. The capsule is lined by the ***synovium***, which consists of an intimal lining layer and the subintimal layer or subsynovium. The lining layer comprises a discontinuous, one to three-cell layer of specialized cells, the synoviocytes, without an underlying basement membrane. Structurally and functionally two types of synoviocytes can be distinguished: a macrophage-like (type A) synoviocyte and a fibroblast-like (type B) synoviocyte, which have predominantly phagocytic or biosynthetic properties, respectively.
The subsynovium is a relatively hypocellular connective tissue, that contains blood vessels, fat cells and fibroblasts (Tak PP, 2000). The number of blood vessels is typically highest near the synovial surface to meet its nutritional demand. Morphometric studies have suggested that normal synovium has a heterogenous, but generally high degree of vascularity with *ca.* 240 capillaries per mm^2 and a modal capillary depth of 35 μm (Stevens CR, *et al.*, 1991b).

Hyaline cartilage consists of chondrocytes (< 5% volume), embedded in a water-rich, complex extra-cellular matrix (ECM). Chondrocytes are zonally arranged, *i.e.* adopting a horizontal orientation in the superficial cartilage layer, changing to a vertical or columnar orientation in deeper layers. This orientation is concordant with an arching framework of type II collagen fibres that form a scaffold for the ECM, ensuring tensile strength. Firmly attached to the collagen fibres are proteoglycans, such as aggrecan, that are rich in hydrophilic, negatively charged carbohydrates, which create high osmotic pressure with strong resilience of normal cartilage. Cartilage is bound to its underlying bone through a thin layer of calcified cartilage, and the strongly staining non-calcified-calcified interface is referred to as the tidemark (Hardingham T, 1998). While chondrocytes in normal adult cartilage do not show signs of proliferation, proteoglycans

are subject to a highly regulated turnover with an estimated half-life between days and months. Importantly, cartilage is aneural and avascular tissue and no significant nutrition is thought to occur via the tidemark. Hence, its metabolic demands are met solely via diffusion from the synovium (Hasselbacher P, 2003). Chondrocytes of normal avascular articular hyaline cartilage have to function at low oxygen tension (down to 1 kPa or less) (Silver IA, 1975). Intra-articular (*i.a.*) pressures in normal joints are subatmospheric during most of the movement range, aiding synovial capillaries to remain perfused. However , *i.a.* pressure have been shown to rise above atmospheric levels during maximum flexion: up to 5 mmHg and over 30 mmHg in rabbit and dog knees, respectively (Levick JR, 1979; Nade S and Newbold PJ, 1983).

1.2.2 Pathology of joint inflammation

Inflammation is a complex process that can be defined as the response of living tissue to injury (Cotran RS, *et al.*, 1999), caused by microbial, immune-mediated, physical or chemical insults. Inflammation requires vascularised tissue. The initial acute inflammatory phase is dominated by vascular responses (causing the signs of swelling and redness) and infiltration by neutrophils and/or mast cells. The longer chronic phase that may (or may not) ensue is characterized by the presence of mononuclear cells and connective tissue fibroblasts to attempt tissue repair. However, features of acute and chronic inflammation may co-exist from early on, depending on the nature of the injury. The inflammatory response depends on many mediators that, apart from reactive nitrogen and oxygen species, include cytokines, histamine, complement, arachidonic acid metabolites, kinins, proteinases and – in order to limit the inflammatory response – anti-inflammatory mechanisms, *e.g.* proteinase inhibitors and anti-oxidants.

1.2.2.1 Rheumatoid arthritis

Rheumatoid arthritis is a human disease, characterised by chronic and frequently destructive inflammation affecting synovial joints in a typical distribution. The cause of this disease is unclear. Based on twin studies, the genetic component of disease susceptibility is estimated to be about 60%. Although auto-antibodies are commonly

found in sufferers, the suspected causative foreign antigen/ auto-antigen remains elusive. Despite advances over the recent decades, current treatment achieves commonly only partial disease control (Hochberg MC, 2003).

In rheumatoid arthritis all components of the synovium, cartilage and bone are altered (Freemont AJ, 1995; Tak PP, 2000). The cells of the ***synovial lining layer*** undergo both hypertrophy and hyperplasia, often in a focal distribution and synovial villi extend into the synovial cavity. At the interface of cartilage and synovium the thickened synovial tissue is usually referred to as pannus.
About two thirds of the synoviocytes in the lining layer are macrophage-like cells and their excess number is thought to be the result of recruitment from bone-marrow derived mononuclear phagocytes (Anathasou NA, 1995). Fibroblast-like synoviocyte numbers are thought to be increased in part due to impaired apoptosis. They also show a very distinctive 'stellate' phenotype in cell culture and show gene mutations (*e.g.* the tumour suppression gene p35) and gene activation (*e.g.* matrix metalloproteinases), suggesting transformation to an invasive cell type [reviewed in (Pap T, *et al.*, 2000)].

In the earlier stages of RA, the ***subsynovium*** is characterised by increased cellularity, blood vessel formation and oedema. Similar to the lining layer changes tend to be focal, *i.e.* vary not only between, but also within individual joints (Tak PP, *et al.*, 1997). The cell types accumulating within the subsynovium are predominantly T cells, plasma cells and macrophages; and to a lesser extent B cells, natural killer cells, mast cells and dendritic cells. In addition to a diffuse infiltration of the subsynovium by these cells, perivascular lymphocyte aggregates, consistent with an antigen-driven cellular and humoral immune response, are commonly observed. As in the lining layer, macrophages often represent the majority of inflammatory cells in the subsynovium and they are characterised by strong CD68 expression. They are the main cellular source of tumor necrosis factor α (TNFα), interleukin-1 (IL–1) and other key pro-inflammatory cytokines within the rheumatoid joint (Firestein GS, *et al.*, 1990). They tend to accumulate around the cartilage-pannus-junction and their number has been shown to correlate with future development of characteristic erosive joint damage, as detected by

radiography, in patients with RA (Mulherin D, *et al.*, 1996). Angiogenesis is a further prominent feature of subsynovial change during RA. While new vessel formation during tissue repair following acute trauma is a generally a beneficial process, vessel growth in the context of chronic inflammation, immune activation and hypoxia is frequently not (Walsh DA, 1999). Furthermore, while arterioles and larger vessels may increase in number, the capillary density close to the synovial surface may be decreased (Stevens CR, *et al.*, 1991b), which may render the synovium prone to hypoxia depite new vessel formation.

Cartilage in RA has been reported to be affected via several routes (Woolley DE, 1995). Synovial pannus tissue may invade into the cartilage margins and adjacent bone to cause characteristic erosions through the release of proteolytic enzymes. Separate from this, chondrocytes may break down their surrounding ECM, leading to an enlargement of the chondrocyte lacunae. Finally, cartilage destruction occurs also from the subchondral area via specialised multi-nucleated osteo-/chondroclasts. It is assumed that cartilage breakdown at these spatially separate sites is mediated through pro-inflammatory cytokines, released from the synovium (Woolley DE, 1995). However, it may indicate the possibility that RA is not primarily a synovial disease (Fujii K, et al., 1999).

1.2.2.2 Osteoarthritis

Osteoarthritis (OA) is the most common joint disease to affect humans worldwide. It can be defined as a condition of synovial joints characterized by cartilage loss and evidence of accompanying periarticular bone response (Doherty M, *et al.*, 1998). However it is recognized that all joint components (such as synovium, ligaments and muscle) demonstrate structural change. It is a very heterogenous disease. Apart from a small minority of cases where a single cause can be identified, its aetiology is considered multifactorial. Hereditary and other susceptibility (*e.g.* obesity) and mechanical factors (*e.g.* previous trauma, repetitive usage) are all thought to play a role.

The focus of pathological change in OA has been on ***cartilage***. Histopathologically the loss of normal cartilage is chararcterized by cartilage fibrillation with cleft formation, altered chondrocyte cellularity and loss of peptidoglycan (Mankin HJ, 1974). Chondrocyte proliferation, often leading to focal 'cell clones', is thought to precede chondrocyte loss with empty lacunae, although the frequency of chondrocyte death may be much lower than previously thought (Aigner T and Kim HA, 2002). Apart from NO, osteoarthritic chondrocytes release a multitude of inflammatory mediators, including pro-inflammatory cytokines, such as IL-1 and TNFα, as well as an increased amount of matrix-metalloproteinases and ECM proteins. The net effect is a catabolic turnover of ECM with collagen disruption and proteoglycan loss, relatively early during the disease (Wollheim FA, 2003). Cartilage change is usually, but not invariably, accompanied by new ***bone*** formation at the subchondral and margins of joints in the form of bone thickening (sclerosis) and bony-cartilaginous overgrowths (osteophytes), respectively. In a mechanical canine knee OA model of anterior-cruciate ligament transaction the earliest pathological changes of OA are cartilage swelling and altered proteoglycan metabolism with bone changes featuring prominently later (Brandt KD, 2002). Nevertheless, the issue of whether OA is primarily a disease of cartilage or bone remains under discussion (Felson DT and Neogi T, 2004).

Chronic ***synovial inflammation*** with synovial production of pro-inflammatory cytokines can be demonstrated even in early radiographic stages of OA (Smith MD, *et al.*, 1997). In end-stage OA these changes may be indistinguishable from rheumatoid arthritis. It is assumed, but not proven, that this synovitis is a secondary event, triggered *e.g.* by joint debris or crystal formation (Wollheim FA, 2003). Angiogenesis in OA is also recognised feature, *e.g.* by vessels crossing the tidemark. It is thought to contribute to inflammation and osteophyte formation (Bonnet CS and Walsh DA, 2005).

1.2.2.3 Animal models of inflammatory arthritis

Several models of arthritis have been characterised, although none of them shares all the known pathogenetic features of rheumatoid arthritis. They are nevertheless extremely

useful in studying individual aspects of arthritis and their response to experimental and therapeutic pharmacological intervention. The principles of some of the more frequently used models are briefly described here.

- ***Adjuvant arthritis*** (AA) (Pearson CM and Wood FD, 1959) is induced by systemic injection of heat-killed pulverized *Mycobacterium tuberculosis*, suspended in liquid paraffin (also called: complete Freund's adjuvant) in rats. This stimulates both cellular and humeral immunity, leading to a granulomatous inflammation in many organs (such as spleen, liver, bone marrow, skin and eyes), and a profound inflammatory and erosive polyarthritis, that lasts for a few months. Practically all drugs used in human RA have shown to be efficacious in AA, which cannot be said of other animal models of arthritis. AA has not been reported in mice or primates. There is evidence of increased NO production in AA (Stefanovic-Racic M, *et al.*, 1994).

- ***Collagen-induced arthritis*** (CIA) (Trentham DE, *et al.*, 1977) is induced by immunisation with homologous or heterologous type II collagen, leading to a severe, erosive polyarthritis, that is usually self-limiting. Like AIA it has strong T- and B-lymphocyte involvement and like human RA it shows association with certain MHC haplotypes. There is evidence of increased NO production in this model (Cannon GW, *et al.*, 1996).

- ***Bacterial cell wall-induced arthritis*** is induced by *intra-peritoneal* injection of bacterial cell wall peptidoglycans (usually from *Streptococcus*, Group A) into susceptible rat strains, *e.g.* inbred Lewis, leading to an acute and chronic erosive polyarthritis, characterized by a relapsing and remitting course (Cromartie WJ, *et al.*, 1977). The acute phase depends on an intact alternative complement pathway, and the the chronic phase is T-cell dependent. Part of the pathology may be mediated by RNS (McCartney-Francis N, *et al.*, 1993), but NO may also have a protective role in the erosive phase (McCartney-Francis NL, *et al.*, 2001).

- ***Antigen-induced arthritis*** (AIA) was first described in rabbits (Dumonde DC and Glynn LE, 1962), where it shares many histopathological features of RA, *e.g.* lymphoid aggregates, synovial hypertrophy and chronic-persistent inflammation. It is produced by immunising the animal with an exogenous foreign antigen, commonly methylated bovine serum albumin (mBSA), in CFA. This is followed by intra-articular administration of the same antigen later. An acute immune complex arthritis develops, characterized by joint swelling and leukocyte infiltration. In mice (Brackertz D, *et al.*, 1977) and rats (Griffiths RJ, 1992) mBSA achieves sufficient retention within the joint, which is necessary to generate a T-cell-mediated hypersensitivity, which in turn is necessary for a chronic arthritis to develop. The chronic arthritis features pannus-like synovial hypertrophy/-plasia with a cellular infiltrate of macrophages, neutrophils, dendritic cells and a few T-cells. Erosions of cartilage and bone are seen from day 14 onwards (Griffiths RJ, 1992). NO appears to be involved in this arthritis model (Veihelmann A, *et al.*, 2001).

1.3 Evidence for a role of reactive nitrogen species in joint inflammation and physiology

There is a plethora of evidence linking nitric oxide and its reactive metabolites to joint disease in humans. As far as human joint disease is concerned, the majority of evidence is indirect, *i.e.* based, for instance, on the demonstration of NOS enzyme activity or relatively stable metabolites such as 3-NT or NO_2^- in biological samples. Experimental animal studies will allow study of the causality of observations, but their applicability of findings to human disease is uncertain. *In vitro* studies have concentrated on the perceived key cells and tissue involved, *i.e.* the inflammatory cells and synovium in RA, and articular chondrocytes and the cartilage in OA.

1.3.1 RNS in rheumatoid and experimental inflammatory arthritis

The suggestion of increased NO synthesis in human inflammatory arthritis *in vivo* first arose in 1992 when Farrell *et al.* found increased serum levels of nitrite,as a metabolite of NO, in subjects with RA, compared to healthy controls and patients with OA (Farrell AJ, *et al.*, 1992). RA synovial fluid (SF) concentrations of NO_2^- were on average over twice as high as paired serum levels, indicating that NO is likely to be generated locally within the joint by inflamed synovium. A larger study confirmed these findings and showed furthermore that serum NO_2^- concentrations of subjects with RA correlated with clinical disease activity and with serum levels of C-reactive protein, TNFα and interleukin-6 (IL-6) (Ueki Y, *et al.*, 1996). The local production of NO in RA was shown by demonstrating spontaneous NO_2^- production and NOS protein and mRNA expression in excised human synovium and cartilage (Sakurai H, *et al.*, 1995). NOS mRNA and protein localized to macrophage-like synoviocytes, endothelial cells and chondrocytes in particular, although other investigators found NOS protein predominantly in fibroblast-like rather than macrophage-like synoviocytes (McInnes IB, *et al.*, 1996). Inducible NOS protein has also been immuno-localized to vascular smooth muscle cells (Grabowski PS, *et al.*, 1997; McInnes IB, *et al.*, 1996). Accordingly, synovial fibrobasts, chondrocytes and osteoblasts from rheumatoid joints can produce

NO *in vitro* in response to pro-inflammatory cytokines (*e.g.* IL-1β, TNFα and interferon γ (IFNγ) (Grabowski PS, *et al.*, 1996). While rodent macrophages readily produce large amounts of NO (Hibbs JBJ, *et al.*, 1987), human macrophages have been reported to show only very modest amounts of NO *in vitro* despite strong stimulation (Albina JE, 1995). In RA and similar inflammatory arthritides expression of iNOS, IL-1β and TNFα protein in the synovium was elevated and strongly correlated, while only weakly present in cartilage (Melchiorri C, *et al.*, 1998). The converse was found for OA subjects. NO has been shown to induced mRNA expression of the pro-inflammatory enzyme cyclooxygenase type 2 (COX2) in rheumatoid synovial cells *in vitro* (Honda S, *et al.*, 2000). Studies of the effects of NO on potential target cells have otherwise focused on articular chondrocytes and cartilage, and will be discussed in the next section.

Kaur and Halliwell reported the first evidence implicating more reactive RNS, such as $ONOO^-$ in rheumatoid arthritis (Kaur H and Halliwell B, 1994). Using HPLC, they demonstrated increased levels of 3-NT in the serum and synovial fluid of patients with RA, compared to osteoarthritic and healthy controls. Immunohistochemically, 3-NT localised to synovial macrophages and blood vessels in rheumatoid synovia, and this was paralleled by staining for iNOS (Mapp PI, *et al.*, 2001; Sandhu JK, *et al.*, 2003). There was disagreement between these two studies as to whether iNOS is expressed in vascular smooth muscle or endothelial cells of the synovium. Nevertheless, there is clear evidence to implicate reactive NO-derived species in rheumatoid arthritis.

Initial studies of pharmacological NOS inhibition, using inhibitors relatively non-selective for individual NOS iso-enzymes, showed amelioration of arthritis in a number of models, *e.g.* rat streptococcal cell wall (SCW)-induced arthritis (McCartney-Francis N, *et al.*, 1993), adjuvant arthritis (Stefanovic-Racic M, *et al.*, 1994) and rabbit antigen-induced arthritis (Palacios FA, *et al.*, 1999). Suppression of chronic joint inflammation and cartilage-bone damage was common to all these studies. But not all aspects of acute joint inflammation were improved by NOS inhibition. For instance, joint swelling was suppressed in SCW-induced arthritis, but leucocyte infiltrates unaffected (McCartney-Francis N, *et al.*, 1993). When using more selective inhibitors of iNOS or iNOS 'knock-out' mouse models in experimental arthritis, the picture was different. SCW-induced rat arthritis (McCartney-Francis NL, *et al.*, 2001) was exacerbated with more severe tissue

destruction and cartilage/bone loss by the iNOS-selective inhibitor N-imino-ethyl-*L*-lysine (*L*-NIL) (Boer R, *et al.*, 2000). Expression of eNOS and nNOS mRNA was not affected by *L*-NIL treatment and it was suggested that constitutive NOS enzymes mediate the destructive arthritis. AIA in iNOS-deficient mice (iNOS -/-) and mice treated therapeutically with L-NIL produced, as expected, lower plasma levels of nitrite, but joint swelling, leucocyte adhesion and adhesion molecule expression during the acute phase was increased, compared with appropriate controls (Veihelmann A, *et al.*, 2001; Veihelmann A, *et al.*, 2002). L-NIL treatment commenced in the chronic phase of arthritis had no effect on articular inflammation or bone destruction of AIA in mice. There are, however, examples where specific iNOS inhibition is protective: Paw inflammation and joint destruction of adjuvant arthritis was shown to be inhibited by *L*-NIL, albeit only when given prophylactically, but not therapeutically (Fletcher DS, *et al.*, 1998). Proteoglycan loss was decreased in zymosan-induced knee monarthritis in iNOS gene 'knock-out' mice compared to wild-type, although acute inflammation was little affected (van de Loo FA, *et al.*, 1998). This heterogeneity of results is likely to reflect differences of disease mechanisms of these arthritis models and the different roles that individual NOS isoenzymes may play at different stages of the inflammatory disease process. In general, it would seem that NOS inhibition has to start prophylactically, *i.e.* during the pre-clinical phase of arthritis development, in order to have any chance to be protective.

There is evidence that a putative $ONOO^-$-scavenger, referred to as tempol (Carroll RT, *et al.*, 2000), is able to ameliorate inflammation and erosive damage in rats with collagen-induced arthritis (Cuzzocrea S, *et al.*, 2000). Accordingly, 3-NT immuno-staining was also dimished by tempol.

No published clinical trials of NOS inhibition exist.

1.3.2 RNS in human and experimental osteoarthritis

Although serum and synovial levels of NO_2^- are considerably lower in patients with OA than RA, there is much evidence to suggest that NO is an important mediator of cartilage pathology in OA. Chondrocytes are both an important source and target cell of NO.

Compared to most other human cell types, chondrocytes from non-diseased joints readily release large amounts of NO (measured as NO_2^-) when stimulated with the pro-inflammatory cytokine IL-1β *in vitro* (Palmer RJM, *et al.*, 1993) while chondrocytes from the cartilage of subjects with OA produce NO spontaneously (Amin R, *et al.*, 1995). This NO production by OA chondrocytes was associated with the expression of iNOS and a neuronal-type NOS enzyme, respectively. NO generation *in vitro* was found to be higher in superficial compared with deeper parts of normal human cartilage (Hayashi T, *et al.*, 1997). Both endogenous (*i.e.* IL-1β-induced) NO and exogenous NO have been associated with apoptosis in human and bovine chondrocytes (Blanco FJ, *et al.*, 1995), reduced ECM synthesis in rabbit cartilage (Taskiran D, *et al.*, 1994) and increased matrix metalloproteinase (collagenase and stromelysin) activity in non-diseased human and bovine chondrocytes (Murrell GA, *et al.*, 1995) *in vitro*. In normal rabbit chondrocytes, exogenous NO inhibited mitochondrial respiration and ECM synthesis, in particular under hypoxia (Tomita M, *et al.*, 2001). *In vivo*, a canine anterior-cruciate transection model of knee OA was associated with increased expression of iNOS and treatment with *L*-NIL decreased cartilage damage and synovial inflammation (Pelletier JP, *et al.*, 1998)

There is, however, also evidence that NO generation is not deleterious for OA cartilage *per se*: iNOS inhibition of human OA cartilage showed increased spontaneous release of prostaglandin E_2 (PGE_2) *in vitro* (Amin AR, *et al.*, 1997).

Some observations suggest that $ONOO^-$ is implicated in chondrocyte dysfunction. *In vitro* normal human chondrocytes required the presence of reactive oxygen species for NO-induced cell death (Del Carlo MJ and Loeser RF, 2002). Human OA cartilage showed 3-NT immunostaining in chondrocytes and ECM, correlating with histological OA severity and IL-1β staining of chondrocytes (Loeser RF, *et al.*, 2002). Staining was mainly in the superficial cartilage layers.

1.3.3 RNS in joint physiology

There is increasing *in vitro* evidence that NO has protective roles in cartilage and chondrocytes from normal joints. Both endogenous and exogenous NO has been shown to inhibit ECM catabolic activity of non-diiseased equine and bovine chondrocytes *in vitro* (Bird JLE, *et al.*, 2000; Stefanovic-Racic M, *et al.*, 1996). Inhibition of iNOS led to increased release of IL-1-induced, pro-inflammatory cytokines, such as IL-6, interleukin-8 and PGE_2, by chondrocytes from non-diseased human joints *in vitro* (Henrotin YE, *et al.*, 1998). NO appears also essential for host defence against bacterial arthritis. Mice lacking iNOS had higher mortality and more joint damage in *Staph.aureus*-induced septic arthritis (McInmes IB, *et al.*, 1998). Recently, NO_2^-, as the main breakdown product of NO, was shown to protect normal human chondrocytes *in vitro* against hypochlorous acid, a neutrophil-derived oxidant mediating cartilage destruction (Whiteman M, *et al.*, 2003). However, evidence that nitrogen species more reactive than NO may have a role in normal jjoint physiology has been lacking.

Previous work of our group determined the immunohistochemical distribution of 3-NT in inflamed and non-inflamed human synoviium (Mapp PI, *et al.*, 2001). In rheumatoid synovium, obtained from patients at the time of replacement arthroplasty, immunoreactivity was found in macrophage-like synoviocytes and vascular smooth muscle cells. This showed co-distribution with immunoreactivity for iNOS protein in serial sections. Control synovium had been taken from *post mortem* examinations and subjects, undergoing arthroscopy for mechanical knee symtoms. The control synovia were histologically normal, but displayed 3-NT immunoreactivity in the majority of vascular smooth muscle cells, as confirmed by staining of serial sections with a monoclonal antibody for smooth muscle α-actin. Co-distribution of iNOS was not observed and vascular smooth muscle cells from a wide range of normal non-synovial tissues (derived from the *post mortem* specimens and a pathological specimen bank) showed no immunoreactivity for 3-NT. Tissues studied, included skin, colon, small intestine, liver, kidney, heart, skeletal muscle and spleen.

These findings suggested a unique capability of synovial vessels to produce potent RNS, such as peroxynitrite, under physiological conditions. If true, this observation was likely to reflect an important biological role rather than a coincidental phenomenon. The questions that arose were as follows: Could this observation be reproduced in other species and by other (*i.e.* non-immunological) methods? If so, when during animal development did it come about? What was the enzymatic origin of the RNS leading to 3-NT formation and would this offer a way of modifying 3-NT in healthy joints? Given its ability to generate both NO and $O_2^{\bullet-}$, was there a role for XOR in generating articular 3-NT formation? Finally the most important question: how does 3-NT in healthy joints affect articular physiology and inflammation?

Chapter 2: Aims and objectives

The ***aim*** of this work was to elucidate the biological role of reactive nitrogen species (RNS) in normal synovial joint tissue and in joint inflammation:

To this purpose the following ***objectives*** were defined:

- To test the hypothesis that 3-nitrotyrosine (3-NT), a marker of peroxynitrite and other RNS formation *in-situ*, is present in joint tissue from normal animals across species.
- To identify a single enzymatic source of nitric oxide (NO), that precedes 3-NT formation in normal joints.
- To study the role of 3-NT in normal joints and in the development of joint inflammation following the induction of arthritis in normal and enzyme-deficient animals.

Previous work had shown that xanthine oxidoreductase (XOR), a ubiquitous enzyme is capable of generating both NO and superoxide, which can form the powerful RNS peroxynitrite.

Therefore a specific ***hypothesis*** to be examined was:

- That XOR contributes to 3-NT formation in normal joints and also during joint inflammation.

Chapter 3: Presence and distribution of 3-nitrotyrosine in joint tissue

3.1 Introduction

It is recognised that nitric oxide (NO) can have both adverse and beneficial effects on joint tissue during inflammation (see section 1.3). However, upon reaction of NO with $O_2^{\bullet-}$, both prevalent during joint inflammation (2000; Halliwell B, 1995), the more reactive species peroxynitrite ($ONOO^-$) is readily formed (Pryor WA and Squadrito GL, 1995). $ONOO^-$, in common with most reactive species derived from NO (RNS), has to date only been shown to be of deleterious consequence for joint tissue. For instance, 3-nitrotyrosine (3-NT), a molecular marker of $ONOO^-$ (Ischiropoulos H, *et al.*, 1992b; Reiter CD, *et al.*, 2000; Sawa T, *et al.*, 2000) and other RNS (Brennan ML, *et al.*, 2002; van der Vliet A, *et al.*, 1997), has been found to be elevated in synovial fluid and serum from subjects with rheumatoid arthritis (RA) compared to those with osteoarthritis (OA) and healthy volunteers, as measured by HPL-chromatography (Kaur H and Halliwell B, 1994). Increased immunoreactivity to 3-NT has been described in experimental forms of inflammatory arthritis (Cuzzocrea S, *et al.*, 2000) and osteoarthritis (Pelletier JP, *et al.*, 1999), as well as RA synovium (Mapp P.I., *et al.*, 2001; Sandhu JK, *et al.*, 2003) , OA synovium (Sandhu JK, *et al.*, 2003) and OA cartilage (Loeser RF, *et al.*, 2002) in human tissue. The correlation of 3-NT staining with histological inflammation in human joint tissue (Mapp PI, *et al.*, 2001; Sandhu JK, *et al.*, 2003) and the reduction of inflammation and 3-NT staining by $ONOO^-$-scavengers (Cuzzocrea S, *et al.*, 2000) is indirect evidence of a pathogenetic role of $ONOO^-$/RNS in arthritis.

In additon to 3-NT being a marker of RNS formation *in situ* there is increasing evidence to suggest that 3-NT itself may play a pathogenetic role (see section 1.1.4.3). Nitration of tyrosine under inflammatory conditions is a selective process with only one to five in 10,000 tyrosine residues (10-50 μmol/mol) detectable as 3-NT (Brennan ML, *et al.*,

2002). There is an increasing literature showing that nitration of single or few tyrosine sites of proteins associate with altered enzyme function and pathological anatomy or physiology, *e.g.* manganese SOD (MnSOD) in human rejected kidney allografts (MacMillan-Crow LA, *et al.*, 1996) or vascular tissue of senescent rats (van der Loo B, *et al.*, 2000b), and prostacyclin (PGI_2) synthase in atherosclerotic bovine artery walls (Zou MH, *et al.*, 1999).

Previous work from our group has shown distinct immunostaining for 3-NT in histologically normal synovium, derived from *post-mortem* examinations or subjects undergoing arthroscopy for knee pain (Mapp PI, *et al.*, 2001). 3-NT immunolocalised in particular to the vascular smooth muscle cells of synovial vessels, but it was not present in other vascular beds, such as in skin, gut, kidney or liver from a human tissue bank. This was a surprising finding, suggesting a physiological RNS-generating mechanism, exclusive to synovium.
But there were several caveats to these findings: Although the *post-mortem* specimens were obtained from subjects without known arthritis, most subjects were of advanced age, and it is now known that increased 3-NT in blood vessels and cartilage occurs as a part of normal aging (Loeser RF, *et al.*, 2002; van der Loo B, *et al.*, 2000a). Furthermore, an inevitable degree of *ante-mortem* and pre-sampling tissue hypoxia could have led to oxidative stress and artefactual formation of RNS, leading to spurious results. Finally, the arthroscopically retrieved synovial samples, although histologically normal, could not be assumed to be normal in the strictest sense.

There was therefore a need to replicate these immunohistochemical findings in other species under controlled conditions. If these findings were reproduced, it would then allow further investigations into the biological role of 3-NT in normal synovium. In addition, it was important to examine 3-NT content by a non-immunological, quantitative method, *e.g.* gas chromatography/ mass spectrometry (GC/MS). Finally, it was of interest to see whether specific tyrosine-nitrated proteins could be identified or whether 3-NT formation affected joint proteins in an indiscrimate way.

3.2 Aims and objectives

- To study the presence and distribution of 3-NT immunoreactivity in the normal joint and other tissues from the rat, mouse and other mammals, to determine whether findings are similar to human tissue.

- To determine at what stage during ontogenetic development 3-NT in normal rat joint tissue is first observed.

- To measure any increased presence of 3NT in the normal rat joint and compare this to other tissues by a sensitive quantitative physico-chemical method.

- To perform immunoblotting for 3-NT on joint homogenates of the rat to determine whether physiological tyrosine nitration affects specific proteins or all proteins indiscrimately.

3.3 Methods

Detailed material lists and protocols on general procedures can be found in the appendix sections. All concentrations are final, unless stated otherwise.

3.3.1 Animal methods

Laboratory rats and mice were kept under standard conditions with water and food *ad lib.* and 12 hour day-night light cycles. Animal husbandry and general procedures were in accordance with the Animal (Scientific Procedures) Act (ASPA), 1986. All experimental procedures were carried out under a Home Office-approved project and personal licence (#30/5652).

3.3.2 Animal tissues

Outbred Wistar rats (Bath strain; Charles River, UK) were killed by cervical dislocation or carbon dioxide overdose in accordance with Schedule 1 (Appropriate methods of humane killing, ASPA 1986). Patella with adjacent synovium was dissected together with other tissues for analysis.

Male SV 129 mice (B&K, Glasgow, UK) were killed by cervical dislocation. Whole knee joints were excised for analysis.

White Frisian cattle tissue samples were obtained from 4 – 6 week old animals, killed by electrical stunning and exsanguination, at the former Bath Abattoir, Cheltenham Street, Bath. Samples (*i.e.* synovial samples and cartilage core biopsies from the stifle joint) were removed within 20 min of slaughter.

3.3.3 Histological methods

3.3.3.1 Fixation and embedding

Joint samples were not decalcified prior to processing, since it was known from previous experiments within the group that the 3-NT antibody does not bind to decalcified sections.

3.3.3.1.1 By immersion

After excision, tissues were fixed in buffered formal saline (10% (v/v), histological grade; BDH, Poole, UK). Formal saline is known to fix tissue by cross-linking proteins via methylene bridges. After 24 -72 hours fixed tissues underwent automated dehydration and embedding in paraffin wax (Shandon Hypercentre XP, UK).

3.3.3.1.2 By perfusion

Compared to immersion-fixation, perfusion-fixation has a shorter time from cessation of circulation to fixation. It is used to demonstrate biomolecules *in situ*, that are very unstable or sensitive to hypoxic modification.

Six week-old, male Wistar rats (weight ca. 200-250 g; n=3) underwent terminal anaesthesia with *intra-peritoneal* (*i.p.*) pentobarbitone (Euthatal ™, 50-75 mg/animal; Rhone-Merieux, UK). Animals were fixed to a dissection board, the cardiac left ventricle cannulated with a surgical hollow probe and the probe clamped with a customized Spencer-Wells artery forceps. Approximately 200 mls phosphate-buffered saline (PBS) with sodium heparin (5 U/ ml PBS; Leo Laboratories, Bucks, UK) were perfused via a peristaltic pump (CP Instruments Co. Ltd, Herts, UK), followed by ca. 500 mls of formal saline per animal. Completed fixation was indicated by profound *rigor mortis*. Specimens were dissected and processed as for immersion-fixed samples.

3.3.3.1.3 By cryofixation

Certain antigens and staining methods, *e.g.* immunofluorescent techniques, require tissue fixation by cryo-preservation, since chemical fixation would mask the antigen or causes tissue autofluorescence. Excised tissue was mounted in OCT compound (TissueTec; RA

Lamb, UK) on cork beds and snap-frozen in isopentane (BDH, UK), pre-cooled in liquid nitrogen. Cryo-fixed samples were stored at -70 °C until sectioning.

3.3.3.2 Sectioning

Since non-decalcified tissue was used, sectioning of joint tissue was technically difficult due to early blade blunting and physical disruption of sections. Joint specimens were (embedded and) sectioned in a sagittal orientation.

3.3.3.2.1 Sledge microtome

Ice-cooled, paraffin-embedded tissue blocks were sectioned at a thickness of 5-8 µm on a sledge microtome (Leitz, Wetzlar, Germany), floated on 35 °C warm H_2O and mounted on microscopy slides. Sections were incubated at 60 °C overnight to improve adherence to the glass slides during the staining procedures. For difficult tissues, *e.g.* joint tissue, adherence was further improved by pre-treatment of glass slides with Vectorbond™ (Vector, UK) or using Superfrost™ glass slides.

3.3.3.2.2 Cryostat sectioning

OCT-embedded frozen samples were cut at 6-8 µm thickness on a cryostat (Bright Instrument Co., Huntingdon, UK). Bone-containing knee synovium samples were cut using a tungsten carbide blade (Bright, UK). Sections were thaw-mounted on Superfrost™ glass slides, air-dried and fixed as appropriate for the histological method.

3.3.3.3 Staining methods

3.3.3.3.1 Covalent-bound stains

Initial histological assessment of tissues will usually employ a stain that forms strong covalent bonds between a dye and a target tissue. In general the advantages of these stains are that they produce quick and durable results with good colour definition. The

disadvantages are that they require higher concentrations of chemical target groups and are less specific than immuno-stains.

One of the most frequently used stains in general pathological practice is the haematoxylin-eosin stain. Haematoxylin stains basophilic cell structures, such as the nucleic acid-rich nucleus, blue, whereas eosin stains the eosinophilic cytoplasm of cells red. Details about the procedure are found in ***Appendix I.***

3.3.3.3.2 Immunohistochemistry (IHC)

Immunohistochemical detection relies on the relatively specific interaction of an antibody with its corresponding antigen. This interaction is made visible via an enzyme, linked to the antibody, which catalyzes a colour reaction (*i.e.* direct IHC). However, since many antigens are present in low concentration, a signal amplification step with a 'tagged' secondary antibody (directed against the primary antibody) is often part of the protocol (*i.e.* indirect IHC), making the immunohistochemical method very sensitive (***Fig. 3.3.3.3.2***). Potential disadvantages include in particular the possibility of non-specific (*i.e.* false positive) staining, which can in part be eliminated by blocking non-specific binding or identified by using appropriate controls. Materials and protocol of the general method will be found in ***Appendix I.***

In the following there is a brief description of the general method with examples for 3-NT IHC in brackets:

After de-paraffinisation in xylene and rehydration in industrial methylated spirit (IMS) tissue sections were rinsed in PBS. Then blocking medium (*e.g.* 5 mg BSA and 333 µg normal goat serum in 10 ml PBS) was added onto the sections, so as to reduce non-specific binding of the secondary antibody. After a short incubation, excess medium was discarded and primary antibody added at pre-determined optimum dilution in blocking medium (*e.g.* polyclonal rabbit *anti*-3-NT antibody, 1:100-150 (v/v)). After incubation overnight at 8 °C, sections were rinsed twice in PBS. Then the biotinylated, secondary antibody (*e.g.* goat *anti*-rabbit Ig G, 1:100 (v/v) in PBS) was added, directed against the bound primary antibody and incubated approx. 30 min at room temperature (RT).

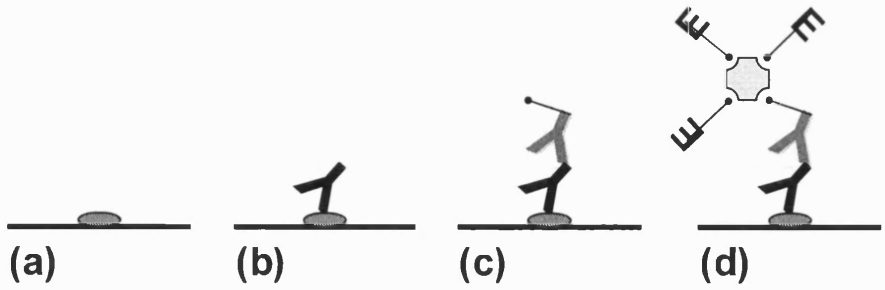

Fig. 3.3.3.3.2: Cartoon outlining the principle of indirect immunohistochemistry: (**a**) an antigen ( ) is shown on a histological section; (**b**) the primary antibody (**Y**) has bound to the antigen; (**c**) secondary antibody (Y), carrying covalently bound biotin (-•), has bound to the primary antibody; (**d**) avidin ,which avidly binds up to four biotin molecules, has bound a number of biotinylated enzyme molecules (**E**) and has cross-linked to a biotinylated secondary antibody, thus amplifying the signal of the primary antibody-antigen complex.

After further washing in PBS, sections were incubated for exactly 30 min with pre-prepared avidin-enzyme complex (reagent A (*i.e.* avidin) and B (*i.e.* biotinylated alkaline phosphatase) in PBS from Vectastain® ABC-AP kit). Each avidin will bind up to four biotin residues, thus amplifying the number of primary antibody-antigen complexes. After rinsing again in PBS, the chromogenic enzyme substrate was added (*e.g.* Sigma Fast™ Fast red, containing TR/ naphthol AS-MX tablets including 0.6 mM levamisole to inhibit exogenous alkaline phosphatase activity in H_2O/Q). Within minutes a colour reaction product (*i.e.* red) could be observed to develop under the microscope. The reaction was terminated by immersion into H_2O/dd, when positive and negative control sections turned positive or remain negative respectively. After counterstaining of nuclei

with Mayer's haematoxylin, sections were mounted in water-based mounting medium and ready for microscopic analysis.

3.3.3.3.3 Immunofluorescence (IF)

Like IHC, immunofluorescence (IF) is based on the specific interaction between an antigen and antibody, but this interaction is then visualized by a fluorescent-labelled secondary antibody. The indirect IF method used here is a modification of the technique described by Viera et al (Viera L, *et al.*, 1999). The protocol is detailed in ***Appendix I.*** In brief the method is as follows (with examples for 3-NT IF in brackets):

Cryo-preserved rat joint tissue was sectioned at 8 μm, air-dried and fixed in 4% para-formaldehyde. After solubilisation with 0.3% Triton X-100 (v/v, in PBS) for 10 min, blocking medium was added (*e.g.* 5 mg BSA, 333 μg normal goat serum in 10 ml PBS). Then primary antibody was added at pre-determined optimum dilution (*e.g.* monoclonal mouse *anti*-3-NT, clone 1A6, 1:200 (v/v) in blocking medium) for one hour at room temperature. After rinsing the sections in PBS, secondary FITC-labelled secondary antibody (*e.g.* goat *anti*-mouse IgG FITC conjugate, 1:150 (v/v) in PBS) was added and the sections from then on protected from light. After incubation for 30 min, the sections were rinsed in PBS and nuclei counter-stained with DAPI for a few minutes. After final rinsing, sections were mounted with a coverslip using an aqueous anti-fading medium and kept protected from light and dehydration at 4°C.

3.3.3.4 Specificity controls

Since immunohistochemical detection is dependent on the specificity of the primary antibody, a number of control sections are required in each assay to ensure that staining is not a result of non-specific binding.

The following controls were performed:

- Omission control: Blocking medium without the primary antibody was added to the sections. This controls for non-specific binding of all IHC media, except of the primary antibody itself, and was performed in every assay.

- Non-immune control: Normal immunoglobulin from non-immunised animals of the same host from which the primary antibody is derived was used instead of the primary antibody at the same final protein concentration. This is a valid control for polyclonal primary antibodies, provided it produces no (or negligible) staining. Given the sensitivity of IHC and the fact that 'non-immune' immunoglobulins are a large pool of different idiotype-specificities, some staining may occur, in particular if the antigen of interest happens to be a naturally common immunogen or when using a monoclonal primary antibody. It is therefore more appropriate to use a so-called isotype control, *i.e.* another primary antibody of identical host and immunoglobulin isotype, directed towards an antigen known to be absent in the tissue under investigation. In this instance, the anti-neurofilament 200 antibody represented such a control for 3-NT IHC in cartilage. Non-immune or isotype controls were employed in at least one out of three assays.

- Adsorption control: The primary antibody is pre-incubated with the purified antigen (if available) which should abolish all staining, if the antibody recognises the antigen it purports to do. In IHC for 3-NT this was performed once at the beginning of a new antibody batch, by pre-incubating the *anti*-3-NT antibody at working dilution, in blocking medium, containing 10 mM 3-nitro-*L*-tyrosine (Sigma, UK; #N-7389), pH-corrected to 7.4 with NaOH. After overnight incubation at 8°C, the medium was centrifuged for 20 min at 13000 rpm (Biofuge Fresco, Heraeus Instruments, Germany) and the supernatant used instead of the *anti*-3-NT antibody.

A positive specimen section control was used in every assay to ascertain that the assay as whole worked technically well. For the *anti*-3-NT antibody, the positive histological control was provided by human RA synovium, containing mononuclear cell infiltrates that stained well for 3-NT (Mapp PI, *et al.*, 2001).

3.3.3.5 Antibodies for IHC/IF

The main antibody used for IHC in this study was the rabbit polyclonal *anti*-3-nitrotyrosine. This immunopurified antibody was developed by Beckman *et al.* (Beckman JS, *et al.*, 1994b) and was generated by immunising mice with $ONOO^-$ - modified keyhole limpet haemocyanin.

Specificity	Host	Type	Source
anti-3-nitrotyrosine	Rabbit	Polyclonal, immunopurified	TCS Biologicals, UK, #06-284
anti-3-nitrotyrosine	Mouse	Monoclonal (clone 1A6), immunopurified	TCS Biologicals,UK, #05-233
anti-bovine neurofilament 200	Rabbit	Polyclonal, immunopurified	Sigma, UK; #N-4142

3.3.3.6 Microscopy

Stained tissue sections were examined on Zeiss Axioskop 2 microscope (Zeiss, UK). Via an interfaced colour video camera (KY-F558; JVC, UK) pictures were acquired digitally, using image analysis software (KS 300, version 3.0, 1997; Zeiss, UK).
Immunofluorescent sections were analysed using the following emission and excitation frequencies: for FITC (359/461 nm; appearance: green) and for DAPI (494/518 nm; appearance: blue).

3.3.3.7 Section analysis

IHC sections for 3-NT were analysed qualitatively for the presence and distribution of 3-NT. Particular attention was paid to the vascular smooth muscle cells in synovium, in comparison to other organs, such as gut, skin, brain, liver, kidney and heart.

As will emerge, 3-NT immunoreactivity was found not only in the synovial vessels, but also the hyaline cartilage chondrocytes, therefore a semiquantitative assessment was performed. The sections of one representative of at least three IHC assays per species or intervention group were coded and scored according to the following rule:

The total number of synovial vessels, defined as having a lumen with endothelium and/or intra-luminal blood cells, in the whole section was expressed as: 0, nil; +, < 5 vessels; + +, 5-15 vessels; + + +, 16 – 50 vessels; + + + +, > 50 vessels. This was done to take into account the variability of number of vessels seen per section.

The sections were then judged according to the proportion of synovial vessels showing unequivocal staining for 3-NT in the vascular smooth muscle layer: 0, no vessels; +, few vessels (*i.e.* <25 %); ++, moderate number of vessels (*i.e.* 25 – 75%); and + + +, most vessels (*i.e.* >75%) stained.

Cartilage, if present, was scored for the proportion of chondrocytes showing 3-NT immunoreactivity: 0, nil; +, few (*i.e.* < 25%); + +, moderate numbers (*i.e.* 25 - 75%); and + + +, most chondrocytes (*i.e.* >75%).

Intra-observer agreement of these semiquantitative scores were calculated as kappa, based on 13 mouse knee joint sections, scored twice four weeks apart and blinded to the label. Kappa (κ) expresses the observed agreement between the scores, as a proportion of the agreement expected by chance (Altman DG, 1991). The κ-value may lie between 0 (*i.e.* agreement no better than chance) and 1.00 (*i.e.* perfect agreement). In practice, κ-values are taken to reflect agreement as follows: < 0.20 equals *poor* level of agreement, 0.21-0.40 *fair*, 0.41-0.60 *moderate*, 0.61-0.80 *good*, and 0.81-1.00 *very good* agreement (Altman DG, 1991). The level of intra-observer agreement was fair for the number of

synovial vessels seen (κ = 0.39), moderate for the proportion of 3-NT-positive synovial vessels (κ = 0.44) and good for the proportion of 3-NT-positive chondrocytes (κ = 0.76).

3.3.3.8 3-NT immunohistochemistry on Wistar rat offspring

The male offspring of two Wistar rats, delivering within one hour of each other, were pooled to be raised by one of the mothers. Random animals (*n=3*, each time point) were sacrificed by cervical dislocation 3 hours, 10 days and 20 days after birth. The following joint tissues were obtained for formal saline fixation: whole limbs (from the newborn pups), whole knee and feet (from 10-day old pups) and patella-synovium preparations (from the weaning age animals, *i.e.* 20 days). Liver, bowel, skin, kidney, heart, lung and brain tissues were also obtained.

3-NT IHC in joint sections from all three time points was performed in the same assay, to ensure comparability of staining. Sections were assessed qualitatively for the absence or presence of 3-NT staining in synovial vessels and cartilage. Negative controls included omission of primary antibody and the use of pooled rabbit immunoglobulin instead of the primary antibody. H&E-stained sections showed no histological tissue pathology.

3.3.4 Nitrotyrosine measurement by gas chromatography/ mass spectrometry

Immunohistochemistry provides information on the localisation of antigens, like 3-NT, but it does not allow quantification of the antigen in question. IHC also relies on and is limited by the quality of the primary antibody, in particular its relative specificity. Several physico-chemical techniques have been used to quantify nitrotyrosine (NT), *e.g.* high-performance liquid chromatography(HPLC) or gas-liquid chromatography (GLC) and/or mass spectrometry (GC/MS, MS) (reviewed in (Herce-Pagliai C, *et al.*, 1998)).

This work had the benefit of collaboration with Prof. Kevin P Moore and Dr Ali R Mani, from the Centre for Hepatology, Department of Medicine, Royal Free & University College Medical School, UCL, London, UK. Prof Moore's group has established a highly sensitive method to quantify nitrotyrosine by GC/MS (Frost MT, *et al.*, 2000). In

principle, the method identifies NT by its molecular mass by inducing detectable fragment ions after a derivative of NT has been separated in a gas-liquid chromatographic column. For the detection of protein-bound NT, firstly protein is extracted from tissue, and NT is isolated by alkaline hydrolysis. This method is avoids artefactual formation of NT from prevalent nitrite, that may occur under the extremely acidic conditions used by acidic hydrolysis (Oldreive C, *et al.*, 1998). After this hydrolytic isolation from proteins, NT is further chromatographically purified and then chemically derivatised into a silylated heptafluoro-compound. This derivate will adopt gas phase state under GC conditions, and interfaced negative-ion chemical-ionization MS, is then able to detect as little as 1 picogram of NT. Both NT and tyrosine concentrations can be estimated in this way, using stable isotopic internal standards from the hydrolysis onwards. This allows expression of nitrotyrosine in ng per mg tyrosine. This is important since the concentration of nitrotyrosine may vary with the protein/solvent ratio used for hydrolysis, whereas the nitrotyrosine/tyrosine ratio is stable. Single measurements of samples were performed. The inter-assay coefficient of variation of the NT/tyrosine ratios, based on 10 determinations of a single plasma sample, was 3.1 % (Ali R Mani; personal communication).

Protein extraction from tissues to yield freeze-dried protein pellets was performed as detailed below and subsequent analytical steps were kindly performed by Dr Ali R Mani in accordance with the method described above (Frost MT, *et al.*, 2000).

3.3.4.1 Sample preparation

Wistar rats (*n=5,* 56 days old; mean weight (±SEM) 316±14 g) were killed by CO_2 gas overdose and knees dissected with a scalpel to isolate the patella and, separately, the peri-patellar synovium. Furthermore liver tissue was dissected.

3.3.4.2 Protein extraction from biological samples

Biological samples were put into 50 ml polypropylene ultracentrifuge bottles, containing 4ml ice-cold PBS, immediately after retrieval and kept on ice throughout. Samples were mechanically homogenised with a polytron (Ultra-Turrax, Jenke&Kunkel, IKA

Labortechnik, Germany) until easy to pipette. Chloroform/Methanol (2:1; v/v) was added to a volume of approximately 20 ml and the solution thoroughly mixed on a vortex. The samples were centrifuged at 9000 g for 15 min (8000 rpm in JA-14 rotor, equivalent to 9820 g at r_{max}, using a J2-MC ultracentrifuge; Beckman, USA). The liquid phases were carefully decanted and the fragile protein pellet at the fluid interphase transferred into an Eppendorf container. The samples were dried in a vacuum centrifuge (SpeedVac 2000, Savant).

3.3.5 Gel electrophoresis and Western blot analysis

While immunohistochemistry allows topographic localization of proteins in tissue sections by means of immuno-affinity, Western blot analysis allows identification of proteins in biological fluids/ homogenates by means of immuno-affinity. Western blotting may also permit a degree of protein quantification. Prior to Western blot analysis, protein concentration in homogenates was measured and proteins separated by gel electrophoresis. The electrophoretic methods used here are standard protocols (see also (Walker JM, 1994) for principles and appendices for step-by-step protocol).

3.3.5.1 Sample preparation

Two male Wistar rats (ca. 250 g) were sacrificed by CO_2 overdose. Synovium and patella with cartilage from both knees were dissected immediately and placed into PBS on ice, containing 10 µg/ ml aprotinin (Sigma, Poole, UK) and 1mM (w/v) phenylmethylsulfonylfluoride (PMSF; Sigma, UK) as protease inhibitors. Samples were homogenised with a polytron including two short sonication bursts (Clifton Ultrasonic Bath; Nickel Electro Ltd, Weston-super-Mare, UK).

3.3.5.2 Protein quantification

The technique to determine the protein content of biological fluids and tissue homogenates was based on the method, described by Bradford (Bradford MM, 1976).

This rapid and simple test is based on the principle that proteins bind avidly to the acidic dye Coomassie Brilliant Blue, resulting in a shift of the photometric absorption maximum from 465 to 595 nm. Comparison to a standard curve provides a relative measurement of protein concentration. A commercially available reagent kit and standard (Bio-Rad Labs, Hemel Hempstead, UK) was used on microtiter plates and the protocol can be found in ***Appendix II***. Inter- and intra-assay coefficients of variation were < 10 and < 5 %, respectively.

3.3.5.3 Gel electrophoresis

Gel electrophoresis is the method of spatially separating proteins in solution in a gel by means of an electrical current. All proteins possess an intrinsic electrical charge, but by covalent binding of sodium dodecyl sulphate (SDS), proteins will separate according to molecular size (and not charge) during polyacrylamide gel electrophoresis (PAGE).

The principle is as follows (see ***Appendix III*** for details): A mini gel is prepared from acrylamide, bis-acrylamide and SDS in water and polymerized by free-radical catalysis through the addition of ammonium persulfate and TEMED. The pore size is determined by the polyacrylamide concentration. Depending on the proteins in question, the polyacrylamide concentration of the separating gel may be 12.5 % for proteins up to 100 kDa, or 8 % for larger proteins. A 4% stacking gel is prepared on top of the separating gel with wells to accept samples. Samples, including standards of known molecular weight and positive controls (for the Western blot analysis), of defined protein concentration are denatured by boiling for 3 min in buffer containing SDS, ß-mercapto-ethanol and tracking dye. The gel set is connected to a constant current of 15-20 mA per gel until the tracking day reaches the bottom of the gel.

3.3.5.4 Western blot analysis

Western blot analysis of proteins involves electrical transfer of the proteins from the gel onto a nitrocellulose (NC) membrane, prior to immunodetection of specific proteins (see

Appendix III). A semi-dry protein transfer method was used and successful transfer onto NC was verified by Ponceau S protein staining. Following blocking of non-specific binding with non-fat dried milk buffer, primary antibody was applied (*e.g.* polyclonal rabbit *anti*-3-NT antibody, 1:2000) and, after washing steps, the secondary antibody/ horse radish peroxidase (HRP) conjugate (*e.g.* swine *anti*-rabbit immunoglobulin/HRP conjugate, 1:2000). The bound antibody/HRP conjugate was then detected by enhanced chemiluminescence (ECL): HRP oxidizes luminal in the presence of H_2O_2 in alkaline solution. Upon oxidation luminol adopts an excited state, which decays to ground state with light emission. This can be enhanced in the presence of phenol, and the chemiluminescence was captured by autoradiography on a blue light –sensitive film. Exposure time was aiming to maximize the signal-to-noise ratio. Negative controls included omitting the incubation with primary antibody.

3.4 Results

3.4.1 *3-NT is located in vascular smooth muscle cells of normal joints in small rodents, but not cattle*

Immunohistochemistry for 3-NT on normal knee joint sections from Wistar rats and SV-129 mice, but not from young cattle, showed immunoreactive vessels.

Table 3.4.1 shows a summary of the findings. In qualitative-descriptive terms 3-NT immunoreactivity (3-NT-IR) in the various species was as follows:

- Wistar rats:

As in the 'normal' human samples, 3-NT-IR localised to the vascular smooth muscle (VSM) cell layer of synovial blood vessels (***Fig. 3.4.1; image A-C***). Sometimes 3-NT-positive vessels could be seen adjacent to 3-NT-negative vessels. Some milder staining was seen also in occasional cells of the synovial lining layer. There was no difference in staining between immersion- and perfusion-fixed joint tissues (***Fig. 3.4.1, image D***). Other organs examined (*i.e.* skin, small intestine, colon, liver, heart, kidney, spleen and brain) did not display clear 3-NT-IR in vascular smooth muscle cells. H&E stains did not show any pathological abnormalities.

- SV 129 Mice:

Allowing for a naturally smaller number of vessels per joint section, mouse knee synovium showed similar 3-NT staining in VSM cells. (***Fig. 3.4.1.B***). Again some degree of milder staining was seen in occasional cells of the synovial lining layer. Skin, heart and gut sections did not show 3-NT-IR in VSM of blood vessels.

- Cattle:

Although synovial sections showed numerous blood vessels, 3-NT-IR in VSM cells was very weak.

Table 3.4.1: **3-NT immunohistochemistry in synovial blood vessels of normal knee joint sections.**

Species	*Animals/Knees (n)*	*Age*	*Synovial Vessels median (range)*	*3-NT-positive vessels median (range)*
Wistar Rat (immersion-fixed)	**5/5**	**5 -8 weeks**	+ + + (+ + - + + +)	+ + + (+ + - + + +)
Wistar Rat (perfusion-fixed)	**3/6**	**6 weeks**	+ + + (+ - + + +)	+ + (++ - +++)
SV 129 Mouse	**3/6**	**7 weeks**	+ + (+ - + +)	+ + + (+ + - + + +)
Cattle	**3/3**	**4 - 6 weeks**	+ + + +	**0 (0 - +)**

Shown is the data of immunohistochemical stains for 3-NT in each species (or intervention group). All sections were coded and scored as follows: the total number of synovial blood vessels, defined as having a lumen with endothelium and/or intra-luminal blood cells, seen in the whole section was expressed as: 0, nil; +, < 5 vessels; + +, 5-15 vessels; + + +, 16 - 50 vessels; + + + +, > 50 vessels. All sections were scored according to the proportion of synovial vessels showing unequivocal staining for 3-NT in the vascular smooth muscle layer: 0, no vessels; +, few vessels (*i.e.* <25%); + +, moderate number of vessels (*i.e.* 25 - 75%); and + + +, most vessels (*i.e.* >75%) stained.

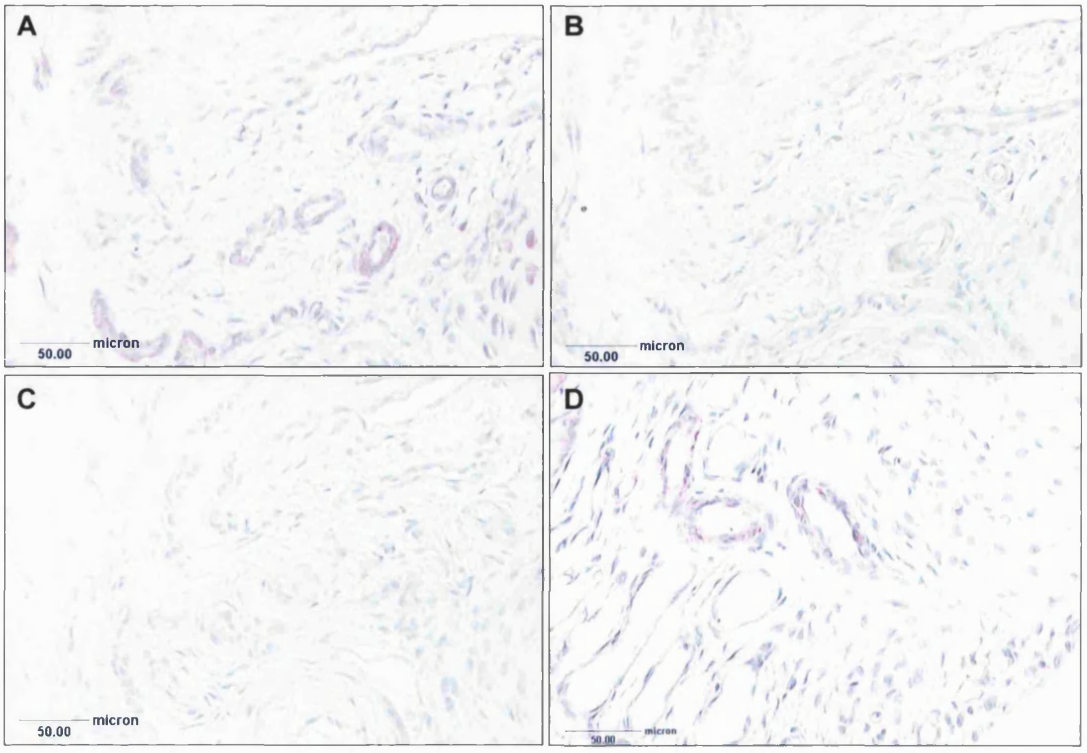

Fig. 3.4.1: Immunohistochemical stain for 3-NT (shown as red) in normal rat knee synovium. **A**, Wistar rat, aged 7 weeks, killed by cervical dislocation. Note widespread staining for 3-NT in the majority of synovial vessels. **B**, negative adsorption control (using 10 mM 3-NT) in a corresponding tissue section to A. **C**, negative omission control (of primary antibody) in a corresponding tissue section to A. **D**, Wistar rat, aged 6 weeks, killed by perfusion-fixation under terminal anaesthesia.

3.4.2 *3-NT immunolocalizes to hyaline cartilage chondrocytes of rats, mice and cattle joints*

Unexpectedly, distinct 3-NT-IR was also found in the hyaline cartilage chondrocytes of knee joints from Wistar rats, SV 129 mice and cattle. ***Table 3.4.2*** summarises the findings.

The qualitative-descriptive findings for the various species were as follows:

- Wistar rats:

Rat patella/ cartilage specimens showed strong 3-NT-IR in the majority of chondrocytes (***Fig. 3.4.2 a, A-C***). The staining pattern of individual cells was consistent with diffuse cytoplasmic and/or membranous antigen localisation.

Table 3.4.2: **3-NT immunohistochemistry in hyaline cartilage of normal knee joint sections**

Species	*Animals/Knees (n)*	*Age (weeks)*	*3-NT-positive Chondrocytes median (range)*
Wistar Rat (immersion-fixed)	**5/5**	**5 -8**	**+ + + (+ + +)**
Wistar Rat (perfusion-fixed)	**3/6**	**6**	**+ + (+ +)**
SV 129 Mouse	**3/6**	**7**	**+ + + (+ + - + + +)**
Cattle	**3/3***	**4 - 6**	**+ + + (+ + +)**

Shown is the data of immunohistochemical stains for 3-NT in each species (or intervention group). All sections were coded and scored as follows: 0, nil; +, few (*i.e.* <25%); + +, moderate numbers (*i.e.* 25 - 75%); and + + +, most chondrocytes (*i.e.* >75%) of the whole section showing immunoreactivity for 3-NT. * included were sections from inter-condylar cartilage biopsies.

Chondrocytes with 3-NT-IR were occasionally adjacent to chondrocytes without 3-NT staining. No consistent zonal distribution of 3-NT-positive cells (*i.e.* apical *vs.*

basal cartilage zones) was observed otherwise. 3-NT-IR in cartilage sections from perfusion-fixed animals appeared less intense, but was still present.

- SV 129 mice:

Mouse knee joints displayed similar widespread 3-NT-IR in chondrocytes of the hyaline cartilage. The staining intensity appeared generally slightly weaker, compared to staining in rat cartilage (***Fig. 4.4.1, F***). There was no differential distribution of 3-NT-postive cells according to central *vs.* peripheral (*i.e.* synovium-near) distribution. In addition, chondrocytes of the proliferative, columnar cartilage layer of the epiphysial growth plate showed similarly intense 3-NT-IR.

- Cattle:

Punch biopsies from calf stifle joints showed similar 3-NT-IR in chondrocytes. Chondrocytes of all horizontal cartilage zones showed staining (***Fig. 3.4.2 a; D,F,G***), irrespective whether they were from cartilage areas of relatively high (*e.g.* tibial plateau) or low (*e.g.* intercondylar area) mechanic load. IHC with an irrelevant antibody (*i.e. anti*-bovine neurofilament) of identical host- and type-characteristics produced no staining at equivalent dilutions (***Fig. 3.4.2 a; E, H***).

Indirect immunofluorescent studies, using the *monoclonal anti*-3-NT antibody in cryo-fixed sections of joints from Wistar rats (8 weeks old), failed to reveal 3-NT staining in synovial vessels or cartilage. ***Fig. 3.4.2 b*** shows a representative photomicrographs.

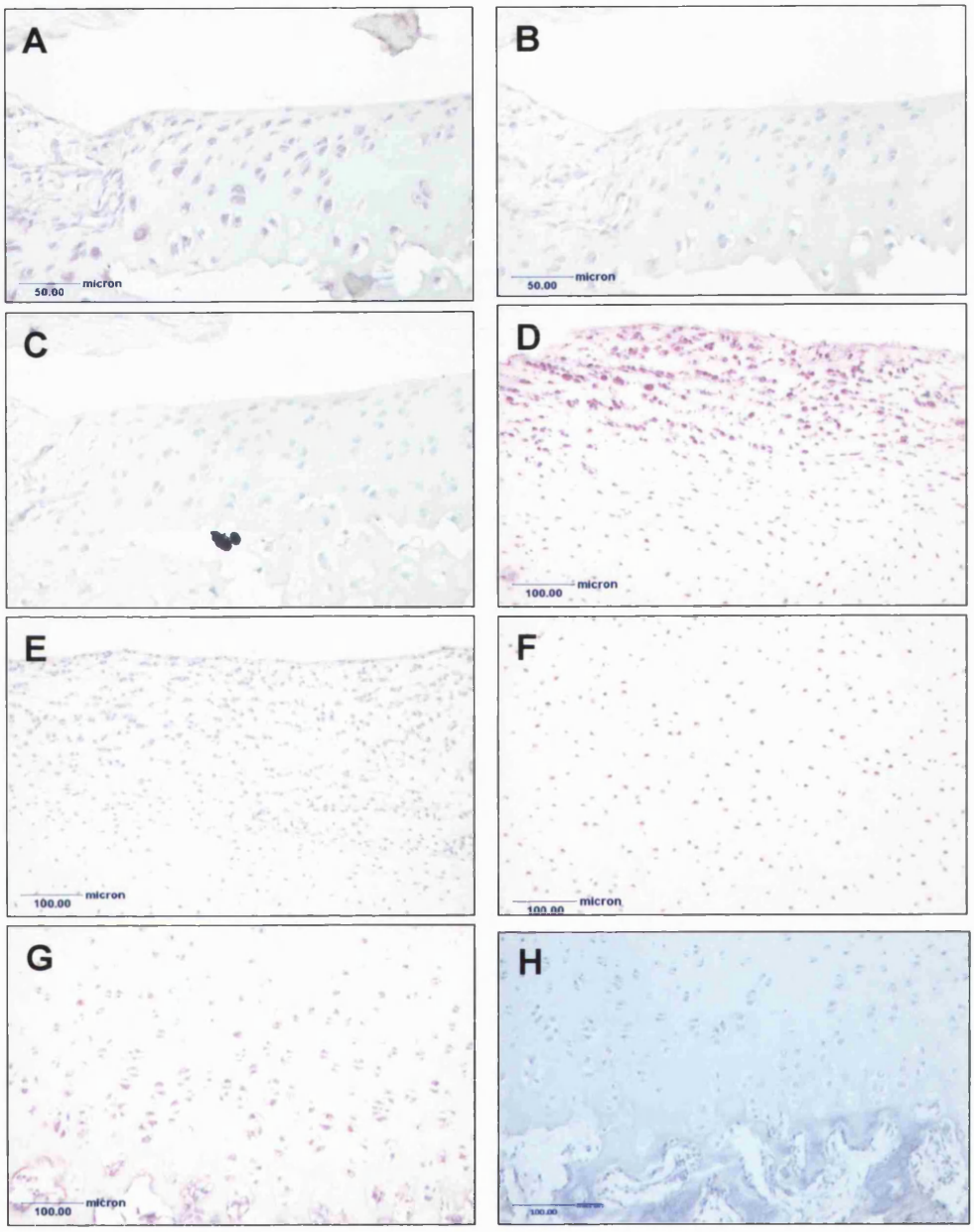

Fig. 3.4.2 a: Immunohistochemical stain for 3-NT (shown as red) in normal knee joint cartilage. **A**, patella cartilage from Wistar rat, aged 7 weeks, killed by cervical dislocation; stained with anti-3-NT. Note the widespread 3-NT staining of chondrocytes; **B**, corresponding section to A, stained with anti-3-NT antibody, preincubated with 10 mM nitrotyrosine; **C**, corresponding section to A, with omitted primary antibody; **D, F, G**, sections from the superficial (D), middle (F) and basal (G) cartilage zone of the tibial plateau of Frisian White cattle, aged 4-6 weeks, stained with anti-3-NT; **E and H**, corresponding sections to D and G, respectively, showing negative staining using anti-bovine neurofilament antibody.

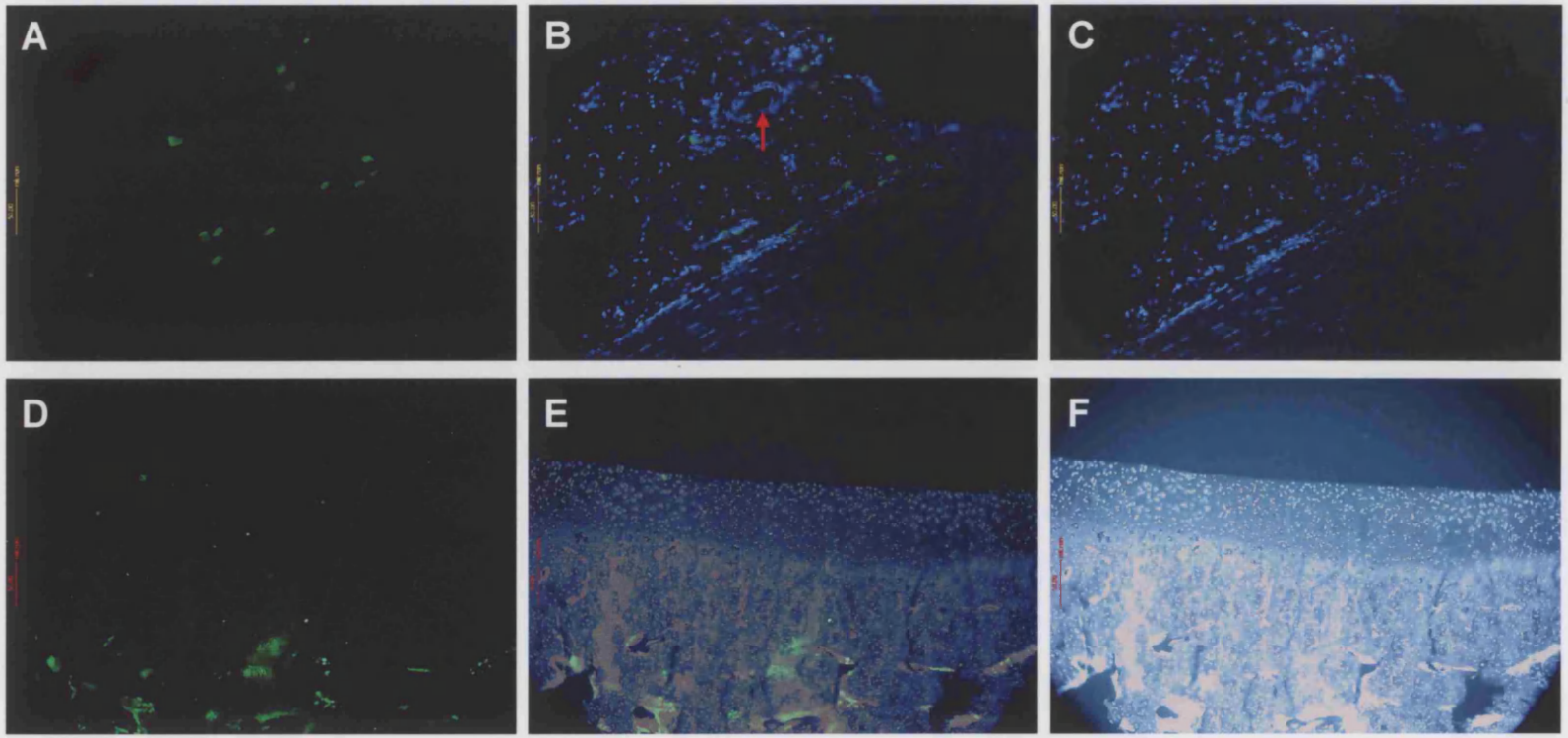

Fig. 3.4.2 b: Immunofluorescent stain for 3-NT of cryo-fixed knee joint tissue from an 8 week-old Wistar rat, using monoclonal anti-3-NT primary antibody. Photomicrographs A-C show the same synovial section, with green (FITC) fluorescence representing 3-NT (**A**) and blue (DAPI) fluorescence of cellular nuclei (**C**). **B** shows a merged image of A and C. Note the absence of 3-NT staining in synovial vessels (arrow). Photomicrographs D-F show the same section of patella with green-fluorescent 3-NT (**D**) and blue nuclear counterstain (**F**). Note the absence of 3-NT in cartilage in the merged image **E**. Bars represent 50 μm.

3.4.3 *3-NT-immunoreactivity in normal joints develops soon after birth in rats*

3-NT staining in synovial VSM cells and hyaline cartilage chondrocytes was absent at birth, but was seen from age 10 days onwards. (***Fig. 3.4.3***).

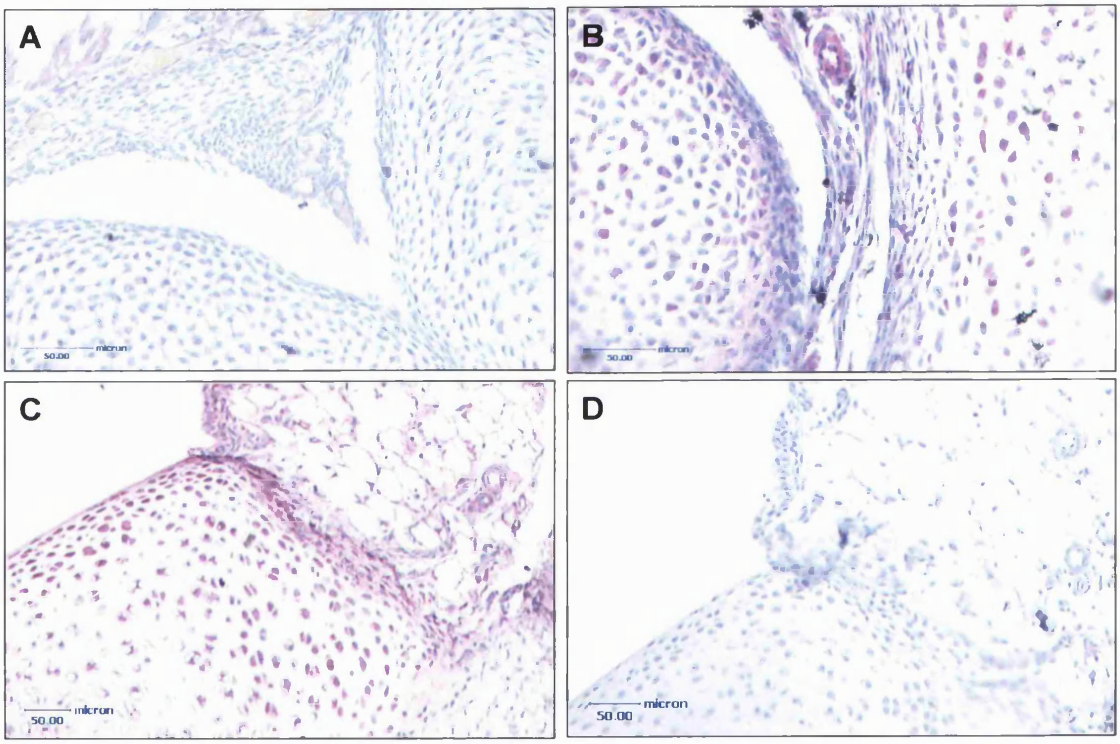

Fig. 3.4.3: Immunohistochemical stain for 3-NT (shown as red) in knee joint tissue of young Wistar rats. The microphotographs show representative examples of one of two assays. **A**, from newborn rat showing absent 3-NT-IR; **B**, from 10 day-old rat; **C**, from 20 day-old rat; **D**, serial section to C, using normal rabbit immunoglobulin as a negative control.

The findings of the experiment, relating to Fig. 3.4.3, are summarized in ***Table 3.4.3***.

Table 3.4.3: **3-NT immuno-localisation in knee joint tissue of young Wistar rats.**

Age	*Specimen (Animal No)*	*3-NT in VSMC*	*3-NT in chondrocytes*
newborn	**Hind limb (I)**	-	-
	Fore limb (I)	-	-
	Hind limb (III)	-	-
	Fore limb (III)	-	-
10 days	**Knee (I)**	+	+
	Foot (II)	NA*	+
	Knee (III)	+	+
20 days	**Synovium-patella (I)**	+	+
	Synovium-patella (II)	+	+
	Synovium-patella (III)	+	+

Sections were scored for the absence (-) or presence (+) of 3-NT staining in synovial vessels and hyaline cartilage chondrocytes. Roman figures refer to different animals. VSMC, vascular smooth muscle cells; *NA, not available due to lack of unequivocal synovial vessels in sections.

3.4.4 *NT content is high in patella tissue compared with synovium and liver*

The mean (±SEM) nitrotyrosine-tyrosine ratios, assessed by GC/MS, in patella ($n=5$), synovium ($n=5$) and liver ($n=2$) of Wistar rats were 423 ± 92, 82 ± 14 and 43 ± 5 pg/μg, respectively ($p<0.05$ for difference between patella *vs* liver and synovium, ANOVA with Bonferroni's multiple comparison test). Due to limitations of the maximum number of samples that can be run in one assay and the anticipated low

standard error for measurements in liver tissue, only 2 of 5 liver samples were measured (***Fig. 3.4.4.***).

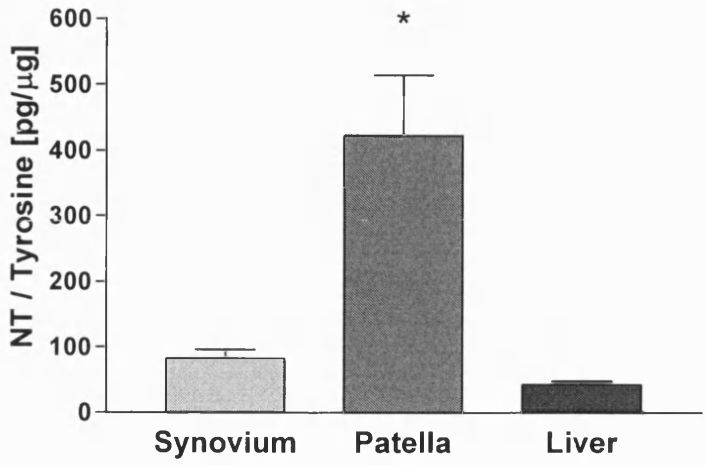

Fig. 3.4.4.: NT/ tyrosine ratios of tissue homogenates from Wistar rats (aged 56 days; killed by CO_2 overdose), as measured by GC/ MS. Bars represent means ± SEM. Synovium (*n=5*), patella (*n=5*), liver (*n=2*). * $p < 0.05$ *vs* liver and *vs* synovium (ANOVA with Bonferroni's multiple comparison test).

3.4.5 *Synovial and patella/cartilage proteins display disparate 3-NT content*

SDS-PAGE and subsequent immunoblotting of synovial and patella/cartilage homogenates from Wistar rats revealed a discrepancy of signal intensity between protein bands and 3-NT bands. ***Fig. 3.5.4*** shows representative gel stains and blots of three separate assays. For instance, the strong protein band between 50 and 75 kDa, which may represent albumin or immunoglobulin heavy chains, shows hardly any 3-NT immuno-reactivity. Conversely, 3-NT staining is seen at sites with relatively little protein staining. The strongest 3-NT signal localises to ca. 150 kDa in both synovium and patellar cartilage, and a weaker one to between 35 and 50 kDa. At least in patella/cartilage, there is a further weak 3-NT band parallel to one of the

peroxynitrite-treated protein standards, *i.e.* the nitrated bovine Cu,Zn-SOD dimer. Negative controls, omitting the primary antibody incubation, were negative.

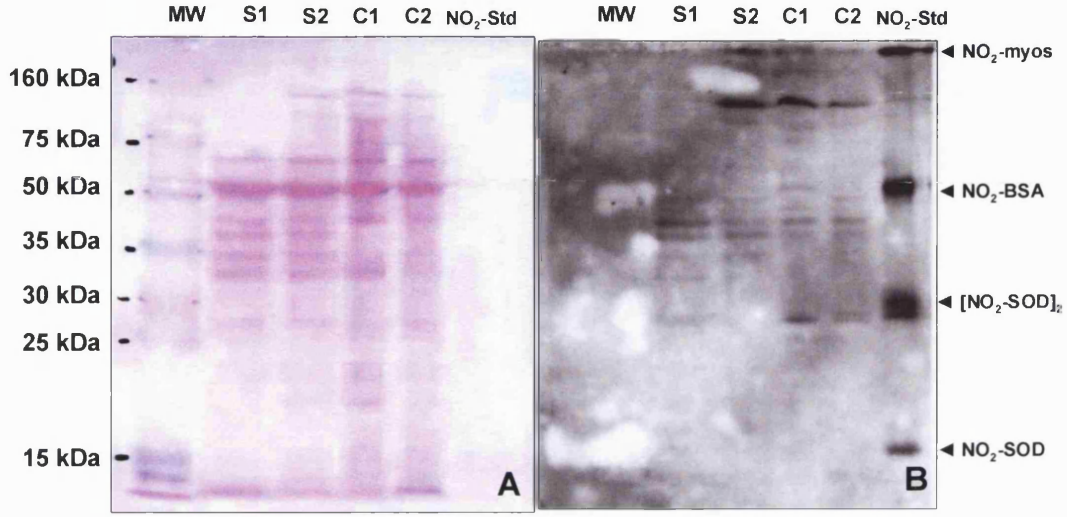

Fig. 3.5.4: Ponceau S protein stain (following 8% SDS-PAGE) of a nitrocellulose blot (**A**) and corresponding immunoblot for 3-NT (**B**), using polyclonal anti-3-NT antibody. Molecular weight markers (MW) and peroxynitrite-treated standards (NO_2-Std) are labelled. Samples include 20 µg protein of homogenates of synovium (S1 and S2) and patella with cartilage (C1 and C2). The nitrated protein standards are: nitrated rabbit myosin (NO_2-myos, ca. 215 kDa), nitrated BSA (NO_2-BSA, ca. 66 kDa), nitrated bovine Cu,Zn-SOD (NO_2-SOD, ca. 16 kDa) and dimer ($[NO_2\text{-SOD}]_2$). Note the discrepancy between protein signal and 3-NT signal, *e.g.* for the protein band above 50 kDa, displaying only very little 3-NT immunoreactivity.

3.5 Discussion

These investigations have shown that normal cartilage and, to a lesser extent, normal synovial vessels from a variety of mammalian species (Wistar rat, SV 129 mice and cattle) contain increased amounts of 3-NT, a molecular marker of RNS formation *in situ*, compared to non-articular tissues. Longitudinal studies in rats indicated that this phenomenon develops shortly after birth and, as perfusion-fixed tissues showed, is not due to *post-mortem* artefact. Electrophoretic and 3-NT immunoblotting studies of rat joint homogenates showed a discordant pattern of protein and 3-NT bands, suggesting that tyrosine nitration of proteins is not a random event. Together, these results indicate an exclusive ability of normal cartilage and synovial vessels to generate specific RNS/3-NT-modification of proteins for reasons yet to be identified.

These findings support the previous observation of our group showing 3-NT in vascular smooth muscle cells of histologically normal human synovium from *post-mortem* and arthroscopic examinations, but not from other vascular beds (Mapp PI, *et al.*, 2001). However, they are at odds with reports by other investigators. Using a rabbit polyclonal *anti*-3-NT antibody, Loeser *et al.* studied 3-NT-IR in cartilage from *post-mortem* human and monkey samples by immunohistochemistry (Loeser RF, *et al.*, 2002). Using a simple dichotomic score of 3-NT staining being positive or negative, they reported 3-NT-IR in chondrocytes, correlating with increasing age and changes of osteoarthritis. They did not find positive 3-NT-IR in human donors without arthritis below the age of 50. Similarly, in normal dog knee joint tissue, only a few cells in cartilage and the occasional synovial lining cell stained positive for 3-NT (Pelletier JP, *et al.*, 1999). In another study of collagen-induced arthritis in the rat, the presence of 3-NT-IR in normal controls is not commented upon (Cuzzocrea S, *et al.*, 2000). Both these studies were pharmacological intervention studies, focussing on the comparison of two experimental groups rather than the normal tissue as control. In those circumstances, it is desirable to terminate the chromogen-reaction step of the IHC assay early to ensure a clear difference between pathological and physiological signal. This may lead to differential staining in normal tissue to remain masked and thus unreported. The absence of staining by immunofluorescence, using the monoclonal *anti*-3-NT antibody, was disappointing,

since it precluded further experiments to try and co-localize 3-NT with putative proteins by double immunofluorescence.

This study is the first report of 3-NT analysis in joint tissue by GC/MS and shows increased 3-NT levels in cartilage, compared to liver and synovium in normal rats. Results were normalized for any potential variation in tyrosine content of different tissues. The discordant pattern of protein and 3-NT bands in synovial and patella/cartilage homogenates from normal rat knee joints, is consistent with other reports in the literature [see 1.1.4.3 and (Ischiropoulos H, 2003)]. These suggest that tyrosine nitration of proteins is a selective process in order to modify protein function. The 3-NT band in patella/cartilage homogenates at the level of the 32 kDa nitrated bovine Cu, Zn-SOD dimer standard raises the possibility that this anti-oxidant enzyme may be nitrated during normal joint physiology. SOD enzymes play an important part in limiting adverse effects of aerobic metabolism. Both cytoplasmic Cu,Zn-SOD and the mitochondrial Mn-SOD protein have been found by immunohistochemistry in chondrocytes but not in the extra-cellular matrix of tracheal cartilage in healthy rats (Frederiks WM and Bosch KS, 1997). However, histochemical SOD *activity* was only encountered in extra-cellular cartilage matrix (Frederiks WM and Bosch KS, 1997). This discrepancy was explained by the presence of a distinct high-molecular (*i.e.* 135 kDa) extracellular form of Cu, Zn-dependent SOD. Using proteomic methods that aim to identify the individual proteins that undergo tyrosine nitration, to date only the mitochondrial Mn-form of SOD has been reported in aging cardiac rat tissue (Kanski J, *et al.*, 2004). This form of SOD was the first to be described to undergo inactivation via selective tyrosine nitration in the pathological context of chronic renal allograft rejection (MacMillan-Crow LA, *et al.*, 1996). It was argued that this forms a positive feed back loop to enhance oxidative stress.

In the absence of identified target proteins for tyrosine nitration, what might be the biological role of 3-NT/RNS in normal joint tissue? In general, one of the best known host-protective functions of RNS, such as $ONOO^-$, is that of anti-microbial action. Experimental studies on mice lacking iNOS showed that NO production is required to protect against staphylococcal septic arthritis (McInnes IB, *et al.*, 1998). It is generally thought that chemical species more reactive than NO are involved in

this bacterial defence mechanism (Fang FC, 1997; Grisham MB, *et al.*, 1999). For instance , $ONOO^-$ is far more toxic to bacteria than NO or $O_2^{\bullet-}$ (Brunelli L, *et al.*, 1995; Umezawa K, *et al.*, 1997). Moreover clinical observations and anatomical factors illustrate the need for an effective anti-microbial defence system within joints. Septic involvement is uncommon in relation to the frequency of septicaemia. This is surprising considering the heavily vascularised nature of the synovium. Having no basement membrane, it could be expected that bacterial spread to the synovial cavity is facilitated (Miller ML, 1998). The avascular and relatively hypoxic cartilage would then be a vulnerable target to direct microbial attack. Furthermore, metabolically active structures of *Chlamydia trachomatis* have been found in the synovium of some asymptomatic human subjects (Schumacher HR, *et al.*, 1999), suggesting that microbial joint invasion may not always be clinically apparent and more common than generally thought. It would therefore be conceivable that 3-NT represents RNS formation to counteract local microbial invasion.

A further beneficial function for $ONOO^-$ is cardioprotection in experimental models of cardiac ischemia-reperfusion injury (CIRI). During reperfusion after temporary complete ischemia, maximally achievable physiological concentrations of $ONOO^-$ (2 μM) restored cardiac contractility and reduced polymorphonuclear (PMN) cell accumulation in an *ex vivo* rat model (Lefer DJ, *et al.*, 1997). In a feline model of CIRI, $ONOO^-$ reduced infarct size and endothelial PMN cell adhesion (Nossuli TO, *et al.*, 1998). Furthermore, $ONOO^-$ was found to be the cardio-protective mediator of ischemic pre-conditioning in rats (Laude K, *et al.*, 2002). The investigators suggested that $ONOO^-$ may exert these effects by nitrosylation of the thiol group of glutathione (GSH) to S-nitrosoglutathione (GSNO), which then acts as a slow and 'good' NO-donor on vascular endothelial cells (Mayer B, *et al.*, 1995). There is good evidence that similar cycles of hypoxia and reoxygenation occur during mobilisation of arthritic joints, which is thought to contribute to pathology (Blake DR, *et al.*, 1989; Mapp P.I., *et al.*, 1995). However, chondrocytes of *normal* avascular articular hyaline cartilage are generally assumed to function at low oxygen tension (down to 1 kPa or less) (Silver IA, 1975). The expression of the transcription factor hypoxia inducible factor-1 alpha in normal as well as osteoarthritic *human* cartilage is further indirect evidence for the functional adjustment of chondrocytes to low oxygen levels

(Coimbra IB, et al., 2004). Intra-articular (*i.a.*) pressures in normal joints are mostly subatmospheric, aiding synovial capillaries to remain perfused. However, during maximum flexion *i.a.* pressure has been shown to rise up to 5 mmHg and over 30 mmHg in rabbit and dog knees, respectively (Levick JR, 1979; Nade S and Newbold PJ, 1983). This could be expected to lead to temporary capillary occlusion. It would therefore seem conceivable that even healthy, moving joints undergo cycles of hypoxia and reoxygenation that could be harmful to cartilage. One could therefore hypothesize that $ONOO^-$ might ensure chondrocyte survival in normal mobilizing joints, comparable to myocardial survival in CIRI. Consistent with this, 3-NT was not seen in cartilage from newborn rats, presumably due to their limited joint mobility. Furthermore, articular chondrocytes have been shown to generate GSH *in vitro* (Carlo MD and Loeser RF, 2003). At millimolar concentrations, nitrosylated GSH induces chondrocyte apoptosis *in vitro*, whereas pretreatment with micromolar GSNO can reduce chondrocyte death (Turpaev KT, et al., 1997). One could therefore speculate that cycles of hypoxia-reoxygenation in healthy joints induce $ONOO^-$ generation in articular chondrocytes, that may nitrosylate the prevalent anti-oxidant GSH to form a slow NO-donor. The slow release of NO would then serve to maintain the regulatory and protective functions of NO, ultimately securing chondrocyte survival and function.

The present investigations have important limitations. The immunohistochemical method depends on the specificity of the antibody used and does not allow reliable quantification of antigen concentration. Appropriate negative controls were employed, but the present data does not eliminate the possibility that the polyclonal *anti*-3-NT antibody may cross-react with antigens other than 3-NT. GC/ MS allowed quantification of 3-NT and confirmed a higher 3-NT to tyrosine ratio in patella compared with liver and synovium in naïve rats. However, this data does not determine whether the 3-NT originates from the cartilage or the bone. These studies will require replication by other investigators and further quantitative analysis of 3-NT in articular and non-articular tissues from other species should be undertaken.

In conclusion, these studies provide evidence of high 3-NT/RNS formation in healthy synovial joints relative to non-articular tissue in several mammalian species. This suggests a physiological role for 3-NT/ RNS that requires further elucidation.

The next aim was to identify an exclusive enzymatic source of NO, the obligatory precursor of 3-NT/RNS in this setting.

Chapter 4: Studies on the enzymatic origins of 3-nitrotyrosine in normal joint tissue

4.1 Introduction

Identification of the biological role of a phenomenon requires the selective modification of the phenomenon and the study of the consequence this has *in vitro* and *in vivo*. In the absence of specific inhibitors of tyrosine nitration or methods to selectively denitrate tyrosine, one approach is to examine the origins of the nitrating species that yield 3-NT.

While it is recognised that $ONOO^-$ is not the only pathway to tyrosine nitration in proteins (see section 1.1.4.1), it is generally accepted that RNS more reactive than NO are necessary to yield 3-NT (Halliwell B, 1997). With very few exceptions (Zweier JL, *et al.*, 1995), the formation of more reactive nitrogen species will require prior enzymatic NO release. There are three isoenzymes of nitric oxide synthase (NOS) that catalyze the oxygen-dependent conversion of *L*-arginine to NO and *L*-citrulline (Förstermann U, *et al.*, 1994). The two calcium-dependent forms are predominantly constitutively expressed on endothelial and neuronal tissue, termed endothelial NOS (eNOS, a.k.a. NOS III) and neuronal NOS (nNOS; a.k.a. NOS I), whereas practically all cell types express a calcium-independent inducible NOS (iNOS, a.k.a. NOS II) upon pro-inflammatory stimulation.

Recently, it was demonstrated that xanthine oxidoreductase (XOR), an ubiquitous enzyme best known for its house-keeping role in purine metabolism, can reduce nitrite to NO under hypoxic (Li H, *et al.*, 2001; Millar TM, *et al.*, 1998) and normoxic (Godber BJL, *et al.*, 2000) conditions *in vitro*. XOR exists in two interconvertible forms: xanthine dehydrogenase (XDH) and xanthine oxidase (XO) (Stirpe F and Della Corte E, 1969), that differ in their substrate specificity. Both will oxidise hypoxanthine to xanthine and xanthine to uric acid as part of purine metabolism. However, XO will only reduce O_2 [1], whereas XDH will reduce O_2 and NAD^+, but with greater affinity for the latter [2] (Waud WR and Rajagopalan KV,

1976). XOR activity to convert xanthine to uric acid has been demonstrated in rheumatoid synovium by radio-isotope assay (Allen RE, *et al.*, 1987). Immunohistochemistry localised XOR protein mainly to endothelial cells in rheumatoid synovium (Stevens CR, *et al.*, 1991a) while XOR protein levels and activity have not been assessed in healthy mammalian joint tissue.

By using animal systems that are selectively deficient for each of these NO-generating enzymes, one might achieve abolition of 3-NT in synovial vessels and hyaline articular cartilage. This will depend on the absence of redundancy between these enzymes, but, if successful, would allow the investigation of how such a system would behave during health and experimental arthritis.

Specific deficiency in whole organisms for individual arginine-dependent NOS enzymes is available in the form of mice carrying targeted gene deletions for the enzymes. At the time of this work no such 'gene knock-out' models were available for XOR. There is, however, a model using dietary tungsten-loading of rats which inhibits XOR enzyme activity by substituting active-centre molybdenum (Johnson JL, *et al.*, 1974). Preliminary work in our group had shown that in tungsten-loaded adult Wistar rats suppression of XOR activity can be achieved within 2 weeks, as measured by the pterin assay in plasma and liver samples (T.Millar; unpublished data). Since my work (see section 3.4.3) had shown that 3-NT in synovial vessels and cartilage is present as early as ten days of age, tungsten-supplementation of chow had to begin in pregnant rats and be continued in the offspring. This has been used successfully in rodents previously (Pitt RM, *et al.*, 1991).

4.2 Aims and objectives

- To determine the enzymatic source responsible for 3-NT formation in synovial vessels and hyaline articular cartilage in small rodents

4.3 Methods

Details of materials and step-by-step protocols on general procedures can be found in the appendices. All concentrations are final, unless stated otherwise.

4.3.1 Animal models

4.3.1.1 Gene knock-out mice for NOS enzymes

The species, source and age of mice, carrying targeted gene deletions, and their controls are summarized in ***Table 4.3.1.1***.

Table 4.3.1.1: **Characteristics of NOS 'knock-out' mice used.**

Deficient NOS	*nNOS*	*iNOS*	*eNOS*
Mouse Strain	B6;129S-*Nos1*^{tm1Plh}	129xMF1 (iNOS -/-)	SV129/C57BL/6 (eNOS -/-)
Reference	(Huang FP, et al., 1993)	(Wei XQ, et al., 1995)	(Huang PL, et al., 1995)
Control	B6129SF2	129	SV129/C57BL/6
Source	The Jackson Laboratory, Maine, USA	B&K Universal Ltd, Hull, UK	Prof J Polak, Dept of Histopathology, Hammersmith Hospital, London
Age (weeks)	6	6	6
Sex	male	male	male
Mode of Killing	Exsanguination under isofluorane/ O_2 anaesthesia	Cervical dislocation	Perfusion fixation under pentobarbitone anaesthesia

Animal tissue was fixed in formal saline, processed and embedded in paraffin as previously described.

4.3.1.2 XOR inactivation by dietary tungsten-loading

Pregnant female outbred Wistar rats (Bath strain; Charles River, UK), kept under standard laboratory conditions, were fed on chow enriched with sodium tungstate (0.7 g/ kg chow; Harlan-Teklad, Oxford, UK) (*n=3*) or continued on standard chow (*n=3*) from 10 days prior term. One tungsten-fed animal did not deliver and was found not to have been pregnant at *post mortem* examination. After weaning, the offspring were continued on their respective diets. From age 21 days three animals of each litter were weighed once weekly.

Animals (*n=3*; each group, where possible one from each litter) were sacrificed at 0, 7, 14, 21, 35 and 56 days of age. This was done by cervical dislocation up to 21 days (inclusively) and by CO_2- overdose thereafter. Apart from knee joint tissue for formal saline fixation and paraffin embedding (see 3.3.3), blood and liver were harvested from each animal. Blood was added to tri-sodium citrate (8mg/ml), gently mixed and centrifuged (4 minutes at 5000 rpm, Biofuge Fresco, Heraeus Instruments, Germany) to retrieve plasma. Liver was snap-frozen in liquid nitrogen. Plasma and liver samples were then stored at -70 °C until further processing.

4.3.2 Histology and microscopy

The histological methods for histopathological analysis and for immuno-localisation of 3-NT have been described previously (see section 3.3.3).

The sections of one representative assay of at least two IHC assays per species or intervention group were coded and scored according to the following rule:

The total number of synovial vessels, defined as having a lumen with endothelium and/or intra-luminal blood cells, in the whole section was expressed as: 0, nil; +, < 5 vessels; + +, 5-15 vessels; + + +, 16 – 50 vessels; + + + +, > 50 vessels. This was done to take into account the variability of number of vessels seen per section.

The sections were then judged according to the proportion of synovial vessels showing unequivocal staining for 3-NT in the vascular smooth muscle layer: 0, no

vessels; +, few vessels (*i.e.* <25 %); ++, moderate number of vessels (*i.e.* 25 – 75%); and + + +, most vessels (*i.e.* >75%) stained.

Cartilage, if present, was scored for the proportion of chondrocytes showing 3-NT immunoreactivity: 0, nil; +, few (*i.e.* < 25%); + +, moderate numbers (*i.e.* 25 - 75%); and + + +, most chondrocytes (*i.e.* >75%).

Intra-observer agreement of these semiquantitative scores were calculated as kappa (κ) (Altman DG, 1991), based on 13 mouse knee joint sections, scored four weeks apart. The level of intra-observer agreement was fair for the number of synovial vessels seen (κ = 0.39), moderate for the proportion of 3-NT-positive synovial vessels (κ = 0.44) and good for the proportion of 3-NT-positive chondrocytes (κ = 0.76) (see also section 3.3.3.7).

4.3.3 XOR activity assay

To determine XOR activity, the spectro-fluorimetric method described by Beckman et al (Beckman JS, *et al.*, 1989) was used. It is based on the detection of fluorescent isoxanthopterin (IXPt), which originates from the oxidation of pterin (2-amino-4-hydroxypteridine), a reaction is catalysed by XO. If methylene blue is added to the reaction as a final electron acceptor, total XOR actvity (*i.e.* XO plus XDH) can be determined. The addition of the XOR-inhibitor allopurinol confirms the enzymatic specificity of the reaction. Comparison with a standard of known IXPt concentration and knowledge of the tissue protein content then allows calculation of the enzyme activity per protein weight of the sample.

The details of method are described in ***Appendix IV***.

In brief, the addition of pterin to a sample in the spectro-fluorimeter containing XOR activity will produce a linear rise in fluorescence over time, due to the production of IXPt. Methylene blue, when added to this reaction, will replace NAD^+ as an electron acceptor and therefore any *increase* of the rate of fluorescence production will reflect the contribution of XDH to pterin oxidation. Allopurinol will stop any further fluorescence, thus confirming that fluorescence production is due to XOR. Finally IXPt of a known concentration is added which will serve as a reference standard to allow the calculation of XOR activity in the sample, as follows:

$$U = \{ dF \text{ x } [IXPt] / F_{IXPt} \} \text{ x } 0.001 \text{ x } V_c / (V_s \text{ x } T) ,$$

where U is the enzyme activity in µmol min^{-1} g^{-1} tissue protein, dF is the change of fluorescence units per minute, $[IXPt]$ is the final assay concentration of IXPt, F_{IXPt} is the increase of fluorescence units produced by the addition of IXPt, V_c is total assay volume in the cuvette in ml, V_s is the sample volume added to the cuvette in ml, and T is the tissue protein content per ml sample (as determined by the protein assay according to Bradford (Bradford MM, 1976)). Samples were measured in triplicate, unless otherwise stated. Inter- and intra-assay coefficients of variation were < 10% and < 5%, respectively.

This method is more sensitive than the previously used spectro-photometric method and can detect activities of as little as 0.1 pmol min^{-1} ml^{-1} cuvette volume. However, the sensitivity of the assay is diminished by increased haemoglobin concentrations. Moreover, peroxidases in samples (*e.g.* from inflamed tissue) may cause pterin oxidation, leading to overestimation of XOR activity (Beckman JS, *et al.*, 1989).

4.3.4 3-NT measurements by GC/MS

The measurement of 3-NT in joint tissues was done by gas chromatography - mass spectrometry (GC/ MS) as described earlier (see section 3.3.4).

4.4 Results

4.4.1 *3-NT is expressed in synovium and cartilage from NOS I, II and III knock-out mice*

Mice, carrying a targeted gene deletion for NOS I, II or III, showed 3-NT immunoreactivity (3-NT-IR) in synovial vessels and articular hyaline cartilage cells, which was no different from control tissues. The findings are summarized in ***Tables 4.4.1a*** for synovium. As in the previous experiments 3-NT-IR localised to the vascular smooth muscle layer of synovial vessels (***Fig. 4.4.1a***).

***Table 4.4.1a*: 3-NT immunohistochemistry in knee synovium from NOS-deficient mice and controls.**

Mouse Strain	*Animals / Knees (n)*	*Synovial Vessels median (range)*	*3-NT-positive Vessels median (range)*
nNOS -/-	5/5	+ + (+ - + + +)	+ + + (+ - + + +)
Control (nNOS)	5/5	+ (0 - + +)	+ + + (+ + +)
iNOS -/-	2/4	+/+ + (0 - + +)	+ + (+ - + + +)
Control (iNOS)	3/6	+ + (+ - + +)	+/++ (+ - + + +)
eNOS -/-	3/6	+/++ (0 - + + +)	+ +/+ + + (+ + - + + +)
Control (eNOS)	2/4	+ + (+ - + +)	+/+ + (+ - + + +)

Shown is the data of an immunohistochemical stain for 3-NT in each species (or intervention group). All sections were coded and scored as follows: the total number of synovial blood vessels, defined as having a lumen with endothelium and/or intra-luminal blood cells, seen in the whole section was expressed as: 0, nil; +, < 5 vessels; + +, 5-15 vessels; + + +, 16 - 50 vessels; + + + +, > 50 vessels. All synovial vessels per section were then judged according to the number showing unequivocal staining for 3-NT in the vascular smooth muscle layer: 0, no vessels; +, few vessels (*i.e.* <25%); + +, moderate number of vessels (*i.e.* 25 - 75%); and + + +, most vessels (*i.e.* >75%) stained.

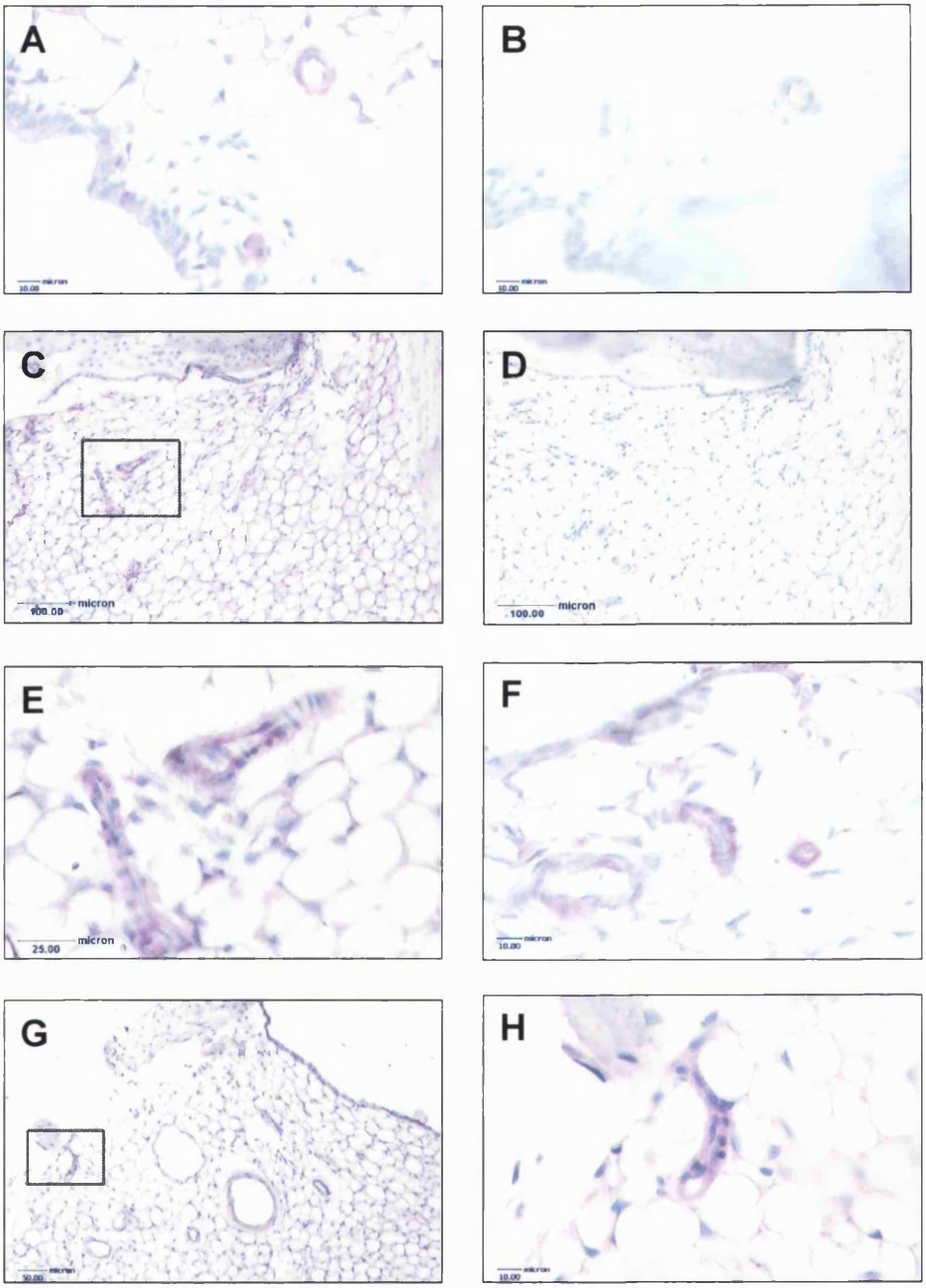

Fig. 4.4.1a: Immunohistochemical stain for 3-NT in normal knee joint tissue from mice deficient in specific NOS genes and controls, respectively. The photomicrographs show representative examples of 3-NT immunoreactivity (shown as red) in synovial vessels from the following species: **A**, nNOS -/- mouse, showing 3-NT-IR in the vascular smooth muscle layer of a synovial blood vessel; **B**, serial control section to image A using normal rabbit immunoglobulin; **C**, iNOS -/- mouse (low-power view); **D**, corresponding omission control to image C; **E**, high-power view of outlined area in image C; **F**, similar 3-NT-IR in synovial vessels of normal SV129 mouse, *i.e.* the control strain for iNOS -/-; **G**, eNOS -/- (low-power view); **H**, high-power view of outlined area in image G, showing distinct 3-NT-IR in the vascular smooth muscle layer.

No obvious macroscopic or microscopic pathology of joints or skin, liver, heart, gut, kidney or spleen was seen in any of the species. The relatively small number of synovial vessels was largely due to difficult sectioning of the non-decalcified samples.

The findings in hyaline knee joint cartilage are shown in ***Table 4.4.1b*** and ***Fig. 4.4.1b***.

Table 4.4.1b: **3-NT immuno-localisation in knee hyaline cartilage from NOS-deficient mice and controls.**

Mouse strain	*Animals/Knees (n)*	*3-NT Staining in Chondrocytes*	
		median	*range*
nNOS -/-	**5/5**	+ + +	+ + - + + +
Control (nNOS)	**5/5**	+ + +	+ + - + + +
iNOS -/-	**2/4**	+ + - + + +	+ - + + +
Control (iNOS)	**3/6**	+ + +	+ - + + +
eNOS -/-	**3/5 ***	+ + +	+ + - + + +
Control (eNOS)	**2/4**	+ + - + + +	+ + - + + +

Shown is the data of immunohistochemical stains for 3-NT in each species (or intervention group). All sections were coded and scored as follows: 0, nil; +, few (*i.e.* <25%); + +, moderate numbers (*i.e.* 25 - 75%); and + + +, most chondrocytes (*i.e.* >75%)of the whole section showing immunoreactivity for 3-NT. * one knee specimen yielded no hyaline cartilage suitable for evaluation.

While the intensity of 3-NT staining for individual chondrocytes was weaker than in rat or calf hyaline cartilage, on average the majority of chondrocytes stained positive for 3-NT.

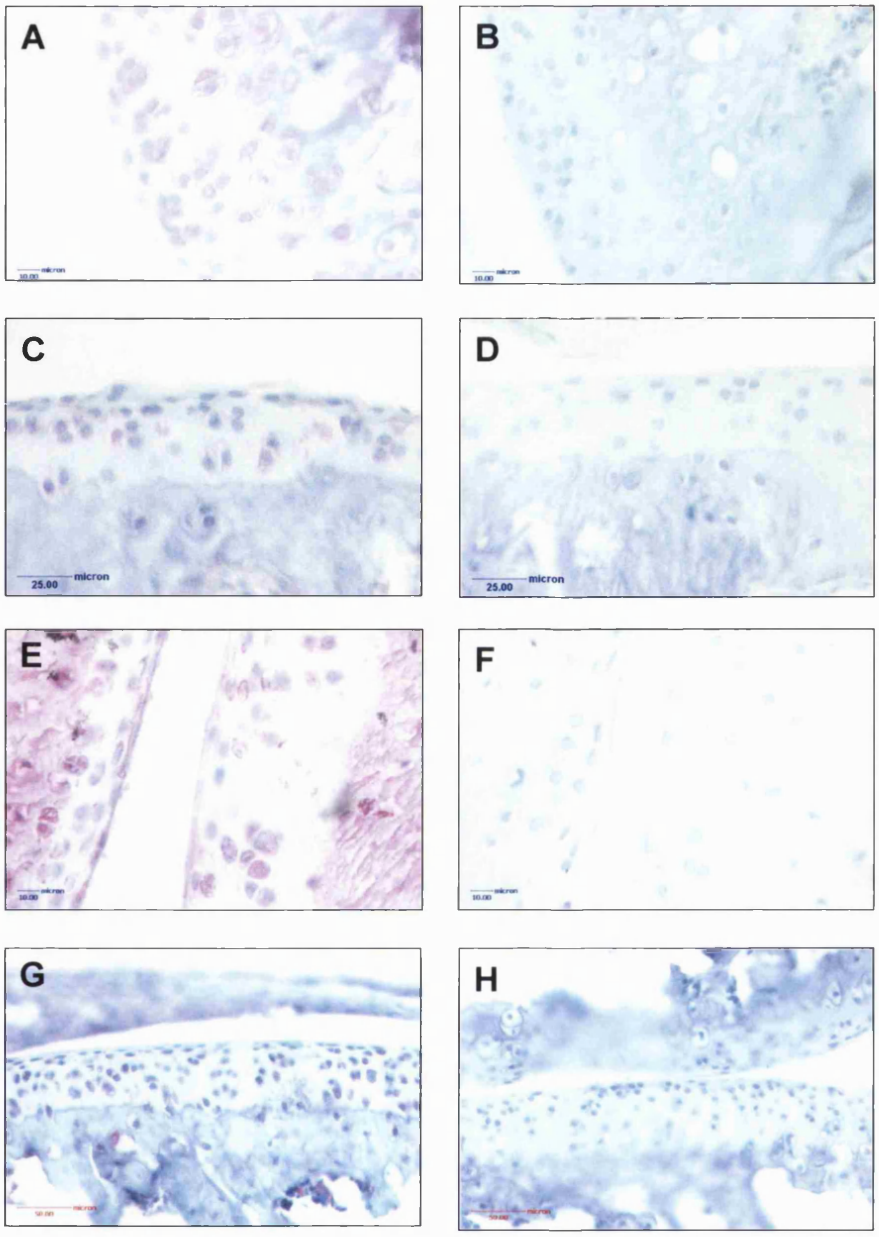

Fig. 4.4.1b: Immunohistochemical stain for 3-NT in normal knee joint tissue from mice deficient of specific NOS genes and controls, respectively (see Table 4.3.1.1 for details of strains and animals). The photomicrographs show representative examples of 3-NT immunoreactivity (shown as red) in hyaline cartilage chondrocytes sections from the following species: **A**, nNOS -/- mouse showing 3-NT-IR in the majority of chondrocytes; **B**, serial control section to image A using normal rabbit immunoglobulin; **C**, iNOS -/- mouse; **D**, corresponding omission control to image C; **E**, Normal SV129, *i.e.* the control strain for iNOS -/-; **F**, corresponding omission control to image E; **G**, eNOS -/-; **H**, serial control section to image G using normal rabbit immunoglobulin.

4.4.2 *Progeny of tungsten-fed rats thrive and have suppressed XOR activity in plasma and liver*

The offspring of rats, which had been fed on a tungsten-supplemented chow from 10 days *pre term* and then maintained on this chow after weaning, thrived as well as the control animals on standard chow. ***Fig. 4.4.2a*** shows the increase of animal weight in time. There was no significant difference between the two diet groups ($p = 0.33$ for difference of mean weight at day 56; Mann-Whitney test).

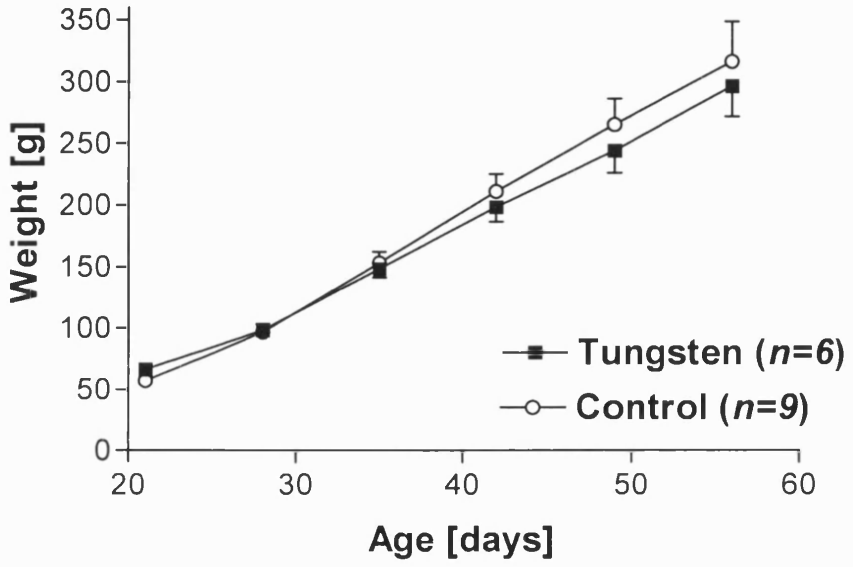

Fig. 4.4.2a: Mean animal weight for tungsten- and control-fed experimental groups over time. Bars represent SEM.

In the tungsten-fed group XOR activity of plasma and liver was suppressed to ≤ 3.0 % (median 0.5%) and ≤ 2.5 % (median 1.9 %), respectively, of the activity in the standard-fed group up to the age of 56 days (***Figures 4.4.2b and 4.4.2c***).

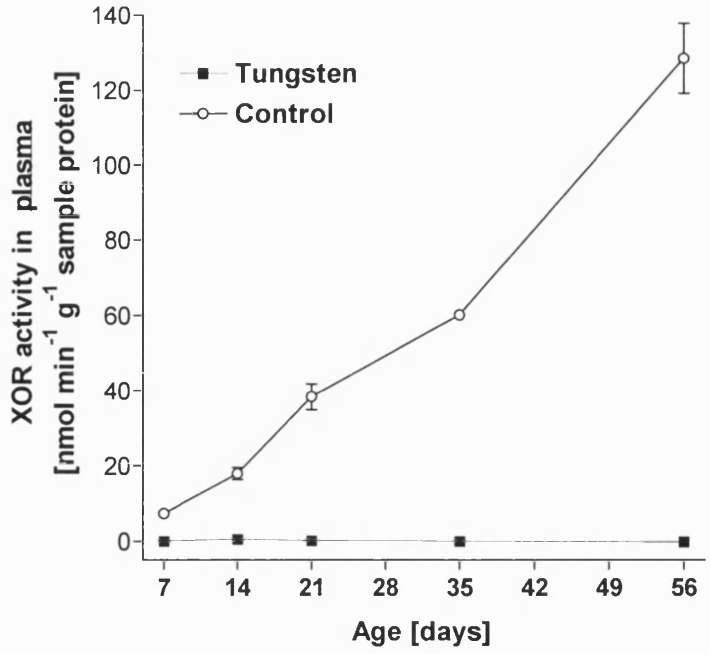

Fig. 4.4.2b: Mean XOR activity, as measured by the pterin assay, in plasma of tungsten- and control-fed Wistar rats (*n=3* for each time point). Bars represent SEM.

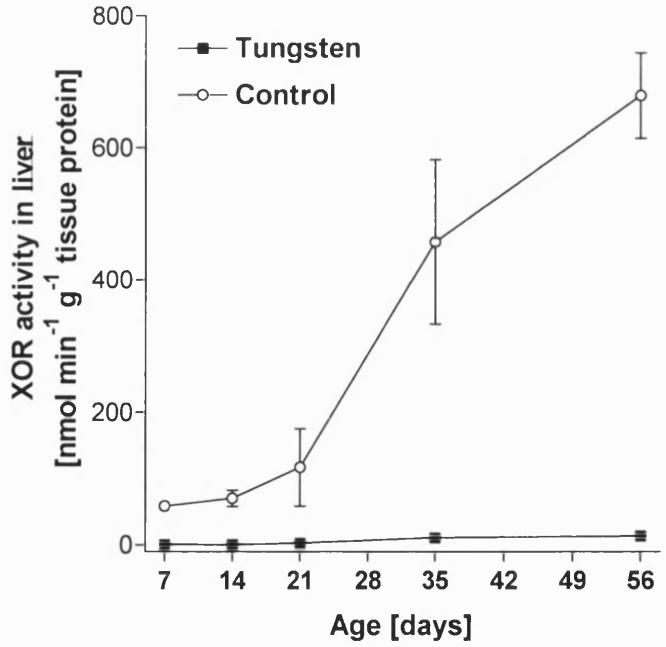

Fig. 4.4.2c: Mean XOR activity, as measured by the pterin assay, in liver homogenates of tungsten- and control-fed Wistar rats (*n=3* for each time point). Bars represent SEM.

4.4.3 *XOR inactivation by dietary tungsten does not alter 3-NT levels in rat joint tissue*

Similar to the observation in NOS gene 'knock-out' mice, the immunohistochemistry for 3-NT in Wistar rat joint tissue did not appear in any way reduced by dietary tungsten-supplementation (***Table and Fig. 4.4.3a***). For semi-quantitative scoring of 3-NT in synovium and articular cartilage, tissue from 35 and 56 day old animals was used.

***Table 4.4.3a*: 3-NT immunohistochemistry in knee joints from tungsten- and control-fed Wistar rats.**

Diet	*Animals/ Knees (n)*	*Synovial Vessels median (range)*	*3-NT +ve Vessels median (range)*	*3-NT +ve Chondrocytes median (range)*
Tungsten	5/5	+ + + (+ + +)	+ + + (+ + +)	+ + + (+ + +)
Control	5/5	+ + + (+ + - + + +)	+ + + (+ + - + + +)	+ + + (+ + +)

Shown are the semi-quantitative scores for synovial vessel number (0 - + + + +) and proportion of 3-NT-positive vessels or chondrocytes (0 - + + +) of coded sections of one representative IHC stain for 3-NT. Animals were 35 and 56 days of age. See section 4.3.2 for further details on the definition of the scores

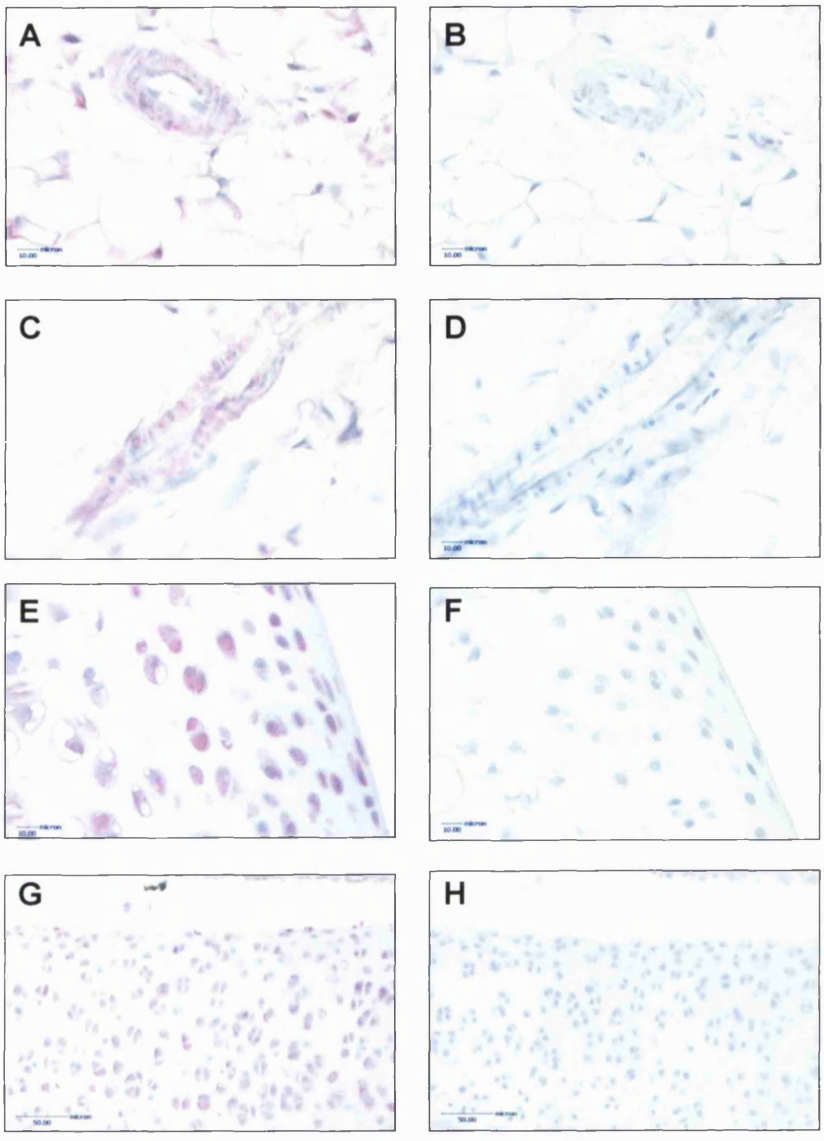

Fig. 4.4.3a: Immunohistochemical stain for 3-NT on knee joint tissue from 35- and 56-day old Wistar rats, deficient of XOR activity due to dietary tungsten treatment, compared with tissues from standard-fed rats. The photomicrographs show representative examples of 3-NT immunoreactivity (shown as red) in synovial blood vessels and hyaline cartilage chondrocytes. **A**, synovial vessel of a tungsten-treated rat, displaying 3-NT in the vascular smooth muscle layer of a synovial vessel; **B**, serial section to that in image A, using normal rabbit immunoglobulin (rIG) as negative control; **C**, synovial vessel of a standard-fed rat; **D**, corresponding section to that in image C, using rIG; **E**, hyaline cartilage of a tungsten-treated rat, showing marked 3-NT in chondrocytes; **F**, serial section to that shown in image E, using rIG; **G**, hyaline cartilage of a standard-fed rat; **H**, negative omission control of a corresponding section to that in image G.

The quantitative analysis of protein-bound 3-NT by GC/MS (***Figure 4.4.3b***) was consistent with the immunohistochemical findings. There was no significant difference of medians between tungsten- and control-fed animals for synovium, patella or liver tissue homogenates ($p>0.05$; Kruskal-Wallis test with Dunn's *post test*). The different sample sizes were a result of limited single assay capacity of GC/MS.

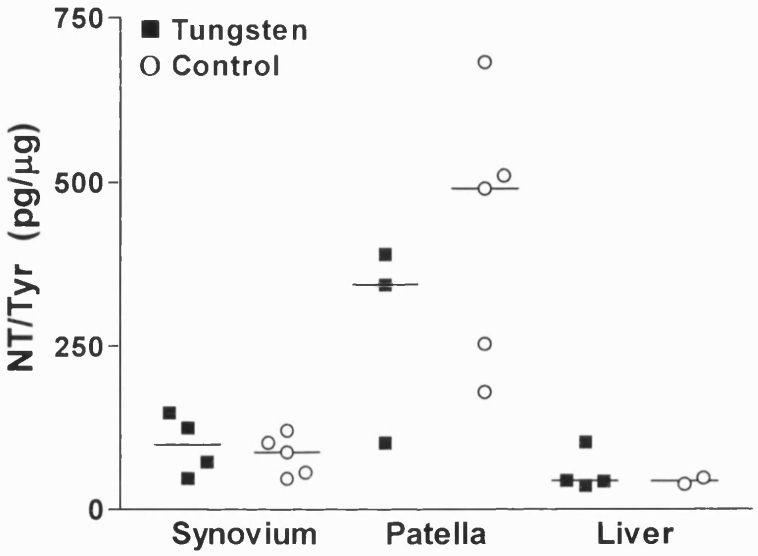

Fig. 4.4.3b: NT/ Tyrosine ratios of tissue homogenates from Wistar rats (*n=5*), fed on either tungsten-supplemented (■) or standard (○) chow. Values represent single measurements of samples by GC/MS and bars represent medians.

4.5 Discussion

Using rodent models, deficient in the NO-generating enzymes nNOS, iNOS, eNOS and XOR, these studies showed that the immunohistochemical presence of 3-NT in synovial vessels and articular hyaline cartilage appeared undiminished compared to corresponding normal control tissues. Since NO can be expected to be an essential precursor to tyrosine nitration (Halliwell B, 1997), these results would imply that more than one mechanism is involved in physiological protein nitration or that inhibition of the responsible NO-generating enzyme can be fully compensated for by increased activity or expression of other enzymes. This suggests further that nitration of tyrosine residues may be an important physiological phenomenon.

Vascular smooth muscle cells (VSMC) are known to express nNOS (Boulanger CM, *et al.*, 1998) and XOR (Hellsten-Westing Y, 1993) and, in response to pro-inflammatory stimuli, iNOS (Nathan C and Xie QW, 1994). eNOS is expressed in the vascular endothelium and in smooth muscle cells of the corpus cavernosum (Boulanger CM, *et al.*, 1998). However, while endothelial eNOS causes VSMC relaxation, there is no evidence of eNOS expression in VSMC. In articular cartilage chondrocytes, gene expression of iNOS (Maier R, *et al.*, 1994) and also nNOS activity (Amin R, *et al.*, 1995) have been demonstrated, but only in an inflammatory setting. There is to date no evidence to show expression of eNOS or XOR by articular cartilage.
Compensatory increased activity for a missing NOS enzyme has been described. For instance, eNOS and nNOS who both cause vasodilatation in meningeal arteries, will each compensate for each other (Meng W, *et al.*, 1996). Such redundancy is thought to be common in biological systems, and could explain the findings of the present study.

There are several important limitations to these studies. The immunohistochemical method to demonstrate 3-NT will not allow the detection of *partial* reduction in 3-NT expression in the selectively NO-deficient rodent species. Due to restriction of resources, it was only possible to assess 3-NT quantitatively in one of the animal models. The XOR-deficient model was chosen, because of the potentially sub-total

degree of pharmacological inhibition of this NO-generating system in comparison to the NOS-gene knock-out models. Although not all samples of XOR-deficient and control rats could be analysed (due to maximally feasible assay sample size), specific nitrotyrosine content was not different in patella and knee synovium homogenates of tungsten-reared animals and controls.

The absence of NOS activity in the 'knock-out' animals was not confirmed. It is therefore possible that residual NOS iso-enzyme expression, *e.g.* by splice variants that have been described for nNOS (Huber A, *et al.*, 1998), may have masked the correct enzymatic source of NO for tyrosine nitration. Since this work was completed we also became aware that the iNOS 'knock-out' species used in this work may continue to express up to 10% of active iNOS protein [F.Y.Liew, Glasgow; personal communication].

If compensatory NOS expression exists, increased protein expression of an alternative NOS could be indirect evidence for the inhibited/deleted enzyme as source of NO. It was therefore attempted to look for increased iNOS protein staining in joint tissue from tungsten-fed rats, compared to normal controls. Rabbit polyclonal anti-mouse iNOS antibody (BD Transduction Laboratories, UK) was used in a standard immunohistochemical stain following enzymatic antigen retrieval by incubation with pronase E (according to (Veihelmann A, *et al.*, 2002)) on paraffin-embedded sections from 56 days-old tungsten- and control-treated rats. However, staining was sparse and weak in synovium and chondrocytes even in the positive technical control tissue (carrageenan-induced acute rat knee arthritis). There were no discernible differences between the two diet groups to allow any conclusions from this work.

This study has provided interesting observations on the expression of 3-NT in joint tissues and its relationship to NOS and XOR enzyme expression/activity. However, a single enzymatic source for 3-NT formation in joint tissue was not identified. In the absence of specific methods to modulate 3-NT (*e.g.* enzyme inhibition, selective de-nitration) the progression of this line of investigation was terminated.

Chapter 5: Xanthine oxidoreductase activity in normal rat joints

5.1 Introduction

The previous chapter provided evidence that 3-NT formation in normal joints is not due to XOR activity alone. However, this does not mean that XOR is not capable of nitrating proteins in joints.

A number of observations would suggest that XOR remains a strong candidate enzyme as a '3-NT generator' in joints. Firstly, it has been shown *in vitro* that XOR does not only produce $O_2^{\bullet-}$ during xanthine metabolism, but also NO from nitrite/nitrate under condition of hypoxia , using either NADH or xanthine as electron donors (Godber BJL, *et al.*, 2000; Li H, *et al.*, 2001; Millar TM, *et al.*, 1998; Zhang Z, *et al.*, 1998). Using SOD as a $O_2^{\bullet-}$ scavenger, XOR-mediated nitrite reduction to $NO^{\bullet}$ has been demonstrated under normoxia *in vivo* (Godber BJL, *et al.*, 2000). This suggests that, under normoxia, nascent NO is 'mopped up' by simultaneously generated $O_2^{\bullet-}$. The most likely product from a reaction of $O_2^{\bullet-}$ and NO would be $ONOO^-$ (Kissner R, *et al.*, 1998; Pryor WA and Squadrito GL, 1995) which can lead to nitration of tyrosine residues under physiological conditions (Ischiropoulos H, 1998). However, while there is evidence that XOR activity in breast milk may be an important anti-bacterial agent as a peroxynitrite synthase in the neonatal gut (Stevens CR, *et al.*, 2000), the production of NO or other RNS by XOR has not yet been proven to occur *in vivo*. Secondly, XOR immunocalisation has been described in human synovium vessels. XOR activity to convert xanthine to uric acid has been demonstrated in rheumatoid synovium by radio-isotope assay (Allen RE, *et al.*, 1987). By immunohistochemistry XOR protein localized predominantly to the endothelial cells in both rheumatoid and normal human synovium (Stevens CR, *et al.*, 1991a). A literature survey did not reveal any reports of XOR expression by articular hyaline chondrocytes.

It remains unclear to what extent XOR protein and activity is expressed in *normal* mammalian joint tissue. Furthermore it is not known whether XOR contributes NO as well as superoxide radicals (Allen RE, *et al.*, 1989) during synovial inflammation.

In order to further investigate the potential role of XOR in 3-NT formation, it was important to characterize the distribution of XOR activity in normal joint tissue. If XOR activity could be demonstrated in joint tissues where immunolocalisation of 3-NT had been found, then XOR would remain a potential candidate for 3-NT formation in joints.

5.2 Aims and objectives

- To look for the presence and distribution of XOR activity by allopurinol-suppressible oxidative activity in homogenates and fresh unfixed frozen section from rat joints.

5.3 Materials and methods

5.3.1 XOR activity assay

XOR activity in rat joint tissue homogenates was determined by the spectro-fluorimetric method (Beckman JS, *et al.*, 1989), described in Section 4.3.3 and ***Appendix IV***. This yielded enzyme activity for XO and XO + XDH as nmol min^{-1} g^{-1} tissue protein, with protein concentrations in samples measured according to Bradford *et al* (Bradford MM, 1976) (see ***Appendix II***).

Three healthy male Wistar rats, aged 4-6 weeks (ca. 250 g), were sacrificed by CO_2 overdose. The following tissues were sampled (in buffer containing proteinase inhibitors) by dissection from each animal: liver, knee synovium, patellar bone, patellar cartilage and quadriceps muscle. Each sample was measured for XOR activity in triplicate.

5.3.2 XOR histochemistry

The localisation *in situ* of XOR activity in rat joint tissue was based on the XOR-mediated reduction of tetra nitro blue tetrazolium (TNBT) to form a dark formazan dye in unfixed cryo-stat sections (Kooij A, et al., 1991). This histochemical assay demonstrates both the oxidase (XO) and dehydrogenase (XDH) activity of XOR. It uses polyvinyl alcohol (PVA) as a tissue protectant and methoxyphenazine methosulfate (MPMS) as an electron carrier. The principles of the method as employed for this study are described here. A detailed protocol, listing all concentrations, can be found in ***Appendix V***.

Wistar rats, aged 4-6 weeks, were continued on standard chow (*n=3*) or fed a diet, supplemented with sodium tungstate (0.7 g/ kg chow; Harlan-Teklad, Oxford, UK) (*n=3*) for six weeks before euthanasia by CO_2 overdose. Patella with adjacent synovium and liver was dissected immediately and cryo-embedded in on cork as described earlier (see section 3.3.3.1.3). 8 μm serial sections were cut using a cryostat, mounted on glass slides and used without fixation. All sections were covered with an incubation medium of 5 mM TNBT and 0.45 mM MPMS in phosphate-buffered 18% PVA plus 0.5 mM hypoxanthine as the reducing substrate.

For each specimen, the following controls were employed: omission of hypoxanthine to determine background staining; addition of the specific XOR inhibitor allopurinol (1 mM) to confirm enzymatic specificity of staining; and addition of 10 mM sodium azide to inhibit mitochondrial cytochromes as a source of $O_2^{\bullet-}$ that could interfere with TNBT reduction (Halliwell B and Gutteridge JMC, 1999). The liver sections, known for their rich XOR activity, served as positive technical controls. After incubation for 30 min at 37°C the viscous incubation medium was washed off in 60 °C, pH 5.3-buffered 0.1 M sodium phosphate and sections rinsed briefly with acetone to fix the sections and remove free monoformazans. The sections were then mounted in glycerol jelly and protected from excessive light exposure until microscopical analysis.

Sections were examined qualitatively and descriptively for the localisation of dark purple staining of reduced TNBT that could be suppressed by allopurinol, to indicate XOR activity *in situ*. Experiments included in the evaluation were repeated three times.

5.4 Results

5.4.1 *XOR activity in normal patellar bone, cartilage and synovium is high, compared to muscle*

Patellar bone of normal joints showed enzyme activities for XO and total XOR (*i.e.* XO plus XDH) of the same magnitude as liver (***Fig. 5.4.1***). Mean enzyme activities were about 20-fold that of quadriceps muscle ($p < 0.001$; ANOVA, Bonferroni's *post*-test). Mean XOR activity of cartilage and synovium was between that of liver and smooth muscle, but, probably due to the high standard error, not significantly different from the low activity of muscle.

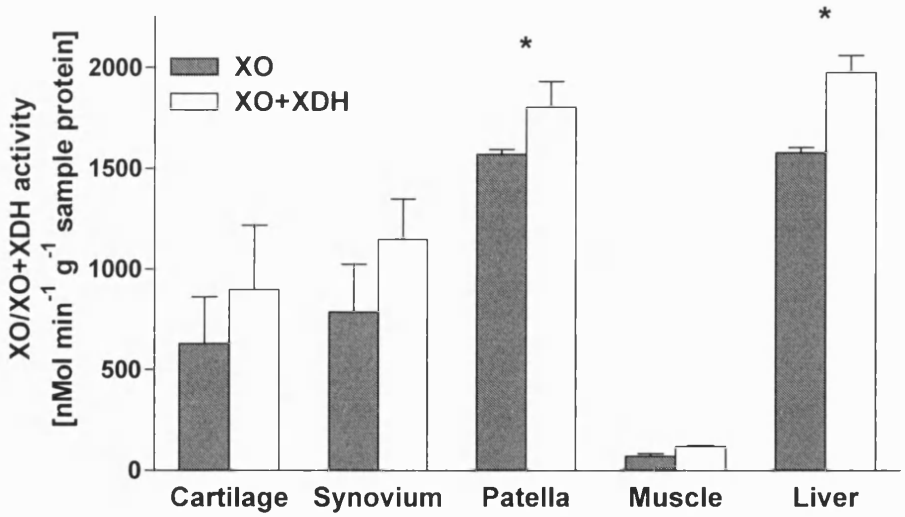

Fig. 5.4.1: Mean activity of XO (*dark columns*) and combined XO + XDH (*light columns*) in tissue homogenates of normal, male, 4- 6 week old Wistar rats (*n=3*), as measured by the pterin assay, in liver homogenates of tungsten- and control-fed Wistar rats (*n=3* for each time point). Bars represent SEM. * $p < 0.001$ for difference to muscle, $p < 0.05$ for difference to cartilage and synovium (ANOVA, Bonferroni's *post*-test).

5.4.2 *Normal hyaline chondrocytes display XOR activity in situ, suppressible by dietary tungsten*

XOR activity in liver (positive control)

Fig. 5.4.2a shows representative photomicrographs of histochemical staining for XOR activity in liver from standard-fed rats.

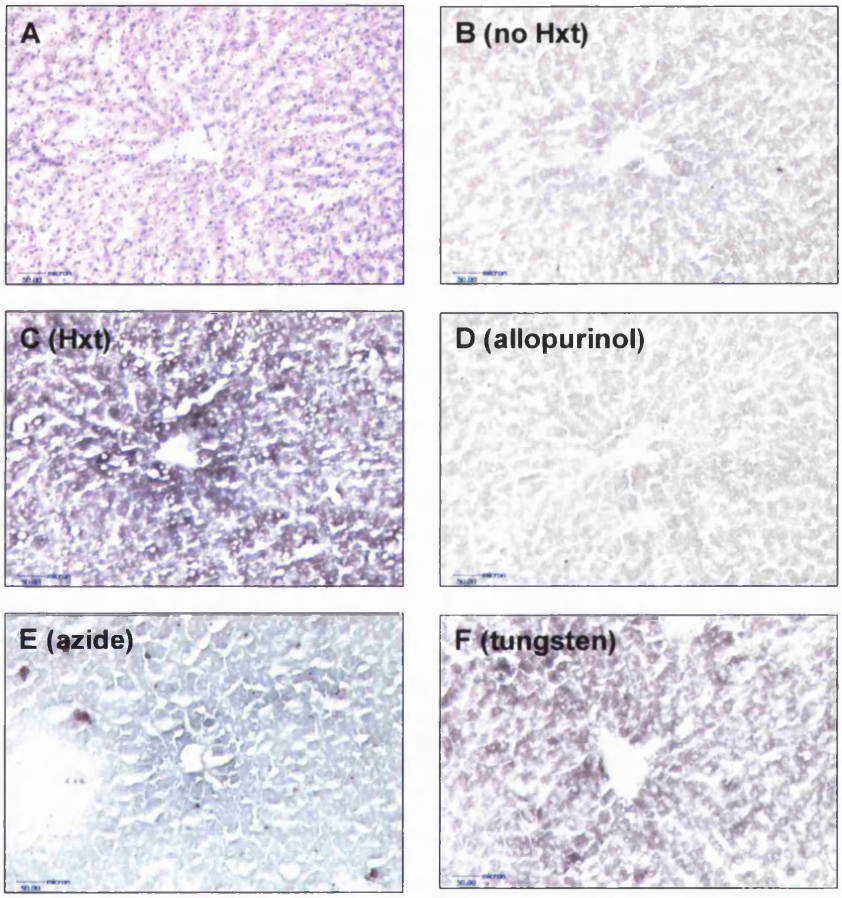

Fig. 5.4.2a: Histochemical staining for XOR activity shown as a TNBT reduction product (*dark purple*) on corresponding, unfixed cryosections of liver from Wistar rats (*n=3*). Photomicrographs are representative of three separate experiments. Bars represent 50 μm. **A**, H&E stain of a liver lobule; **B**, weak staining in the absence of hypoxanthine (Hxt) as substrate; **C**, marked staining in the presence of 0.5 mM Hxt, especially around the central vein; **D**, conditions as in image C with added 1 mM allopurinol showing suppressed XOR activity; **E**, conditions as in image C with added 10 mM sodium azide, showing partial suppression of XOR activity; **F**, partial suppression of XOR activity in liver from a tungsten-fed rat, in the presence of Hxt.

In the presence of hypoxanthine as substrate there was marked staining by reduced TNBT, especially around the central lobular vein (***image C***). Additon of 10 mM allopurinol diminished XOR activity to less than that seen in the absence of hypoxanthine as a substrate (***image D and B***), confirming that a substantial amount of staining reflects XOR activity. The inhibition of mitochondrial cytochrome enzymes by addition of 10 mM azide resulted in partial loss of staining (***image E***). Liver sections from rats, fed on tungsten-supplemented diet for six weeks, showed partial loss of XOR activity (***image F***), but the effect appeared less than of allopurinol.

XOR activity in hyaline cartilage

Rat patellar cartilage sections were stained in the same assay as liver sections. ***Figure 5.4.2 b*** shows representative photomicrographs of one of three experiments. In the presence of 0.5 mM hypoxanthine, the majority of chondrocytes showed marked XOR activity (***image C***). Staining was particular intense in the superficial cartilage layers and appeared as intense as in hepatocytes (see Figure 5.4.2 a). Staining was similar in both central cartilage and cartilage near synovium. In slight contrast to staining in liver sections, allopurinol and azide produced similar partial reduction in staining (***image D and E***), whereas cartilage from tungsten-fed animals achieved the best suppression of XOR activity (***image F***).

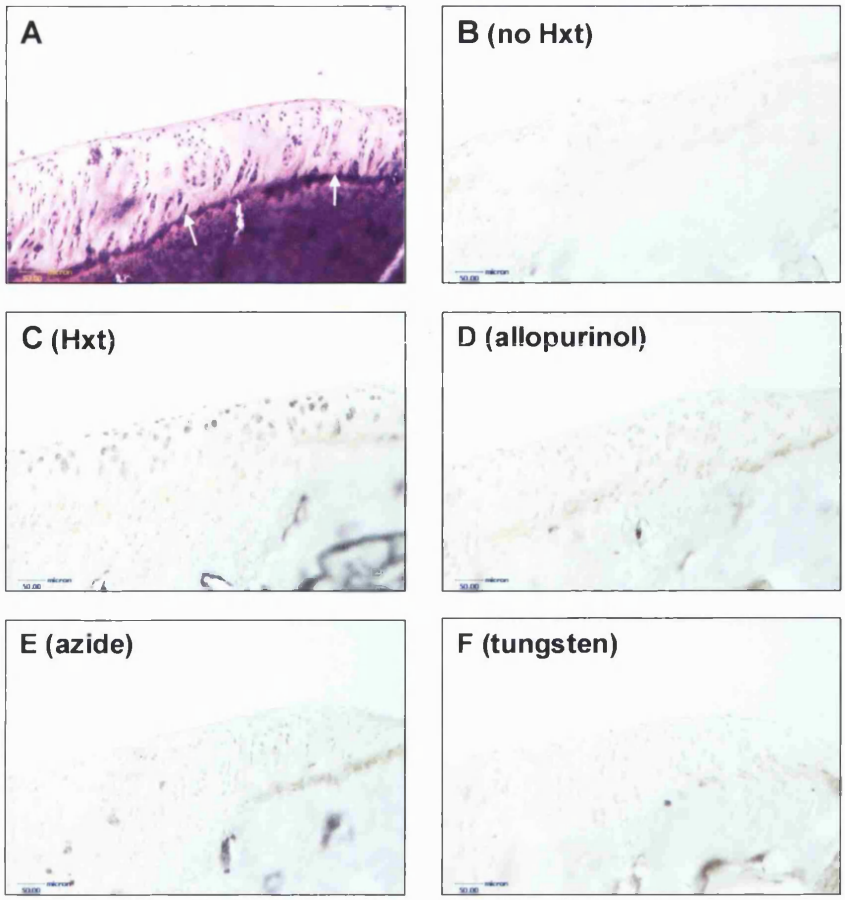

Fig. 5.4.2 b: Histochemical staining for XOR activity shown as a TNBT reduction product (*dark purple*) on corresponding, unfixed cryosections of patellar cartilage from Wistar rats (*n=3*). Photomicrographs are representative of three separate experiments. Bars represent 50 μm. **A**, H&E stain, arrows mark the 'tide mark', *i.e.* the border between calcified and apical non-calcified cartilage; **B**, weak staining in the absence of hypoxanthine (Hxt) as substrate; **C**, marked staining in the majority of chondrocytes, in the presence of 0.5 mM Hxt, especially in the superficial layers; **D**, conditions as in image C with added 1 mM allopurinol, showing suppressed XOR activity; **E**, conditions as in image C with added 10 mM sodium azide, showing diminished staining; **F**, marked suppression of XOR activity in patellar cartilage from a tungsten-fed rat in the presence of Hxt.

XOR activity in synovium

Strong staining for reduced TNBT was seen in the synovial lining and sub-synovial layer including skeletal muscle of normal Wistar rats. ***Fig. 5.4.2 c*** shows

representative photomicrographs of one of three experiments. Noteworthy is the relative lack of staining seen in sub-synovial small arteries (***image A***). Similar to hyaline cartilage chondrocytes (see Fig. 5.4.2 b), dietary supplementation with tungsten produced good suppression of XOR activity staining (***image D***).

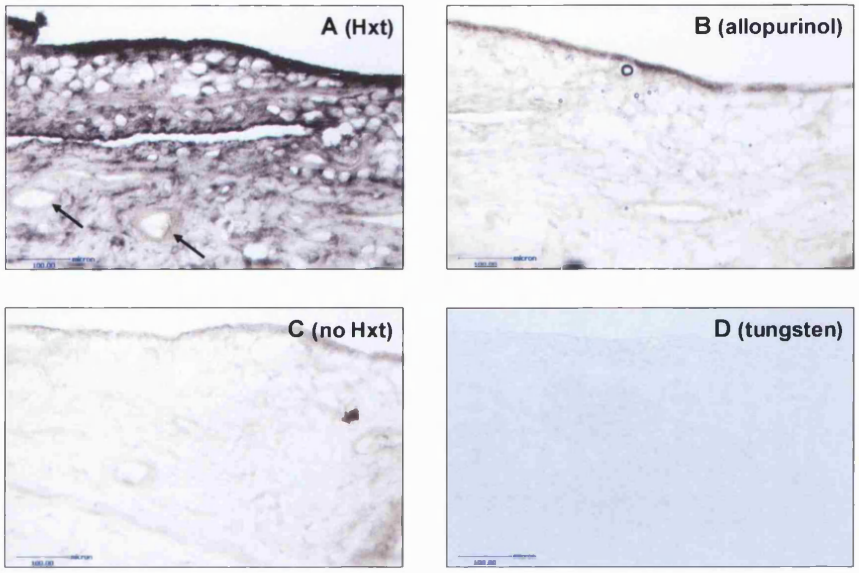

Fig. 5.4.2 c: Histochemical staining for XOR activity shown as a TNBT reduction product (*dark purple*) on corresponding, unfixed cryosections of knee synovium from Wistar rats ($n=3$). Photomicrographs are representative of three separate experiments. Bars represent 100 µm. **A**, marked staining of synovial lining layer and subsynovium in the presence of 0.5 mM hypoxanthine (Hxt); note the relative weak staining in the media of small arteries (*arrows*); **B**, conditions as in image C with added 1 mM allopurinol, showing suppressed XOR activity; **C**, weak staining in the absence of Hxt; **D**, marked suppression of XOR activity in synovium from a tungsten-fed rat in the presence of Hxt.

5.5 Discussion

These experiments showed that in normal rats, homogenates of patellar bone - and to a lesser extent synovium and cartilage – are high in XOR activity in comparison to skeletal muscle and liver. Enzyme histochemistry of normal rat cartilage and synovium sections showed XOR activity localising strongly to hyaline cartilage chondrocytes and the synovial lining cells, but only weak to synovial vessels.

The finding of relative high activity of XOR activity in rat liver by histochemistry and spectro-fluorimetric enzyme assay is concordant with the literature (Beckman JS, *et al.*, 1989; Kooij A, *et al.*, 1992a; Moriwaki Y, *et al.*, 1998) and served as a positive technical control for the assay methods. Consistent with reports of XO protein and XDH mRNA expression in skeletal muscle (Moriwaki Y, *et al.*, 1996; Moriwaki Y, *et al.*, 1997), the present study showed XOR histochemical activity in subsynovial striated muscle cells. However, rat quadriceps muscle showed only low XOR activity in tissue homogenates and the cause for this discrepancy is not clear.
In humans, inflamed joints showed increased XOR activity using radio-labelled substrate (Allen RE, *et al.*, 1987) and immuno-localisation of XO protein has been reported in inflamed and normal synovial vessels (Stevens CR, *et al.*, 1991a). However, no reports on localisation of XOR protein or activity in synovial joints of rats were found. While it would seem very likely that endothelial cells in synovium will express XOR as they do in other rat organs (Kooij A, *et al.*, 1992a), in the present study histochemical XOR activity was weak compared to activity elsewhere in the joint.
The finding of XOR activity in hyaline cartilage chondrocytes, and at a level comparable to that in liver sections, was unexpected. Therefore I attempted to demonstrate XOR protein immunohistochemically in cartilage. A variety of immunohistochemical conditions (*i.e.* paraffin- *vs* cryo-embedded specimen, 5-10 % normal goat serum and/or 10 % foetal calf serum to block non-specific binding, alkaline phosphatase/ Fast Red™ *vs* peroxidase/ diaminobenzidine as enzyme/dye combinations) were tested with a commercial polyclonal anti-(bovine buttermilk)XO primary antibody (Chemicon, Eastleigh, UK). However, no convincing XO staining could be demonstrated in rat hyaline cartilage chondrocytes. Similarly, human

cartilage specimen, obtained from subjects with osteoarthritis at the time of joint replacement surgery, did not show specific immunohistochemical staining for XO protein. This may be due to bovine origin of the immunogen against which the XO antibody was raised. A web search did not reveal any commercially available antibodies raised against XO of rat origin. Nevertheless, there is one report using *anti*-rat XOR antibody (made by the investigators), but XO immunoreactivity in joints was not mentioned (Moriwaki Y, *et al.*, 1996).

What is the purpose of XOR activity in articular chondrocytes? It could simply reflect the role of XOR in purine metabolism. However, the avascular and hence relatively hypoxic environment of articular cartilage with a physiologically slow metabolic rate would appear unlikely to produce a purine load requiring a level of XOR activity similar to that seen in liver. The potential and need for XOR as an $O_2^{\bullet-}$-generator in normal cartilage would appear similarly small. The distribution of XOR activity in articular cartilage closely resembled the distribution of 3-NT immunoreactivity (see Chapter 3.4.1 and Figure 3.4.1). Although co-localisation immunohistochemistry was not possible for reasons explained above, this similarity suggests that XOR activity remains a possible cause of 3-NT and RNS formation. Whether this 3-NT/RNS formation serves to protect chondrocytes against microbial attack (Brunelli L, *et al.*, 1995; Stevens CR, *et al.*, 2000; Umezawa K, *et al.*, 1997) or against the effects of low oxygen tension (Levick JR, 1979; Silver IA, 1975) remains speculative (see discussion 3.5).

There are limitations to this study. The histochemical evidence of XOR activity in cartilage is of a qualitative nature. Due to the heterogeneity of tissue section morphology for anatomical and technical reasons (*e.g.* difficult sectioning across non-calcified patellar bone), joint tissue does not render itself readily suitable for computer-assisted optical density image analysis, as it is possible for liver sections (Frederiks WM, *et al.*, 1995). Because of the difficulties in demonstrating corresponding XOR protein expression in cartilage, it may be be more feasible to investigate XOR mRNA expression.

In both humans and rats most XOR activity exists as XDH *in vivo* (Della Corte E, *et al.*, 1969; Waud WR and Rajagopalan KV, 1976). The high proportion of XO in total XOR activity seen in homogenates of all rat tissues in this study was therefore

unexpected. However, this observation could reflect that, despite proteinase inhibitors and keeping samples cold, conversion of XDH to XO may not be preventable under *in vitro* conditions.

Finally, the distinct, yet apparently incomplete suppression of TNBT reduction in the presence of allopurinol compared to the better suppression seen in tungsten-treated animal tissue suggests that a significant part of the TNBT reductase activity could be provided by aldehyde oxidase (AO). Like XOR, AO is a molybdo-enzyme (and as such will be inactivated by a tungsten diet) which may share many of the substrate specificities and tissue distribution of XOR in rats (Moriwaki Y, *et al.*, 1996; Moriwaki Y, *et al.*, 1998). However, to date AO has not been implicated in joint physiology or pathology.

The finding of XOR activity in rat articular cartilage, mirroring the localisation of 3-NT and suppressible by dietary tungsten, opened the way to study the possible contribution of XOR activity to cartilage/ bone damage and 3-NT formation during experimental arthritis. This will be the subject of the next chapter.

Chapter 6: Pathogenesis of antigen-induced arthritis in xanthine oxidoreductase-deficient rats

6.1 Introduction

The previous chapters have described studies showing that normal rat patellar cartilage contains 3-NT, a marker of *in situ* formation of reactive species derived from NO (Halliwell B, 1997). Rodent models, lacking individual nitric oxide synthases I-III, did not abolish 3-NT expression in cartilage, indicating compensatory enzyme activity. As was shown by several investigators, XOR is capable of generating both $O_2^{\bullet-}$ and NO from nitrates *in vitro* (Godber BJL, *et al.*, 2000; Li H, *et al.*, 2001; Millar TM, *et al.*, 1998). However, inactivation of XOR by a tungsten-supplemented diet (Johnson JL, *et al.*, 1974) did not affect 3-NT in rat joints, arguing against XOR as the only source of RNS *in vivo*. Nevertheless strong XOR activity was found in articular cartilage chondrocytes of normal Wistar rats, in a distribution resembling that of 3-NT. This XOR activity was strongly suppressed by dietary tungsten. Therefore it remains conceivable that XOR may contribute to 3-NT/RNS formation in joints, under conditions of tissue stress, such as experimental arthritis.

There is considerable evidence that arthritis is associated with increased 3-NT formation in cartilage. This has been described in human osteoarthritis (OA) (Loeser RF, *et al.*, 2002; Matsuo M, *et al.*, 2001) and experimental canine (Pelletier JP, *et al.*, 1999) and lapine (Hashimoto S, *et al.*, 1998) OA models. It has also been reported in chondrocytes of type II collagen- (Cuzzocrea S, *et al.*, 2000) and zymosan-induced (Bezerra MM, *et al.*, 2004) inflammatory arthritis in small rodents. In these experimental studies, diminished 3-NT expression was associated with less joint inflammation and cartilage damage.

If XOR contributes to 3-NT formation in cartilage in experimental arthritis, one would expect that inactivation of XOR in rats through dietary tungsten suppresses 3-NT formation in joint tissue. One would further expect an associated reduction of joint inflammation and damage. This is important, since if true, it would point

towards a role for XOR inhibition (*e.g.* with allopurinol) in the treatment of inflammatory arthritis *per se*.

Antigen-induced arthritis (AIA) in Wistar rats was chosen for these studies. AIA is induced by intra-articular injection into the knee joint of a defined antigen (*e.g.* methylated bovine serum albumin (mBSA)) in animals, previously sensitized to the antigen by immunisation. It was originally described in rabbits (Dumonde DC and Glynn LE, 1962) and shares many features with human rheumatoid arthritis (RA), *e.g.* synovial histopathology, chronicity, T-cell responsiveness, cytokine pattern and response to anti-inflammatory and anti-cytokine therapy . In mice (Brackertz D, *et al.*, 1977) and rats (Griffiths RJ, 1992) the initial acute arthritis is a localised, non-destructive, immune complex disease of a few days duration. The development of a chronic destructive arthritis depends on T-cell hypersensitivity and antigen-retention within the joint [reviewed in (Pettipher ER and Blake S, 1995)]. This model was chosen since most of the present work on 3-NT had been carried out on Wistar rat knee joints. Furthermore, previous experience within our group had shown this model to produce a chronic, erosive arthritis in Wistar rats by three weeks *post* induction (Mapp PI, *et al.*, 2001). Three groups of animals were studied: (a) animals fed on a tungsten-enriched diet from three weeks prior to systemic immunisation, or (b) on standard-diet throughout the experiment, and (c) animals on a standard diet treated with the XOR inhibitor allopurinol prior to arthritis induction. The main outcome measures were radiographic and histological analysis of knee joints, and 3-NT/tyrosine ratios by gas chromatography/ mass spectrometry (GC/MS) in patellar/synovium homogenates three weeks after arthritis induction.

6.2 Aims and objectives

The hypotheses to be tested were:

- that XOR contributes to articular 3-NT formation; and
- that XOR inactivation is protective against antigen-induced arthritis(AIA).

The objectives were:

- to study the course of methylated bovine serum albumin-induced knee arthritis in rat groups, treated with tungsten-enriched diet, normal control diet or the XOR inhibitor allopurinol;
- to study 3-NT/tyrosine concentration by GC/MS and radiographic and histological changes in rat knees three weeks after arthritis induction.

6.3 Materials and methods

A list of materials can be found in the ***Appendix VI.*** All concentrations are final, unless stated otherwise.

6.3.1 Animals

Male out-bred Wistar rats of weaning age (Charles River, Margate, UK) were mixed at random from different litters and housed in cages under standard conditions for one week before experimental interventions began. Procedures complied with the Animals (Scientific Procedures) Act 1986, UK and with Home Office (UK) licence. For all invasive interventions, animals were under 4% isofluorane/oxygen (2 l/min) anaesthesia, delivered in an anaesthetic chamber. Apart from dietary interventions, animals were kept under standard laboratory conditions with water *ad lib.*

6.3.2 Materials

Chemicals were obtained from Sigma, Poole, UK, unless stated otherwise. All concentrations are expressed as final concentration.

Normal protein rat chow, supplemented with sodium tungstate (0.7 g/kg; ICN, Basingstoke, UK); standard rat chow (SDS, Witham, UK); methylated bovine serum albumin (mBSA); complete Freund's adjuvant (CFA); 0.9 % aqueous sodium chloride for injection (0.9 % NaCL; Braun, UK); allopurinol; sodium carboxymethylcellulose (medium viscosity).

6.3.3 Pharmacological inhibition of XOR and protocol of antigen-induced arthritis (AIA)

For reasons of clarity the pharmacological inhibition of XOR and the protocol of AIA are described together (***Fig. 6.3.3***).

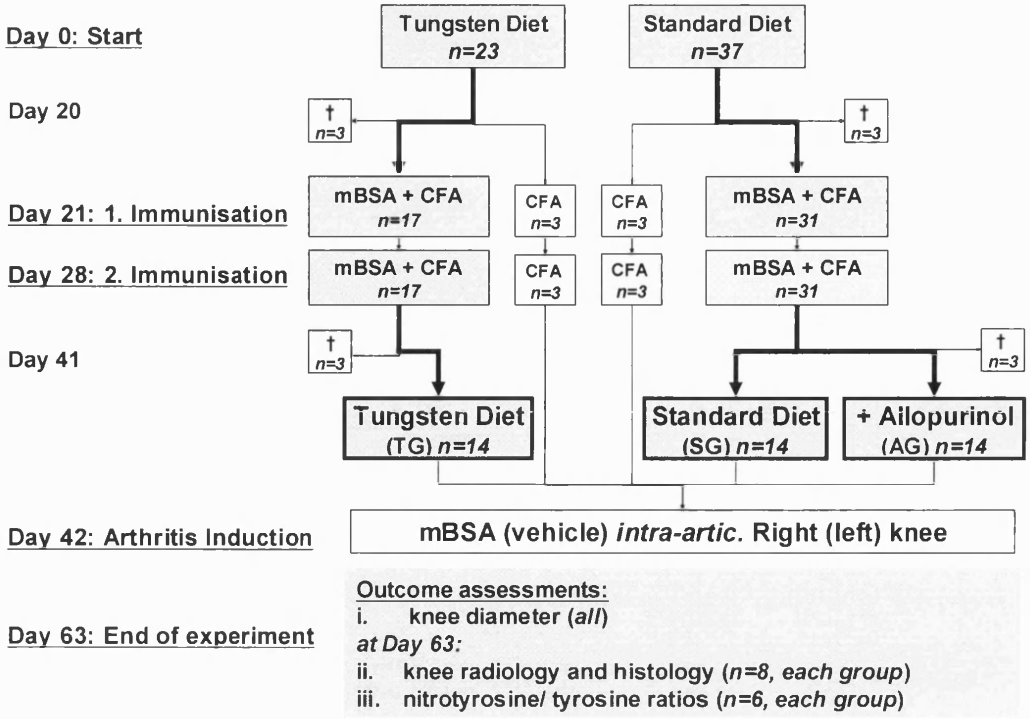

Fig. 6.3.3: Flow chart outlining the experimental protocol of the antigen-induced arthritis in Wistar rats. CFA, complete Freund's adjuvant, †, animals sacrificed to determine XOR activity.

Rats were fed on either a standard diet (SG) or tungsten-enriched chow (TG). A subgroup of animals of the SG group was treated with the XOR-inhibitor allopurinol. AIA in the right knee was induced by a single *intra-articular* (*i.a.*) injection of mBSA in rats previously immunised with mBSA in complete Freund's adjuvant (CFA). CFA is a suspension of heat shock-killed mycobacteria in mineral oil, commonly used to enhance an immune response to achieve hypersensitivity in experimental arthritis. The following protocol was previously described by Mapp *et al.* and known to lead to a chronic erosive knee monarthritis by three weeks (Mapp P.I., *et al.*, 1993).

From Day 0 onwards Wistar rats (28 days old, mean weight ± SEM: 132 ± 2 gm) were fed on a tungsten or standard diet. After three weeks (Day 21) animals were immunised with 500 µg mBSA (as 100 µl of 10 mg mBSA/ml in 0.9 % saline, mixed 1:1 (v/v) with CFA) by *subcutaneous* (*s.c.*) injection into the shaved scruff. Three

control animals in each diet group were injected with vehicle alone (*i.e.* saline/CFA). This immunisation was repeated one week later (Day 28). One day before arthritis induction, a subgroup of the standard diet group was started on allopurinol (50 mg/kg/day, suspended in 1 ml of 1 % (w/v) carboxymethylcellulose in H_2O/Q), administered *per os* with a gavage. The following day (Day 42), all animals were injected with 500 µg mBSA (as 100 µl of 5mg mBSA/ml sterile 0.9% NaCl) and vehicle via *i.a.* injection into the right and left knee, respectively. Three weeks later (Day 63) all animals were sacrificed. A proportion of animals in each treatment group (*n=6*) had blood removed for plasma and patella-synovium dissected from each knee under terminal 4% isofluorane/O_2 (2 l/min) anaesthesia. The remaining animals in each treatment group (*n=8*) and the sham-immunised animals of the tungsten- and standard-diet group (*n=3*) were killed by CO_2 overdose, and knees were excised and put into formal saline for radiographic and histological assessment. All animals underwent *post mortem* examination for macroscopic pathological changes.

6.3.4 Clinical Assessment

Animals were inspected daily for signs of ill health and weighed once per week throughout the experiment.

Medio-lateral knee diameters of both knees were measured on non-anaesthetised animals with digital electronic callipers (Mitutoyo, Andover, Hampshire, UK) before and 1, 2, 5, 7 and 14 days following *i.a.* mBSA/vehicle injection. Measurements were undertaken blinded to the intervention group, and recorded to the nearest 0.1 mm. Baseline evaluation of the inter-observer agreement of transverse knee diameter measurement with covered display was performed between my supervisor Dr. Paul Mapp (PIM; an experienced experimental pathologist) and myself (RK) on the right knees of the Standard Diet animals (n=14) prior to arthritis induction. The result display of the digital callipers was covered during measurement. The level of agreement was calculated as the intra-class correlation coefficient (ICC).

6.3.5 Delayed-type hypersensitivity assessment

In order to determine whether the tungsten diet interferes with the hypersensitisation to mBSA, the development of T cell-dependent hypersensitivity (Type IV, according to the classification by Coombs & Gell (Roitt IM, et al., 1985)) had to be verified in each diet group. This was done by assessing the clinical signs of delayed-type hypersensitivity (DTH) to mBSA.

Seven days after the second mBSA immunisation (Day 35) , a subgroup of animals (*n=5*, from each tungsten- and standard-diet group) were injected intradermally into the pinna of the right and left ear with 2.5 μg mBSA (as 50 μl of 0.5 mg mBSA/ml 0.9% saline) and vehicle, respectively. After 48 hrs, local skin reaction was assessed in coded animals for redness and induration (*i.e.* firm swelling), using the following qualitative score: '0', no redness or induration; '1', redness only; '2', redness and induration. Suffixes 'a' and 'b' (*e.g.* '1a') denoted whether the changes were considered 'mild' or 'more than mild', respectively.

6.3.6 XOR activity assay

XOR analysis was measured in plasma (prior to *s.c.* mBSA immunization, prior to and three weeks after *i.a.* mBSA/vehicle injection; see Fig 6.3.3) and in homogenates of snap-frozen patella-synovium (in PBS with 10 μg/ml aprotinin and 0.5 mM phenylmethylsulfonylfluoride). XOR activity was analyzed as xanthine oxidase activity using a fluorospectrometric method of pterin oxidation (Beckman JS, *et al.*, 1989). Details of sample preparation and the assay are described in ***Section 4.3.3*** and ***Appendix IV***. Samples were measured in triplicate and XOR activity was calculated and expressed as nmol min^{-1} g^{-1} sample tissue protein, with protein concentration determined according to the method of Bradford (Bradford MM, 1976) (see ***Appendix II***).

6.3.7 Quantification of nitrotyrosine

Nitrotyrosine and tyrosine content were measured in homogenates of patella-synovium 21 days *post* arthritis induction by gas chromatography/ mass spectrometry (GC/MS), as previously described (Frost MT, *et al.*, 2000). Sample preparation and protein extraction was performed by myself and further analytical steps of the

method by Dr Ali R Mani, from the Centre for Hepatology, Department of Medicine, Royal Free & University College Medical School, UCL, London, UK (see section 3.4.3). Results were expressed as nitrotyrosine/ tyrosine [pg/μg]. This method avoids artefactual nitration of tyrosine under the acidic conditions commonly employed.

6.3.8 Radiographic analysis

Knee joints were contact X-rayed in the medio-lateral and antero-posterior plane (Faxitron X Ray Systems, Field Emission Ltd., London, UK). Exposure was at 40 kV for 20 min, using a 'Kodalith, Orthotype, Grade 3' film (Sigma, Poole, UK). Blind-label X-ray films were examined with a magnifying glass (x 20) for bone changes of inflammatory arthritis. X-rays were scored for erosions, defined as a cortical break, osteopenia and periosteal reaction, as described by Clark *et al.* (Clark RL, *et al.*, 1979). Results were independently verified by two experienced investigators (Drs Paul I. Mapp and Chris J. Morris) of our group.

6.3.9 Histological analysis

After radiography knees were decalcified in 10% formic acid, (v/v) in formal saline. To accelerate the decalcification, specimen containers were under continuous motion on a rocker roller at room temperature, and the decalcifying solution was replaced twice a week. After six weeks decalcification was complete (as verified by X-ray). Sections were trimmed, processed and embedded in paraffin. 6 μm-thick sections were cut along the sagittal knee joint plane and stained with haematoxylin and eosin (H&E). Blind-label sections were examined for intra-articular fibrin, cellular infiltrates and synovial proliferation, bone and cartilage destruction by pannus and periostitis and all scored individually on a semi-quantitative scale (ranging from 0 to 3+ according to occurrence) (Kruijsen MWM, *et al.*, 1983). Results were independently verified by my co-supervisor Dr Paul I. Mapp.

6.3.10 Statistical Methods

Continuous data was analysed by unpaired t-test or one-way analysis of variance (ANOVA) to compare means between two or three groups, respectively. A repeated measures-ANOVA was used to compare changes within treatment groups from

baseline. If the ANOVA showed significantly different means (at $p < 0.05$), Dunnett's *post*-test was applied, comparing the Tungsten Diet and Allopurinol group to the Standard Diet group or baseline, respectively. Statistical calculations and graphic display of results were carried out using the software program GraphPad Prism, version 3.02, 2000 (GraphPad Software, San Diego, U.S.A.).

6.4 Results

6.4.1 General observations

Animals of all three groups thrived well throughout the duration of the experiment (***Fig. 6.4.1***). Although there was a trend of mean weight being higher in the Tungsten group compared to the Standard Diet group just prior to arthritis induction, these difference became only significant from 7 days *post* induction. *Post-mortem* examination did not reveal any macroscopic abnormality of internal organs in any animal.

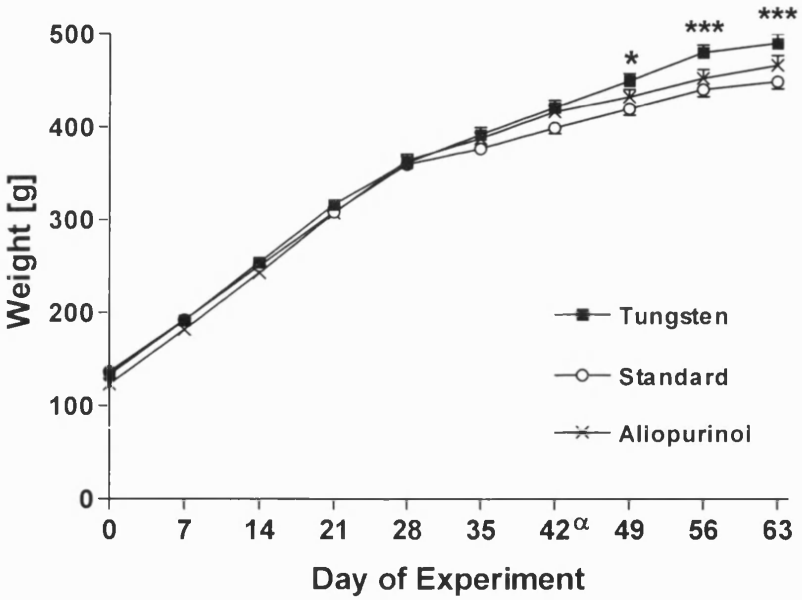

***Fig. 6.4.1*: Mean weight of Wistar rats over time of the experiment** ($n \geq 14$ per experimental group). Day 0 marks the beginning of experimental diets, and Day 42 (**α**) arthritis induction with *i.a.* mBSA. Allopurinol dosing began on Day 41. Bars represent SEM. * $p<0.05$, *** $p<0.001$ for difference between tungsten- *vs.* standard-fed animals (ANOVA with Dunnett's *post*-test).

6.4.2 Tungsten diet, but not allopurinol, suppresses XO activity in joint homogenates.

The Tungsten Diet group had markedly suppressed activity of plasma XO activity from the first mBSA immunisation until the end of the experiment (see ***Table 6.4.2***). XO activity in patella-synovium homogenates from rats (n=3, right and left knee analysed

separately), sacrificed 21 days post arthritis induction (*i.e.* Day 63), showed < 0.9 % activity of joint homogenates of the control Standard Diet group ($p<0.001$, ANOVA with Dunnett's post-test). In the Allopurinol group mean *plasma* XO activity 3 weeks *post i.a.* mBSA injection (*i.e.* Day 63) was decreased to 7.3 % (*n=6*; $p < 0.001$). However, XO activity in patella-synovium homogenates was not significantly different from control animals. Mean XO activity in plasma of Standard Diet animals did not change significantly over time from Day 20 (ANOVA, Dunnett's *post*-test).

***Table 6.4.2*: XO activity in rat plasma, and patella-synovium homogenates.**

	Tungsten Diet	Standard Diet	Allopurinol
Plasma			
Day 20	**0.3 ± 0.4**	**172 ± 16 ***	**NA**
Day 41	**ND**	**219 ± 5**	**NA**
Day 63	**ND**	**162 ± 11 †**	**12 ± 2**
Patella-Synovium			
Day 63	**1.1 ± 3.1**	**127 ± 22 β**	**160 ± 17**

Values are mean XO activity (± SEM), as nmol x min^{-1} x g tissue $protein^{-1}$, measured by spectro-fluorimetric pterin assay. Sample sizes were *n=3* animals for each group, except for plasma of day 21 (*n=6*). Left and right patella-synovium samples were analysed separately. Each sample was measured in triplicate. Experimental days were: Day 20, after 3 weeks on experimental diet and prior to *s.c.* mBSA immunisation; Day 41, prior to *i.a.* mBSA injection; Day 63, three weeks after *i.a.* injection.

ND, not detectable; NA, not applicable. * $p < 0.001$ *vs.* Tungsten Diet (unpaired t-test); † $p < 0.001$ *vs.* Allopurinol and β $p < 0.001$ *vs.* Tungsten Diet (ANOVA with Dunnett's *post*-test).

6.4.3 Tungsten diet does not affect development of DTH to mBSA

On blind-label assessment, three out of five (60 %) animals tested in each diet group developed a positive DTH to mBSA. One animal showed mild redness and induration (score '2a') (see ***Fig. 6.4.3***) and two had mild redness (score '1a') in each dietary group. None of vehicle injected left ears showed a positive DTH reaction. Similarly, none of four randomly interspersed animals, that did not have an *intra-dermal* mBSA challenge, were judged to have a positive DTH reaction.

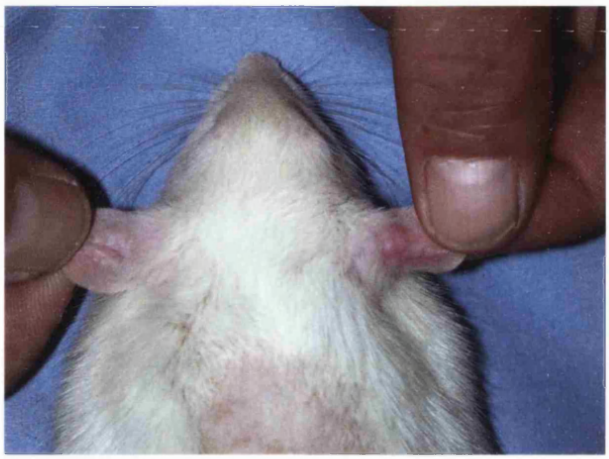

Fig. 6.4.3: Delayed-type hypersensitivity reaction on the right pinna of a tungsten-fed Wistar rat, 48 hours after *intra-dermal* mBSA (2.5 μg). Note the redness and swelling, in comparison to the vehicle-injected left side. The DTH score given was '2a' (see section 6.3.5 for details).

6.4.4 Tungsten-fed, but not allopurinol-treated animals show greater acute joint swelling.

The inter-observer agreement between PIM, the experienced investigator, and RK was low, as signified by an ICC of r^2=0.16. As a result all further knee measurements were taken by PIM.

Mean baseline diameters ± SEM of mBSA-injected knee joints were comparable in the TG, SG and AG groups (*n=14*, each group) with 12.3 ± 0.2, 12.5 ± 0.2 and 12.5 ± 0.1 mm, respectively. At 24 and 48 hours after *i.a.* mBSA-injection, the mean right knee diameters of all treatment groups had increased from baseline ($p < 0.001$; repeated measure ANOVA). At both these time points, knee diameters showed a greater increase in the tungsten- compared with the standard diet group (***Fig. 6.4.4***).

The mean differences (95% confidence interval) were 1.3 (0.3, 2.4) mm and 1.2 (0.2, 2.1) mm, at 24 and 48 hours, respectively ($p<0.05$; ANOVA with Dunnett's *post*-test). There was no significant change in mean diameter of left (*i.e.* sham-injected) knees and mBSA-injected knees of the CFA-immunised animals. By five days post arthritis induction mean knee diameters had returned to normal in all treatment groups.

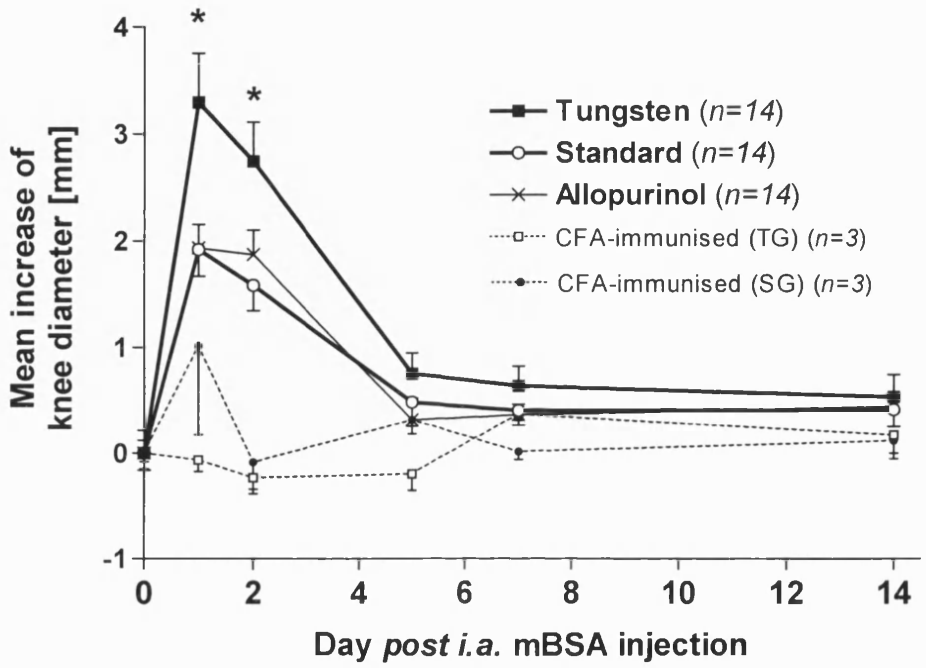

Fig. 6.4.4: Mean change of transverse diameter of mBSA-injected knees from baseline (*i.e.* prior to *i.a.* mBSA) over time. Bars represent SEM. * $p < 0.05$ *vs* . Standard Diet group (ANOVA with Dunnett's post-test). TG, tungsten diet; SG, standard diet; CFA, complete Freund's adjuvant.

6.4.5 Tungsten-fed, but not allopurinol-treated animals have higher 3-NT content in inflamed knee joints

At 21 days post arthritis induction mean nitrotyrosine-tyrosine ratios (±SEM) of right patella-synovium homogenates were higher in the Tungsten Diet group, compared with the Standard Diet and Allopurinol group: 12.3 ± 0.7 pg/µg, 9.6 ± 0.8 pg/µg and 10.4 ± 0.5 pg/µg, respectively ($p < 0.05$, TG *vs* SG; ANOVA with Dunnett's post-

test) (***Fig. 6.4.5***). There was no significant difference of 3-NT/tyrosine ratios between right and left knee homogenates in the treatment groups (paired t-test).

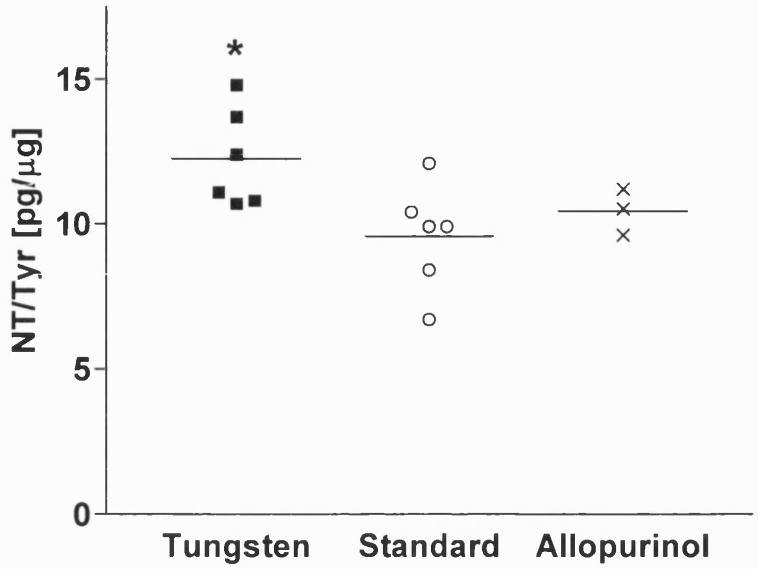

Fig. 6.4.5: Nitrotyrosine-tyrosine ratios of patella-synovium homogenates (3 weeks post *i.a.* mBSA injection). Bars represent mean values. * $p < 0.05$ for difference of means between tungsten- *vs.* standard-diet group (ANOVA with Dunnett's post-test).

6.4.6 Radiographic or histological features of arthritis were not detected at 21 days post i.a. mBSA injection

Close scrutiny of joint radiographs ($n=8$, each group; except sham-immunized animals: $n=3$) by two experienced experimental pathologists revealed no convincing signs of bone changes in any of the treatment groups.

Similarly, histological analysis of H&E stains of sagittal knee joint sections ($n=8$, each group; except sham-immunized animals: $n=3$) showed no convincing evidence of chronic inflammation, bone erosions or periosteal reactions in any of the treatment groups.

6.5 Discussion

It had been hypothesized that XOR contributes to the formation of RNS and nitration of articular proteins during joint inflammation and that thus inhibition of XOR would ameliorate the course of experimental arthritis. In contrast, here I have shown that inactivation of articular XOR activity by tungsten was associated with a significantly greater increase of knee swelling during acute mBSA-induced arthritis compared to controls. Furthermore, tungsten-treated animals showed increased nitrotyrosine formation in arthritic joints compared with the animals on standard diet, as measured by a highly sensitive gas chromatographic-mass spectrometric method. Together, these observations suggested that inactivation of XOR enhanced joint inflammation early during the course of AIA. Although the effect is relatively modest, this is the first study to indicate that XOR may have a protective effect in immune complex-mediated disease, and supplements our previous observation that suggests a beneficial role for XOR in innate immune responses (Stevens CR, *et al.*, 2000). The present study does not suggest XOR to be a significant source of RNS in acute antigen-induced arthritis.

Tungsten-treated animals thrived well and their development of immunity to mBSA was unaffected. Moreover, the tungsten-treated group showed marked suppression of mean xanthine oxidase activity in plasma and joint tissue to < 0.9 % of controls. In contrast, allopurinol achieved partial inhibition of plasma, but not joint XOR activity, which may explain why joint swelling was not enhanced in the allopurinol group.
A literature search revealed no published studies of tungsten-induced XOR inactivation in antigen-induced arthritis. However, using the *M.tuberculosis*-adjuvant arthritis model in Lewis rats with dietary tungsten treatment or oral allopurinol, our group has previously observed a reduction in radiographic erosion and bone demineralisation scores in the tungsten-treated animals compared to controls, suggesting that XOR contributes to joint damage in this model (Speden DJ, *et al.*, 2002). Pathogenetic differences between animal models may account for these contrasting results. Acute antigen-induced arthritis is a localised, non-destructive, immune complex disease of a few days duration (Griffiths RJ, 1992). T-cell hypersensitivity and antigen-retention within the joint are required for the

development of a chronic, destructive arthritis. In contrast, adjuvant arthritis is a destructive, T-cell mediated disease from the outset, that affects primarily periarticular soft tissues and bone (Pearson CM and Wood FD, 1959). It may be that XOR has divergent effects on acute synovial inflammation and chronic bone/cartilage destruction in arthritis. Indeed, distinct anti-inflammatory activity is increasingly recognised as an integral part of enzymes, such as iNOS (McCartney-Francis NL, *et al.*, 2001; Veihelmann A, *et al.*, 2001) and cyclooxgenase-2 (Gilroy DW, *et al.*, 1999), previously thought of as exclusively pro-inflammatory. This dual role of enzymes, central to joint inflammation, may hold clues to explain the clinical observation of progressive joint damage despite inactive synovial inflammation in rheumatoid arthritis (McQueen FM, *et al.*, 1999; Mulherin D, *et al.*, 1996). Alternatively, the enhanced acute inflammatory response seen during XOR inhibition with tungsten may in part explain the common, but poorly understood, clinical observation of exacerbation of gout when treatment with allopurinol is started (McLean L, 2003).

How may XOR limit protein nitration and acute AIA inflammation?

Uric acid, the final oxidation product of XOR-mediated purine metabolism, is a potent inhibitor of peroxynitrite-induced tyrosine nitration under physiological conditions *in vitro* (Whitemann M and Halliwell B, 1996). Furthermore, endogenously generated uric acid was identified as an inhibitor of protein tyrosine nitration in rat heart homogenates (Teng RJ, *et al.*, 2002). Pharmacological administration of uric acid has been shown to reduce both tissue damage and 3-NT tissue levels in experimental chronic autoimmune encephalitis, an animal model of multiple sclerosis, (Hooper DC, *et al.*, 1998) and acute zymosan-induced rat knee arthritis (Bezerra MM, *et al.*, 2004). However, uric acid does not inhibit all peroxynitrite-induced reactions. For instance, peroxynitrite-induced inactivation of α_1- antiproteinase (Whitemann M and Halliwell B, 1996), oxidation of sulfhydryl groups and lipid peroxidation (Santos CX, *et al.*, 1999) *in vitro* are not suppressed and may even be enhanced by uric acid (Whitemann M, *et al.*, 2002). This suggests that protein tyrosine nitration itself could be an important mediator of tissue inflammation and damage. This may occur via the nitration of specific tyrosine residues in proteins, leading, for example, to the alteration of enzyme function and cell signalling [reviewed in (Ischiropoulos H, 2003)]. One could therefore speculate

that in the present experiment, inhibition of XOR led to reduced generation of uric acid, with an increase of protein nitration and acute joint inflammation as a consequence. Future studies will have to incorporate the measurement of serum and tissue uric acid during the acute phase of AIA to examine this possibility further.

This study has important limitations.

Firstly, it lacks histological evidence of enhanced acute inflammation in the XOR-inactivated animals. This is due to the fact that study design and power considerations were aimed at the detection of a difference in the development of chronic destructive arthritis, as the outcome most relevant in comparison to rheumatoid disease in humans. Although a majority of animals developed delayed-type hypersensitivity to mBSA, radiographic and histological analysis 21 days after intra-articular arthritis induction did not reveal any convincing destructive or chronic inflammatory joint damage in any of the animals. This was in contrast to earlier experience by our group, using the same AIA induction protocol (Mapp P.I., *et al.*, 1993). It is possible that subtle strain variation in Bath out-bred Wistar rats may account for this observation. Increased 3-NT formation in joints can be taken as strong indirect evidence that increased inflammation has occurred, but future studies should include histological data during the early phase of AIA. They should also consider using an alternative rat species, shown by other investigators to be more prone to developing chronic AIA, *e.g.* Lewis rats (Griffiths RJ, 1992). Secondly, tungsten is not a specific XOR inhibitor, but will inhibit all three molybdenum-enzymes known to exist in rat and man. Apart from XOR, these are sulfite oxidase (SO) and aldehyde oxidase (AO) [reviewed in (Moriwaki Y, *et al.*, 1997)]. SO is a ubiquitous, mitochondrial enzyme whose only known function is the oxidative degradation of sulphur dioxide and bisulfite. As discussed in the previous chapter, AO has been shown to share substrates and localisation in rat tissues with XOR. However, neither of these enzymes is known to play a role in arthritis to date. It would therefore appear reasonable to attribute the observed effects of tungsten-supplementation in our experiment to the suppression of XOR.

In conclusion, it has been shown that inactivation of XOR by dietary tungsten was associated with increased acute joint swelling and increased nitration of articular

proteins, indicating increased joint inflammation during acute antigen-induced arthritis. This suggests that XOR may have a novel protective role in immune complex -mediated arthritis, which requires further clarification.

Chapter 7: General discussion and future work

Nitric oxide (NO) exerts both beneficial and deleterious effects on healthy and inflamed joint tissue (see section 1.3). Reactive species that derive from the interaction of NO and oxygen or superoxide ($O_2^{\bullet-}$), however, are known to have adverse effects in arthritis, but no beneficial role in joint physiology. For instance, NO and $O_2^{\bullet-}$ react rapidly to form the highly reactive peroxynitrite ($ONOO^-$) (Pryor WA and Squadrito GL, 1995), which is implicated in tissue damage of a wide variety of diseases. $ONOO^-$ may lead to nitration of tyrosine to form the relatively stable 3-nitrotyrosine (3-NT) (Ischiropoulos H, *et al.*, 1992b; Reiter CD, *et al.*, 2000). There is increasing evidence that 3-NT is not only an *in situ* marker of $ONOO^-$ (Ischiropoulos H, *et al.*, 1992b) and other RNS (Halliwell B, 1997; van der Vliet A, *et al.*, 1996), but that its formation is a specific process to regulate protein function (see section 1.1.4.3).

The work described in this thesis was developed from the striking observation of 3-NT immunoreactivity in synovial vessels of apparently normal human joints, but not in other vascular beds (Mapp PI, *et al.*, 2001). The present work sought to investigate the distribution of 3-NT in normal mammalian joint tissue, its enzymatic origin and its implications for inflammatory joint disease. Since the enzyme xanthine oxidoreductase (XOR), present in synovium (Allen RE, *et al.*, 1987; Stevens CR, *et al.*, 1991a), can generate both NO and $O_2^{\bullet-}$ during purine metabolism *in vitro* (Li H, *et al.*, 2001; Millar TM, *et al.*, 1998), a specific hypothesis to be tested was that XOR contributes to 3-NT formation in joints.

Main findings

The studies presented here have shown that synovial vessels from knee joints of healthy rodent species (*i.e.* Wistar rats and Sv 129 mice) also display immunoreactivity to 3-NT, not found in vessels of other organs (*e.g.* skin, small intestine, colon, liver, heart, kidney, spleen and brain). Moreover, even stronger 3-NT immunoreactivity was seen in hyaline cartilage chondrocytes of healthy, young rodents and cattle. This 3-NT immunoreactivity developed within 10 days after birth in rats and perfusion-fixation did produce similar findings, compared with immersion-fixation of animals/tissues. In normal rats 3-NT content, measured by a

highly sensitive gas chromatography-mass spectrometry (GC/MS), was significantly higher in patella/cartilage, compared to synovium and liver. Electrophoretic and 3-NT immunoblotting studies of normal rat joint tissue suggested that tyrosine nitration of proteins is not a random process. Immunohistochemistry (IHC) on small rodents, lacking functional individual nitric oxide synthases (NOS) 1, 2 or 3 (by targeted gene deletion) or XOR (by dietary tungsten-supplementation) showed unchanged articular 3-NT distribution. Tungsten-supplementation starting *in utero* achieved substantial inactivation of XOR, but GC/MS did not show reduced articular 3-NT content. Histochemistry for XOR activity showed marked activity in hyaline cartilage chondrocytes, suppressible by tungsten, and resembling the distribution of 3-NT immunoreactivity. In order to test whether XOR could contribute to articular 3-NT formation in 'stressed' animals, antigen-induced arthritis (AIA) was induced in Wistar rats on tungsten diet or standard diet (with or without allopurinol from arthritis induction onwards). Unexpectedly, XOR inactivation by tungsten led to increased joint swelling during the acute arthritic phase and increased 3-NT content in knee joint homogenates.

Implications

These findings provide evidence for tyrosine nitration of specific proteins in cartilage and synovial vasculature of healthy mammalian joints The 3-NT formation appears exclusive to the synovium as far as vasculature is concerned, and of higher magnitude than liver, an organ characterized by high metabolic activity. This articular tyrosine nitration does not appear to be a consequence of perimortal anoxia or aging. It seems secured by several enzymatic pathways, suggesting a protected physiological function. XOR is active in healthy articular chondrocytes, but is not involved in articular 3-NT formation in healthy rats or in rats, stressed by antigen-induced arthritis. XOR may, however, be protective in the acute phase of antigen-induced, immune complex-mediated arthritis.

General discussion

This work challenges the widely held opinion that NO, but not more reactive chemical species derived from NO, occur in significant amounts in healthy joints. Studies that have looked at the immunohistochemical distribution of 3-NT in normal joint tissue have done so by comparing pathological or aged tissue with normal

controls in primates (Loeser RF, *et al.*, 2002), dogs (Pelletier JP, *et al.*, 1999) or rats (Cuzzocrea S, *et al.*, 2000). Consistent with physico-chemical methods of 3-NT quantitation (Kaur H and Halliwell B, 1994), these studies found that 3-NT is increased in diseased or aged joints compared to normal joints. By design, however, immunohistochemical studies of this kind aim to *contrast* the abnormal tissue with the normal one, and this is technically achieved by terminating reactions when the positive control becomes positive while the negative technical and normal tissue controls remain negative. Therefore these studies are not helpful to draw conclusions on 3-NT in normal joint tissue. When investigating 3-NT in normal tissue, several issues need consideration. Firstly, how normal is normal tissue? Normal human tissue from asymptomatic donors is difficult to obtain for ethical reasons, and the absence of macro- and microscopical tissue abnormalities in *post mortem* incidental samples does not equate normality. But even when tissue is derived in a controlled fashion from animals, hypoxia occurring until tissue fixation may alter the *in vivo* situation. Perfusion-fixation of animals is one way of minimizing this problem, and my studies showed no significant reduction of 3-NT staining in joint tissue, sampled in this way. Secondly, there is potential for bias by 'creating' immunoreactivity by prolonged assay incubation, in particular during the final chromogenic reaction. Negative normal immunoglobulins or isotype controls guard against this source of bias, and such controls were employed in this work. The finding that newborn and 10 day-old tissue were stained in the same assay but produced a marked difference in 3-NT staining of synovial vessels and cartilage indicates that articular 3-NT indeed develops during animal ontogeny. The increasing sensitivity of highly specific methods of 3-NT measurement has also been helpful here. Clearly, it would have been desirable to compare the relatively high 3-NT content of patella bone and cartilage, measured by gas chromatography/ mass spectrometry, to more tissues than synovium and liver. This was not possible due to logistic constraints. It is intriguing to note how a range of normal can now be estimated for free 3-NT in plasma of healthy human volunteers, using gas chromatographic tandem mass spectrometry (*i.e.* mean 2.8 nM, range 1.4 – 4.2 nM) (Schwedhelm E, *et al.*, 1999).

However, even when the definition of what should be regarded as normal for healthy joint tissue has been verified, the bigger problem is to determine what, if any, difference this makes to the function of joints. This question requires first the identification of a method to alter 3-NT in joints both substantially *and* specifically.

In principle, 3-NT content could be altered by preventing new 3-NT synthesis, or by accelerating the metabolism of existing 3-NT. Since there was no known mechanism to increase metabolism, e.g. by denitration of 3-NT, the origins of 3-NT were examined. Apart from the extreme acidic gastric environment (where dietary NO_2^- may directly nitrate tyrosine), endogenous NO is usually considered the necessary precursor for 3-NT (Halliwell B, 1997). It seemed therefore appropriate to look at animal models deficient in the NO-producing enzymes NOS 1, 2, 3 and XOR, but these did not show altered 3-NT immunoreactivity in joints compared to their wild-type/ normal controls. This was not too surprising, given that phenotypically these animal models have not been reported to display any spontaneous joint problems (Johnson JL, *et al.*, 1974; McKusick VA, 2005a; McKusick VA, 2005b; McKusick VA, 2005c; McKusick VA, 2005d). These observations also indicated a degree of redundancy of articular 3-NT formation in healthy joints. However, I did not assess whether compensatory over-expression of the remaining NO-generating enzymes occurred in these enzyme-deficient animals to investigate the possibility of redundancy further.

While the role of enzymes and biological phenomena may not be obvious during healthy normal function, they may become unmasked during environmental or experimental stress. For instance, iNOS-deficient mice are not particularly prone to develop spontaneous infection, but their inoculation with infective agents reveals a disposition to increased morbidity and mortality (McInnes IB, *et al.*, 1998).

Several experimental arthritis studies have shown reduced NO production in iNOS-deficient animals, although this was not always associated with less inflammation or tissue damage (see section 1.3.1 and 1.3.2). While *in vitro* studies have shown that XOR can generate NO under physiological conditions (Godber BJL, *et al.*, 2000; Li H, *et al.*, 2001) there was only indirect evidence that this may be an essential part of the anti-microbial activity in human breast milk *in vivo* (Stevens CR, *et al.*, 2000). At the same time there was good evidence for XOR as a good candidate for 3-NT generation in cartilage chondrocytes and synovial vessels: (1) XOR is present in human normal and rheumatoid synovium (Allen RE, *et al.*, 1987); (2) XOR localizes to the synovial endothelium (Stevens CR, *et al.*, 1991a); (3) XOR can generate *both* NO and $O_2^{\bullet-}$ (Godber BJL, *et al.*, 2000; Li H, *et al.*, 2001; Millar TM, *et al.*, 1998). This study has added to this evidence by showing that XOR actvity is present in

normal hyaline cartilage chondrocytes and in a distribution resembling that of 3-NT immunoreactivity.

Nevertheless, as I have discovered, acute antigen-induced arthritis in Wistar rats with substantially inactivated XOR activity did not show the expected suppression of articular inflammation and 3-NT content compared to animals with normal XOR activity.

What could be the biological role of 3-NT in normal mammalian joint tissue?

Two of the best documented beneficial functions of highly reactive NO-derived species, such as $ONOO^-$, are tissue protection in animal models of cardiac ischemia-reperfusion injury/ pre-conditioning (Laude K, *et al.*, 2002; Lefer DJ, *et al.*, 1997; Nossuli TO, *et al.*, 1998) and superior anti-microbial properties compared to NO and $O_2^{\bullet-}$ (Brunelli L, *et al.*, 1995; Fang FC, 1997; Umezawa K, *et al.*, 1997). The avascular cartilage that depends nutritionally on the synovium has to function at low oxygen levels (estimated to be 1 kPa or less) (Silver IA, 1975). Intra-articular pressure fluctuations during joint movement (Levick JR, 1979; Nade S and Newbold PJ, 1983) may cause cycles of hypoxia-reoxygenation. Mitochondrial proteins from rat liver have recently been shown to undergo rapid and selective cycles of tyrosine nitration and denitration synchronous with alternating normoxia and hypoxia/anoxia *in vitro* (Koeck T, *et al.*, 2004). In this study, Koeck *et al.* identified a number of respiratory chain enzymes undergoing nitration/denitration, and it was suggested that protein nitration forms a mechanism to adjust cellular respiration to a variable oxygen supply. Consistent with this, my studies did not show 3-NT in cartilage from newborn rats, presumably due to their limited weight-bearing joint activity. Other mechanisms of chondrocyte protection can be considered. Articular chondrocytes have been shown to generate glutathione (GSH) *in vitro* (Carlo MD and Loeser RF, 2003). At millimolar concentrations, nitrosylated GSH (GSNO) induces chondrocyte apoptosis *in vitro*, whereas pretreatment with micromolar GSNO can reduce chondrocyte death (Turpaev KT, *et al.*, 1997). One could therefore speculate that cycles of hypoxia-reoxygenation in healthy joints induce $ONOO^-$ generation in articular chondrocytes which may nitrosylate the prevalent anti-oxidant GSH to form a slow NO donor. The slow release of NO would then serve to maintain the

regulatory and protective functions of NO, ultimately securing chondrocyte survival and function.

Clinical observations and anatomical factors illustrate the need for an effective anti-microbial defence system within joints. Septic involvement is uncommon in relation to the frequency of septicaemia. This is surprising considering the heavily vascularised nature of the normal synovium (Stevens CR, *et al.*, 1991b). Having no basement membrane, it could be expected that bacterial spread to the synovial cavity is facilitated (Miller ML, 1998). The avascular and relatively hypoxic cartilage would then be a vulnerable target to direct microbial attack. Ribosomal RNA of *Chlamydia trachomatis*, suggesting metabolically active organisms, have been found in the synovium of some asymptomatic human subjects (Schumacher HR, *et al.*, 1999). This indicates that microbial joint invasion may not always be clinically apparent and may be more common than generally thought. It would therefore be conceivable that 3-NT represents RNS formation to counteract local microbial invasion.

How can we explain that, contrary to expectation, XOR protected against tyrosine nitration and acute antigen-induced, immune complex-mediated joint inflammation?

In the *M.tuberculosis*-adjuvant arthritis model in Lewis rats our group had previously observed a reduction in radiographic erosion and bone demineralization scores in the tungsten-treated animals compared to controls, suggesting that XOR contributes to joint damage in this model (Speden DJ, *et al.*, 2002). Pathogenetic differences between animal models may account for these contrasting results (see section 1.2.2.3). While *acute* antigen-induced arthritis is a localised, immune complex disease of a few days duration (Griffiths RJ, 1992), adjuvant arthritis is a destructive, T-cell mediated disease from the outset, affecting primarily periarticular soft tissues and bone (Pearson CM and Wood FD, 1959). Therefore it may be that XOR has divergent effects on acute synovial inflammation and chronic bone/cartilage destruction in arthritis, *i.e.* suppressing the former and mediating the latter. XOR has indeed been shown by our group to mediate cytokine-induced bone loss, as occurs during inflammatory arthritis (Kanczler JM, *et al.*, 2003), but it is not known whether this requires NO generation. Such divergent activity for acute joint inflammation and cartilage/bone destruction would not be unique. It is increasingly

recognised as an integral part of enzymes, such as iNOS (McCartney-Francis NL, *et al.*, 2001; Veihelmann A, *et al.*, 2001; Veihelmann A, *et al.*, 2002) and cyclooxgenase-2 (Gilroy DW, *et al.*, 1999), previously thought of as exclusively adversarial in joint disease. This dual role of enzymes, central to joint disease, may hold clues to explain the clinical observation of progressive joint damage despite inactive synovial inflammation in rheumatoid arthritis (McQueen FM, *et al.*, 1999; Mulherin D, *et al.*, 1996). Alternatively, the enhanced acute inflammatory response seen during XOR inhibition with tungsten may in part explain the common, but poorly understood, clinical observation of exacerbation of gout when treatment with allopurinol is started (McLean L, 2003).

By what mechanism may XOR limit protein nitration and acute AIA inflammation?

The main catalytic products of XOR *in vitro* are NO, $O_2^{\bullet-}$ and uric acid (see section 1.1). Although NO is generated during AIA, iNOS-derived NO may be protective in acute AIA (Veihelmann A, *et al.*, 2001; Veihelmann A, *et al.*, 2002). XOR-derived NO could be similarly protective, but the present studies do not indicate that XOR is a relevant source of NO/RNS in this inflammatory *in vivo* model. Transfer of extra-cellular SOD and catalase genes, which will scavenge $O_2^{\bullet-}$ and hydrogen peroxide, has been shown to ameliorate AIA in Wistar rats (Dai L, *et al.*, 2003). This indicates that reactive oxygen species contribute pathology in AIA. However, if XOR were to be a relevant source of $O_2^{\bullet-}$ in AIA, one would have expected similar amelioration from XOR inactivation by tungsten.

Uric acid, the final oxidation product of XOR-mediated xanthine metabolism, is a potent inhibitor of peroxynitrite-induced tyrosine nitration under physiological conditions *in vitro* (Whiteman M and Halliwell B, 1996). Furthermore, endogenously generated uric acid was identified as an inhibitor of protein tyrosine nitration in rat heart homogenates (Teng RJ, *et al.*, 2002). Pharmacological administration of uric acid has been shown to reduce both tissue damage and 3-NT tissue levels in experimental autoimmune encephalitis, an animal model of multiple sclerosis, (Hooper DC, *et al.*, 1998) and zymosan-induced rat knee arthritis (Bezerra MM, *et al.*, 2004). However, as previously stated, uric acid does not inhibit all peroxynitrite-induced reactions. For instance, peroxynitrite-induced inactivation of α_1-antiproteinase (Whiteman M and Halliwell B, 1996), oxidation of sulfhydryl groups

and lipid peroxidation (Santos CX, *et al.*, 1999) *in vitro* are not suppressed and may even be enhanced by uric acid (Whiteman M, *et al.*, 2002). This suggests that protein tyrosine nitration itself could be an important mediator of tissue inflammation and damage. This may occur via the nitration of specific tyrosine residues in proteins, leading, for example, to the alteration of enzyme function and cell signalling and/or to neo-epitope formation [reviewed in (Ischiropoulos H, 2003)]. One could therefore speculate that in the present studies, inhibition of XOR led to reduced generation of uric acid, with an increase of protein nitration and acute joint inflammation as a consequence.

Limitations and future work

Studies that need to be addressed in future work arise in part from weaknesses of the present work.

The largely immunohistochemical and descriptive evidence of 3-NT in normal mammalian joint tissue would benefit from further studies of 3-NT measurements in tissues by GC/ MS. There are several rat tissues that would merit further investigation in this way: (1) cartilage, bone and synovial rat tissue, harvested by micro-dissection, to determine the relative 3-NT content of cartilage *vs.* bone; (2) rat joint tissue in comparison to a wider range of non-articular tissues; (3) joint tissue from rats at different stages of development (including newborn rats that did not display articular 3-NT immunoreactivity); and (4) rat tissue, retrieved by perfusion-fixation vs. immersion-fixation (to assess a potential contribution of peri-mortal hypoxia/anoxia on 3-NT formation). Clearly more important is the question as to whether the present findings apply to human joints. Given the relative difficulty of obtaining normal human joint tissue that has not been exposed to prolonged hypoxia/anoxia prior to sampling, it would seem more realistic and appropriate to obtain more information from animal studies first.

Quantitative 3-NT estimation would also have been desirable for tissue of the gene knockout models for iNOS, eNOS and nNOS, to see whether a partial suppression of 3-NT could be detected. In order to identify a more substantial reduction of articular 3-NT other strategies are required. For instance, double e,nNOS knockout mice (Wu

HH, *et al.*, 2000) or tungsten-feeding of individual NOS knockout models may be more likely to achieve 3-NT suppression, provided there is no undue toxicity.

In order to approach the potential biological role of 3-NT in normal articular cartilage more directly, it may be more promising to search for individually nitrated proteins in normal rat cartilage by more elaborate electrophoretic and mass-spectrometric techniques (*e.g.* two-dimensional gel electrophoresis and subsequent analysis of the 3-NT immunospots by matrix-assisted laser desorption ionization/ time-of-flight mass spectrometry) (Aulak KS, *et al.*, 2001). It would be of interest to see whether chondrocytes in suspension culture and exposed to cycles of hypoxia and re-oxygenation show similar changes of denitration and nitration of energy and anti-oxidant enzymes, as has recently been described for rat liver mitochondria (Koeck T, *et al.*, 2004). A similar analysis could prove useful to compare joint tissue from newborn with weaning-age rats, to determine in what way protein nitration differs. Although a soluble factor denitrating protein tyrosine residues has been described in homogenates of rat lung, spleen, brain and heart (Kamisaki Y, *et al.*, 1998; Kuo WN, *et al.*, 1999), it may be some time before 3-NT formation in articular chondrocytes can be specifically reversed to assess its biological role.

The antigen-induced arthritis experiment on tungsten-fed animals did not follow the chronic-destructive course, expected from a previous study of our group (Mapp P.I., *et al.*, 1993), which may have been due to variations of the out-bred 'Bath' Wistar strain. The experimental design and power calculations focussed on chronic destructive arthritis as the main end-point, and as a consequence, histological material was not available to assess whether acute joint inflammation had occurred. Clearly, this experiment needs to be repeated before firm conclusions about the protective properties of XOR can be made. A repeat experiment that aims to produce a chronic destructive arthritis should use inbred Lewis rats as in the original description of AIA in rats (Griffiths RJ, 1992). It would also be important to analyse venous blood or better synovial fluid for XOR activity, nitrite and uric acid at key stages of the arthritis, to try and elucidate the role of uric acid in this model.

In conclusion, this work has produced evidence to suggest that cartilage and synovium of normal joints contain relatively high amounts of 3-NT/RNS in several mammalian species, ensured by multiple enzymatic sources of NO, indicating a protective physiological function. XOR is not a significant source of RNS during antigen-induced arthritis, but it may protect against RNS formation and acute antigen-induced joint inflammation.

Appendices

Appendix I: Materials and protocols for histological staining techniques, including immunohistochemistry and immunofluorescence

Materials & solutions

Consumables were obtained from BDH, Poole, UK, unless otherwise stated.

Aquamount® (R.Lamb, UK),
bovine serum albumin (BSA) (Sigma, UK),
eosin,
DPX mounting media,
DAPI (Sigma, UK),

- Stock solution: 10 mg/ml (w/v) in H_2O/Q, stored light-protected at 4°C,

formaldehyde,
goat *anti*-mouse IgG FITC conjugate (Sigma, UK; #F 5262),
Harris' haematoxylin,
industrial methylated spirit (IMS),
Mayer's haematoxylin,
mouse monoclonal *anti*-3-nitrotyrosine antibody, clone 1A6 (TCS Biologicals, UK, #05-233),
normal goat serum (Vector Labs, UK),
normal rabbit immunoglobulin (Vector Labs, UK),
phosphate-buffered saline (PBS, diluted in H_2O/Q),
rabbit polyclonal *anti*-3-nitrotyrosine antibody (TCS Biologicals, UK, #06-284),
Sigma Fast® Red (Sigma, UK; containing TR/ naphthol AS-MX tablets including 0.6 mM levamisole to inhibit endogenous alkaline phosphatase activity, and buffer tablets, dissolve 1 tablet each in 10 ml H_2O/Q immediately prior use),
Triton X-100 (Sigma, UK),

Vectastain® ABC-AP kit, for rabbit primary antibody, # AK-5001 (Vector Labs, UK),
Vectashield® anti-fade mounting medium (Vector Labs, UK),
xylene.

Haematoxylin-Eosin (H&E) Staining

i) Dewax in xylene for 30-60 sec (x2) (Omit for cryostat sections).
ii) Rehydrate in 70% IMS for 30-60 sec (x2).
iii) Immerse in running water for 3 min.
iv) Stain with Harris' haematoxylin (1:3 dilution) for 5 min.
v) Immerse in running water for 5 min.
vi) Immerse in acid alcohol (1% concentrated hydrochloric acid (v/v) in 70% IMS) for 1 min.
vii) Immerse in running water for 5 min.
viii) Stain with eosin for 30 sec.
ix) Immerse in running water for 5 min.
x) Dehydrate in 70% IMS for 30 sec (x2).
xi) Immerse in xylene (x2).
xii) Mount with DPX mounting media and a cover slip.
xiii) Dry at room temperature.

Indirect Immunohistochemical Staining

with example of staining for 3-NT in brackets:

i) Dewax in xylene for 30-60 sec (x2) (omit for cryostat sections!).
ii) Rehydrate in 70% IMS for 30-60 sec (x2).
iii) Rinse sections in PBS for 5 min (x2).
iv) Apply blocking medium (e.g. 5 mg BSA, 333 µl normal goat serum in 10 ml PBS) for 20 min at room temperature.
v) Discard excess medium.

vi) Apply primary antibody at a pre-determined optimum dilution in blocking medium (e.g. rabbit polyclonal anti-3-nitrotyrosine antibody; 1:100) and incubate in wet chamber at 8 °C overnight.

vii) Discard and rinse sections in PBS for 5 min (x2).

viii) Apply biotinylated secondary antibody (e.g. goat anti-rabbit immunoglobulin 1:100 in PBS) for 30 min at room temperature.

ix) Discard and rinse in PBS for 5 min (x2).

x) Apply avidin-bound enzyme probe (*e.g.* 2 drops from reagent A (*i.e.* avidin) and B (*i.e.* alkaline phosphatase) in 10 ml PBS from Vectastain® kit, prepared 30 min prior use) for exactly 30 min at room temperature.

xi) Discard and rinse in PBS for 5 min (x2).

xii) Apply Sigma Fast ® chromogenic enzyme substrate to cover whole section.

xiii) Observe the development of a red reaction product under the microscope and stop reaction by immersion in H_2O/dd.

xiv) Counterstain nuclei with Mayer's haematoxylin for 1 min.

xv) Immerse in running water for 5 min.

xvi) Mount with Aquamount® and coverslip.

xvii) Dry at room temperature.

Indirect Immunofluorescence Staining

with example of staining for 3-NT in brackets:

i) Fix air-dried cryo-stat sections with 4% formaldehyde (v/v) in PBS for 10 min.

ii) Rinse sections in PBS for 5 min (x2).

iii) Permeabilize sections in 0.3% Triton-X (v/v) in PBS for 10 min.

iv) Rinse sections in PBS for 5 min (x2).

v) Apply blocking medium (*e.g.* 5 mg BSA, 333 µl normal goat serum in 10 ml PBS) for 20 min at RT.

vi) Discard excess blocking medium.

vii) Apply primary antibody at a pre-determined optimum dilution in blocking medium (e.g. mouse monoclonal *anti*-3-nitrotyrosine antibody; 1:200) and incubate in wet chamber for 1 hr at RT.

viii) Discard medium and rinse sections in PBS for 5 min (x2).

ix) Apply FITC-conjugated secondary antibody (*e.g.* goat *anti*-mouse IgG FITC conjugate, 1:150 (v/v) in PBS) and incubate in wet chamber for 30 min at RT under light protection.

x) Discard medium and rinse sections in PBS for 5 min (x2).

xi) Counterstain nuclei with DAPI (diluted 1:5000 from stock in PBS) for 5 min at RT under continued light protection.

xii) Discard medium and rinse sections in H_2O/dd (x2).

xiii) Mount with Vectashield® anti-fade mounting medium and store light-protected at 4°C until fluorescence microscopy.

Appendix II: Materials and protocols for protein quantification according to Bradford (Bradford MM, 1976)

Materials & Solutions

dye reagent concentrate (Bio-Rad Labs, Hemel Hempstead, UK),
protein standard (1.4 mg BSA/ml; Bio-Rad Labs, Hemel Hempstead, UK),
96-well microtiter plates (Nunc, Fisher Scientific, UK),
microtiter plate reader (Dynex Revelation, US),
GraphPad® software programme (version 3.02, GraphPad Software Incorporated, US).

Assay

i) Prepare nine serial dilutions (1:2), beginning with 100 µg BSA / ml (from BSA standard) in H_2O/Q, in a 96-microwell plate (80 µl per well) for a standard concentration curve.

ii) Dilute test samples 1:100 or higher, if required, in H_2O/Q. Set up all standards and samples in triplicates.

iii) Add 20 µl dye reagent concentrate to each well with a multi-pipette.

iv) Read optical density at 595 nm after 5-10 min.

v) Generate a standard curve, which should have an $r > 0.95$ on linear regression in the concentration range, relevant to the test samples. Calculate the assay protein concentration of your samples from the mean absorbance. Consider any dilution factor, when calculating the protein concentration of the original sample.

Appendix III: Materials and protocols for SDS-PAGE electrophoresis and Western blot analysis

The method described is that for SDS- PAGE mini slab gels, followed by semi-dry protein transfer. Immunodetection uses primary antibody/ secondary antibody-HRP interaction, which is demonstrated by chemiluminescence on autoradiography.

Materials & solutions

Consumables were obtained from BDH, Poole, UK, unless otherwise stated.

Acrylamide (Bio-Rad Labs., Hemel Hampstead, UK),
Ammonium persulphate (AMPS; Sigma,UK),
autoradiography film (Hyperfilm™ ECL, Amersham Pharmacia Biotech Ltd, Little Chalfont, UK),
Bis (*N,N'*-methylene-bis-acrylamide; Bio-Rad Labs.),
bromophenol blue (Sigma, UK),
butan-2-ol,
ECL™ Western blotting detection reagents (Amersham Pharmacia Biotech Ltd, Little Chalfont, UK; #RPN 2106),
filter paper (Whatman, UK),
glycine (Sigma, UK),
2-ME (2-mercaptoethanol; Sigma, UK),
methanol (Sigma, UK),
nitrocellulose blotting paper (Hybond™ ECL, Amersham Pharmacia Biotech, UK),
rabbit polyclonal *anti*-3-nitrotyrosine antibody (TCS Biologicals, UK, #06-284),
nitrotyrosine immunoblotting control (TCS Biologicals, UK, #12-354),
non-fat, dried milk (Marvel™, UK),
Ponceau S dye (*red*, Sigma, UK),
Rainbow™ molecular weight (MW) markers, range 10-250 kDa (Amersham Int., Little Chalfont, UK),
SDS (sodium dodecyl sulfate, Sigma, UK),
sucrose,

swine *anti*-rabbit immunoglobulin/horse radish peroxidase (HRP) conjugate (Dako Ltd, UK; #P0217),

TEMED (*N,N,N',N'*-tetramethylenediamine; Sigma, UK),

Tris (tris(hydroxylmethyl)methylamine base; Promega, UK),

Tween-20 (polyoxyethylene (20) sorbitan monolaurate; Sigma, UK)

Hardware:

ATTO mini-PAGE chamber (Genetic Research Instr. Ltd, Rayne Braintree, UK),

ATTO semi-dry blotting tank (Genetic Research Instr. Ltd, UK),

DC power supply,

flat tweezers,

flat small plastic containers,

film cassette,

film developing facilities.

Stock solutions

All made in good water (at least H_2O/dd) and kept at 4°C, unless otherwise stated.

Gel buffers:

Separating gel buffer: 1.5 M (w/v) Tris, adjusted to pH 8.8 with conc. HCl,

Stacking gel buffer: 0.5 M (w/v) Tris, HCl, pH 6.8,

30 % acrylamide (29.2 g acrylamide plus 0.8 g Bis to 100 ml H_2O),

10 % (w/v) AMPS/ H_2O (prepare fresh!),

water-saturated butan-2-ol (i.e. 50 ml butan-2-ol plus 50 ml H_2O, mixed well and left to settle),

Reducing sample buffer:

2.0 g SDS,

20.0 g sucrose,

5.0 ml 2-ME,

7.5 ml 0.5 M Tris/HCl, pH 6.8,

10 mg bromophenyl blue,

in 67.5 ml H_2O;

Running buffer:

14.4 g glycine,

3.06 g Tris,

10.0 ml 10% (w/v) SDS in H_2O, to 1,000 ml H_2O;

Blotting buffer:

200 ml of 5 x conc. running buffer,

200 ml 100% methanol, to 1,000 ml H_2O,

Ponceau S protein staining solution (0.1% (w/v) in 1 % acetic acid),

TBS (Tris-buffered saline, 50 mM (w/v) Tris and 150 mM (w/v) NaCl in H_2O, adjusted to pH 7.6 with conc. HCl),

TBS/0.5% Tween-20.

SDS-PAGE electrophoresis

Wear gloves during all procedures. Use acrylamide, Bis, 2-ME and AMPS under exhaust vent.

i) Thoroughly clean glass plates with detergent and de-grease with acetone.

ii) Assemble glass plates, rubber gasket and clips and stand plates vertically.

iii) Prepare **separating gel**:

	8% *	**12.5%**
30% acrylamide	6.65 ml	10.30 ml
Tris/HCl, pH 8.8	6.25 ml	6.25 ml
10% SDS	0.25 ml	0,25 ml
H_2O	8.00 ml	11.65 ml,

degas for 10 min and then add:

TEMED	15 µl	15 µl
10% AMPS	150 µl	150 µl.

* used in this thesis, to separate proteins > 100 kDa.

iv) Pipette mixture between plate sandwich to about 2 cm from top avoiding air bubbles.

v) Overlay with water-saturated butan-2-ol (to remove gel meniscus) and leave at least 30 min to polymerize.

vi) Prepare **4% stacking gel**:

30% acrylamide	2.6 ml,
Tris/HCl, pH 6.8	5.0 ml,
10% SDS	0.1 ml,
H_2O	12.2 ml,

degas for 10 min and then add:

TEMED	15 µl,
10% AMPS	150 µl.

vii) Fill gel sandwich to the top with stacking gel and insert combs without trapping air and leave to polymerize.

viii) Pour running buffer into ATTO mini-PAGE chamber, carefully remove combs and rubber gaskets from gel plates and lower them into the chamber, avoiding trapped air bubbles. Fill up central chamber with running buffer.

ix) Prepare Rainbow™ MW markers, immunoblotting standards (*i.e.* nitrotyrosine immunoblotting control and 20 µg sample protein with an equal amount of reducing SDS sample buffer (NB: Total volume per gel well must not exceed 25 µl). Seal and place in boiling water bath for 3 min.

x) Add samples and controls into wells immediately and put lid onto ATTO chamber.

xi) Connect to DC power source and apply constant current of 20 mA/gel for approx. 2 hr or until the tracking dye bromophenol blue has reached the bottom of the gel).

xii) After turning off power and disassembling the plates, the gel is carefully removed and marked.

Western blot analysis

Wear gloves during all procedures.

Protein Transfer

i) Soak electrode pads in blotting buffer.

ii) Place gel carefully in blotting buffer.

iii) Cut gel-size pieces of nitrocellulose (NC) (1) and filter paper (8) and soak in blotting buffer.

iv) Starting from the *cathode* side, assemble the blotting cassette in the following order:

cathode pad
4 filter paper,
gel,
NC membrane,
4 filter paper,
anode pad,

avoiding air bubbles being trapped between layers.

v) Assemble semi-dry blotting apparatus and apply constant current 1 mA/ cm^2 gel for 2 hr.

vi) Disassemble apparatus and stain NC membrane for protein with Ponceau S solution for 1 min.

vii) Scan protein-stained NC and mark MW markers on membrane with sharp pencil.

Immuno-detection

The protocol uses the immuno-detection of 3-NT as an example.

i) Destain NC membrane in TBS/0.5% Tween-20.

ii) Block non-specific binding with 5% (w/v) dried milk/ TBS/0.5% Tween-20 for for 1 hr..

iii) Wash 10 min x 2 with TBS/0.5% Tween-20.

iv) Incubate with primary antibody (*i.e.* rabbit polyclonal *anti*-3-nitrotyrosine antibody, diluted 1:2000 in TBS/0.5% Tween-20) for 2 hr.

v) Wash 10 min x 2 with TBS/0.5% Tween-20.

vi) Incubate with secondary antibody/ HRP conjugate (*i.e.* swine anti-rabbit immunoglobulin/ HRP conjugate, 1:2000 in TBS/0.5% Tween-20) for 2 hr.

vii) Wash 10 min x 2 with TBS/0.5% Tween-20.

viii) Mix equal volume of ECL™ detection solution 1 and solution 2.

ix) Drain excess TBS/Tween and place NC membrane on cling film with protein-side facing up.

x) Apply detection solution to cover the whole of the membrane and incubate precisely for 1min at RT.

xi) Drain off excess detection solution and wrap NC membrane in cling film, smoothing out any air pockets.

xii) Place the wrapped NC membrane in a film cassette protein-side facing up.

xiii) In the darkroom, place a sheet of autoradiography film on top of the wrapped NC membrane, close cassette and expose initially for ca. 15 sec.

xiv) Develop film and determine further exposure times based on the 'signal-to-noise' ratio of the initial exposure.

Appendix IV: Materials and protocols for spectro-fluorimetric XOR activity assay (Beckman JS, *et al.*, 1989)

Material & solutions

Consumables were obtained from BDH, Poole, UK, unless otherwise stated.

Protease inhibitors:

aprotinin (from bovine lung, 7.8 IU/mg; Sigma, # A-1153,Poole, UK),
phenylmethylsulfonylfluoride (PMSF; Sigma; FW 174.2).

Reagent solutions:

allopurinol (Sigma, # A-8003; FW 136.1):

- 1mM solution in PBS, freshly prepared from a 10 mM solution (*i.e.* 1.36 mg/ml PBS after first dissolving allopurinol in small aliquot of 1M NaOH first),

isoxanthopterin (IXPt; Sigma, # I-7388, UK; FW 179.1):

- 10 μM solution in PBS, freshly prepared from a 10 mM solution (*i.e.* 1.79 mg/ ml PBS after first dissolving IxPt in small aliquot of 1M NaOH first),

methylene blue (Sigma, UK; FW 373.9):

- 1 mM solution in PBS (*i.e.* 3.74 mg / 10 ml PBS),

pterin (Sigma, # P-1132, UK; FW 163.1)

- 1 mM solution in PBS, freshly prepared from 10 mM solution (*i.e.* 1.63 mg/ml PBS after first dissolving pterin in small aliquot of 1M NaOH first).

All solutions, except methylene blue, must be freshly prepared daily and kept on ice and protected from light until immediate use.

Hardware:

desktop centrifuge (Biofuge Fresco, Heraeus Instruments, Germany),
quartz glass cuvettes (Fisher Scientific, UK),
polytron blender (Ultra-Turrax, Jenke&Kunkel, IKA Labortechnik, Germany),
spectro-fluorimeter F4500 (Hitachi, UK).

Sample preparation

Samples for the pterin assay were harvested from animals without delay in the following way:

- Plasma: Add blood 10:1 (v/v) to tri-sodium citrate (8mg/ml in H_2O/Q), gently mix, centrifuge (4 min at 5,000 rpm) and pipette the supernatant plasma off.
- Joint Tissue: Add dissected samples to ice-cold proteinase-inhibiting buffer (10 µg/ml Aprotinin, 1mM PMSF; in PBS) and homogenise with the polytron until easy to pipette. Short bursts of sonication ($\leq$ 5s, twice) may be used to achieve this. Centrifuge (10 min at 12,500 rpm, 8 °C) and take off clear supernatant.
- Liver: Prepare as joint tissue for comparative studies. Otherwise dissected samples may be snap-frozen in liquid nitrogen and homogenised as above at a later date.

All samples were stored at -70 °C until further processing.

The Pterin Assay

i) Allow the spectro-fluorimeter to equilibrate to 37.0 °C with the following settings: λ excitation/emission: 345/390 nm; photo-multiplier: 700 - 950 V, depending on sensitivity.

ii) Insert a quartz cuvette (cleaned in 1M HCL and rinsed in H_2O/Q, containing a small magnetic flea) into the spectro-fluorimeter (SPF).

iii) Add 920 µl PBS and 10 µl of the sample and the SPF will start to display graphically fluorescence over time.

iv) After stabilization of background fluorescence, add the following solutions sequentially at intervals sufficient to reach a linear or static change of fluorescence over time (1-3 min):

(final concentrations in parenthesis; total volume 1.0 ml)

- 20 µl 1mM pterin (20 µM),
- 10 µl 1mM methylene blue (10 µM),
- 20 µl 1mM allopurinol (20 µM),
- 20 µl 10 µM IXPt (200 nM).

v) Terminate the measurement once a static reference standard of fluorescence after adding IXPt has been reached. Generate a report via the software menu, showing fluorescence units for specific time points.

vi) Calculate from a mean of at least triplicate measurements, the enzyme activity U as µmol min^{-1} g^{-1} tissue protein as follows:

$$U = \{ dF \times [IXPt] / F_{IXPt} \} \times 0.001 \times V_c / (V_s \times T).$$

dF is the change of fluorescence units per minute, $[IXPt]$ is the final assay concentration of IXPt in nM, F_{IXPt} is the absolute increase of fluorescence units produced by the addition of IXPt, V_c is total assay volume in the cuvette in ml, V_s is the sample volume added to the cuvette in ml, and T is the tissue protein content in g per ml sample (as determined by the protein assay according to Bradford, see Appendix II).

Appendix V: Materials and protocols for XOR activity histochemistry (Kooij A, *et al.*, 1991)

Material & solutions

Consumables were obtained from BDH, Poole, UK, unless otherwise stated.
Except for phosphate buffer and buffered polyvinyl alcohol, which keeps in the fridge for several weeks, all incubation solutions were prepared daily fresh.

- 0.1 M phosphate buffer (PB, NaH_2PO_4/Na2HPO4 in H_2O/Q), pH 8.0 and pH 5.3,
- 18 % buffered polyvinyl alcohol (PVA; average FW 70,000-100,000; Sigma, # P-1763, Poole, UK) in 0.1 M PB, pH 8.0, dissolved by gentle heating,
- 50 mM tetranitro blue tetrazolium (TNBT, Sigma # T4000;FW 907.6; light-sensitive), supended in H_2O/Q,
- 18 mM 1-methoxyphenazine methosulfate (MPMS, Sigma #M8640; FW 336.4; light-sensitive), dissolved in H_2O/Q,
- 20 mM hypoxanthine (HXT, Sigma #H9377, FW 136.1): dissolve HXT in a small aliquot of 1 M NaOH and dilute in 0.1 M PB, pH 8.0,
- 20 mM allopurinol (Sigma #A8003, FW136.1): dissolve HXT in a small aliquot of 1 M NaOH and dilute in 0.1 M PB, pH 8.0,
- 400 mM sodium azide (Azide; BDH #103692K, FW65.01; highly toxic!), dissolved in. H_2O/Q,

Glycerol jelly.

Protocol

i) Prepare all solutions as above.

ii) Cut 8 µm serial sections on the cryotome and leave at -25 °C without fixation.

iii) Soften buffered PVA by heating to 37 °C and stir in the solutions in the following order (final concentrations in parenthesis):

TNBT:	1:10	(5mM)
MPMS:	1:40	(0.45 mM)
HXT:	1:40	(0.5 mM).

Prepare separate control incubation media:

a)	without HXT,			-to determine background activity;
b)	with allopurinol:	1:20	(1 mM),	- to inhibit XOR;
c)	with azide	1:40	(10 mM),	- to inhibit mitochondrial cytochromes as a source of interfering $O_2^{\cdot-}$.

iv) Apply incubation medium onto the sections with a wooden applicator and incubate in the dark at 37 °C for 30 min.

v) Wash sections twice in 60 °C warm 0.1 mM PB, pH 5.3 to terminate reaction and remove the viscous incubation medium.

vi) Wash in H_2O/dd and rinse sections with acetone (to fix sections and remove unbound pink monoformazan).

vii) Mount sections with glycerol jelly (liquified in a microwave) and protects from excessive light exposure until microscopy.

Appendix VI: Materials for experimental animal work

Consumables:

(from Sigma, Poole, UK, unless otherwise stated)

allopurinol (# A-8003),
complete Freund's adjuvant (CFA; # F-5881),
methylated bovine serum albumin (mBSA; # A-1009),
normal protein rat chow, supplemented with sodium tungstate (0.7 g/kg; ICN, Basingstoke, UK; # 960350),
standard rat chow (SDS, Witham, UK),
sodium carboxymethylcellulose (medium viscosity; # C-4888),
0.9 % sodium chloride (aqueous, for injection) (0.9 % NaCL; Braun, UK).

Hardware:

digital weighing scales (Sartorius BP 1200; BS Blance Service, Worthing, UK),
digital calipers (Mitutoyo, Andover, Hampshire, UK).

References

Abadeh S, Case PC, Harrison R. Purification of xanthine oxidase from human heart. Biochem Soc Trans 1993;21:99S.

Abadeh S, Killacky J, Benboubetra M, Harrison R. Purification and partial characterization of xanthine oxidase from human milk. Biochim Biophys Acta 1992;1117:25-32.

Aigner T, Kim HA. Apoptosis and cellular vitality: issues in osteoarthritic cartilage degeneration. Arthritis Rheum 2002;46:1986-1996.

Albina JE. On the expression of nitric oxide synthase by human macrophages. Why no NO? J Leukoc Biol 1995;58:643-649.

Allen RE, Blake DR, Nazhat NB, Jones P. Superoxide radical generation by inflamed human synovium after hypoxia. Lancet 1989;2:282-283.

Allen RE, Outhwaite JM, Morris CJ, Blake DR. Xanthine oxidoreductase is present in human synovium. Ann Rheum Dis 1987;46:843-845.

Altman DG. Some common problems in medical research. In: Practical statistics for medical research. London :Chapman&Hall, 1991:396-439.

Ames BN, Cathcart R, Schwiers E, Hochstein P. Uric acid provides an antioxidant defense in humans against oxidant- and radical-caused aging and cancer: a hypothesis. Proc Natl Acad Sci U S A 1981;78:6858-6862.

Amin AR, Attur M, Patel RN, Thakker GD, Marshall PJ, Rediske J *et al.* Superinduction of cyclooxygenase-2 activity in human osteoarthritis-affected cartilage. Influence of nitric oxide. J Clin Invest 1997;15:1231-1237.

Amin R, Di Cesare PE, Vyas P, Attur M, Tzeng E, Billiar TR *et al.* The expression and regulation of nitric oxide synthase in human osteoarthritis-affected chondrocytes: evidence for up-regulated neuronal nitric oxide synthase. J Exp Med 1995;182:2097-2102.

Anathasou NA. Synovial macrophages. Ann Rheum Dis 1995;54:392-394.

Aulak KS, Miyagi M, Yan L, West KA, Massillon D, Crabb JW *et al.* Proteomic method identifies proteins nitrated in vivo during inflammatory challenge. Proc Natl Acad Sci U S A 2001;98:12056-12061.

Babior BM. Oxygen dependent microbial killing by phagocytes (in two parts). N Engl J Med 1978;298:659, 721-668, 725.

Bachschmid M, Thurau S, Zou MH, Ullrich V. Endothelial cell activation by endotoxin involves superoxide/NO-mediated nitration of prostacyclin synthase and thromboxane receptor stimulation. FASEB J 2003;17:914-916.

Balafanova Z, Bolli R, Zhang J, Zheng Y, Pass JM, Bhatnagar A *et al.* Nitric oxide induces nitration of protein kinase C epsilon, facilitating PKC epsilon translocation via enhanced PKC epsilon -RACK2 interactions. J Biol Chem 2002;277:15021-15027.

Beckman JS, Chen J, Ischiropoulos H, Crow JP. Oxidative chemistry of peroxynitrite. Methods Enzymol 1994a;233:229-240.

Beckman JS, Parks DA, Pearson JD, Marshall PA, Freeman PA. A sensitive fluorometric assay for measuring xanthine dehydrogenase and oxidase in tissues. Free Radic Biol Med 1989;6:607-615.

Beckman JS, Ye YZ, Anderson PG, Chen J, Accavitti MA, Tarpey MM *et al.* Extensive nitration of protein tyrosines in human atherosclerosis detected by immunohistochemistry. Biol Chem Hoppe Seyler 1994b;375:81-88.

Berry CE, Hare JM. Xanthine oxidoreductase and cardiovascular disease: molecular mechanisms and pathophysiological implications. J Physiol 2004;555:589-606.

Bezerra MM, Brain SD, Greenacre S, Jeronimo SM, De Melo LB, Keeble J *et al.* Reactive nitrogen species scavenging, rather than nitric oxide inhibition, protects from articular cartilage damage in rat zymosan-induced arthritis. Br J Pharmacol 2004;141:172-182.

Bird JLE, May S, Bayliss MT. Nitric oxide inhibits aggrecan degradation in explant cultures of equine articular cartilage. Equine Vet J 2000;32:133-139.

Blake DR, Merry P, Unsworth J, Kidd BL, Outhwaite JM, Ballard R *et al.* Hypoxic-reperfusion injury in the inflamed human joint. Lancet 1989;1:289-293.

Blanco FJ, Ochs RL, Schwarz H, Lotz M. Chondrocyte apoptosis induced by nitric oxide. Am J Pathol 1995;146:75-85.

Boer R, Ulrich WR, Klein T, Mirau B, Haas S, Baur I. The inhibitory potency and selectivity of arginine substrate site nitric-oxide synthase inhibitors is solely determined by their affinity toward the different isoenzymes. Mol Pharm 2000;58:1026-1034.

Bonnet CS, Walsh DA. Osteoarthritis, angiogenesis and inflammation. Rheumatology 2005;44:7-16.

Boota A, Zar H, Kim YM, Johnson B, Pitt B, Davies P. IL-1 beta stimulates superoxide and delayed peroxynitrite production by pulmonary vascular smooth muscle cells. Am J Path 1996;271:L932-L938.

Boulanger CM, Heymes C, Benessiano J, Geske RS, Levy BI, Vanhoutte PM. Neuronal nitric oxide synthase is expressed in rat vascular smooth muscle cells: activation by angiotensin II in hypertension. Circ Res 1998;83:1271-1278.

Brackertz D, Mitchell GF, Mackay IR. Antigen-induced arthritis in mice. I. Induction of arthritis in various strains of mice. Arthritis Rheum 1977;20:841-850.

Bradford MM. A rapid and sensitive method for the quantitation of microgram quantities of protein utilizing the principle of protein-dye binding. Anal Biochem 1976;72:248-254.

Brandt KD. Animal models of osteoarthritis. Biorheology 2002;39:221-235.

Brennan ML, Wu W, Fu X, Shen Z, Song W, Frost H *et al.* A Tale of Two Controversies. Defining both the role of peroxidases in nitrotyrosine formation in vivo using eosinophil peroxidase and myeloperoxidase-deficient mice, and the nature of peroxidase-generated reactive nitrogen-species. J Biol Chem 2002;277:17415-17427.

Brito C, Naviliat M, Tiscornia AC, Gualco G, Dighiero G, Radi R *et al.* Peroxynitrite inhibits T lymphocyte activation and proliferation by promoting impairment of tyrosine phosphorylation and peroxynitrite-driven apoptotic death. J Immunol 1999;162:3356-3366.

Brunelli L, Crow JP, Beckman JS. The comparative toxicity of nitric oxide and peroxynitrite to Escherichia coli. Arch Biochem Biophys 1995;316:327-334.

Campbell WH, Kinghorn KR. Functional domains of assimilatory nitrate reductases and nitrite reductases. Trends Biochem Sci 1990;15:315-319.

Cannon GW, Openshaw SJ, Hibbs JBJ, Hoidal JR, Huecksteadt TP, Griffiths MM. Nitric oxide production during adjuvant-induced and collagen-induced arthritis. Arthritis Rheum 1996;39:1677-1684.

Capelletti G, Tedeschi G, Maggioni MG, Negri A, Nonnis S, Maci R. The nitration of tau protein in neurone-like PC12 cells. FEBS Lett 2004;562:35-39.

Carlo MD, Loeser RF. Increased oxidative stress with aging reduces chondrocyte survival: correlation with intracellular glutathione levels. Arthritis Rheum 2003;48:3419-3430.

Carreras MC, Pargament GA, Catz SD, Poderoso JJ, Boveris A. Kinetics of nitric oxide and hydrogen peroxide production and formation of peroxynitrite during the respiratory burst of human neutrophils. FEBS Lett 1994;341:65-68.

Carroll RT, Galatsis P, Borosky S, Kopec KK, Kumar V, Althaus JS *et al.* 4-Hydroxy-2,2,6,6-tetramethylpiperidine-1-oxyl (Tempol) inhibits peroxynitrite-mediated phenol nitration. Chem Res Toxicol 2000;13:294-300.

Cassina AM, Hodara R, Souza JM, Thomson L, Castro L, Ischiropoulos H *et al.* Cytochrome c nitration by peroxynitrite. J Biol Chem 2000;275:21409-21415.

Clark RL, Cuttino JTJ, Anderle SK, Cromartie WJ, Schwab JH. Radiologic analysis of arthritis in rats after systemic injection of streptococcal cell walls. Arthritis Rheum 1979;22:25-35.

Coimbra IB, Jiminez SA, Hawkins DF, Piera-Velazquez S, Stokes DG. Hypoxia inducible factor-1 alpha expression in human normal and osteoarthritic chondrocytes. Osteoarthritis Cart 2004;12:336-345.

Cotran RS, Kumar V, and Collins T, Robbins pathologic basis of disease. In: WB Saunders, 1999.

Cromartie WJ, Craddock JG, Schwab JH, Anderle SK, Yang C. Arthritis in rats after systemic injection of streptococcal cells or cell walls. J Exp Med 1977;146:1585-1602.

Crowley JR, Yarasheski K, Leeuwenburgh C, Turk J, Heinecke JW. Isotope dilution mass spectrometric quantification of 3-nitrotyrosine in proteins and tissues is facilitated by reduction to 3-aminotyrosine. Anal Biochem 1998;259:127-135.

Cuzzocrea S, McDonald MC, Mota-Filipe H, Mazzon E, Costantino G, Britti D *et al.* Beneficial effects of tempol, a membrane-permeable radical scavenger, in a rodent model of collagen-induced arthritis. Arthritis Rheum 2000;43:320-328.

Dai L, Claxson A, Marklund SL, Feakins R, Yousaf N, Chernajovski Y *et al.* Amelioration of antigen-induced arthritis in rats by transfer of extra-cellular superoxide dismutase and catalase genes. Gene Ther 2003;10:550-558.

Del Carlo MJ, Loeser RF. Nitric oxide-mediated chondrocyte cell death requires the generation of additional reactive oxygen species. Arthritis Rheum 2002;46:394-403.

Della Corte E, Gozzetti G, Novello F, Stirpe F. Properties of the xanthine oxidase from human liver. Biochim Biophys Acta 1969;191:164-166.

Denicola A, Freeman BA, Trujillo M, Radi R. Peroxynitrite reaction with carbon dioxide/bicarbonate: kinetics and influence on peroxynitrite-mediated oxidations. Arch Biochem Biophys 1996;333:49-58.

Doherty M, Jones A, and Cawston TE. Osteoarthritis. In: Maddison, P. J., Isenberg, D. A., Woo, P., and Glass, D. N.eds.Oxford Textbook of Rheumatology. Oxford University Press, 1998:1515-1553.

Dumonde DC, Glynn LE. The production of arthritis in rabbits by an immunological reaction to fibrin. Brit J Exp Path 1962;43:373-383.

Eiserich JP, Cross CE, Jones AD, Halliwell B, van der Vliet A. Formation of nitrating and chlorinating species by reaction of nitrite and hypochlorous acid. J Biol Chem 1996;32:19199-19208.

Enroth C, Eger BT, Okamoto K, Nishino T, Nishino T, Pai E. Crystal structures of bovine milk xanthine dehydrogenase and xanthine oxidase: Structure-based mechanism of conversion. Proc Natl Acad Sci U S A 2000;97:10723-10728.

Estevez AG, Spear N, Manuel SM, Radi R, Henderson CE, Barbeito L *et al.* Nitric oxide and superoxide contribute to motor neuron apoptosis induced by trophic factor deprivation. J Neurosci 1998;18:923-931.

Fang FC. Mechanisms of nitric-oxide-related antimicrobial activity. J Clin Invest 1997;99:2818-2825.

Farrell AJ, Blake DR, Palmer RM, Moncada S. Increased concentrations of nitrite in synovial fluid and serum samples suggest increased nitric oxide synthesis in rheumatic diseases. Ann Rheum Dis 1992;51:1219-1222.

Felson DT, Neogi T. Osteoarthritis: is it a disease of cartilage or bone? Arthritis Rheum 2004;50:341-344.

Firestein GS, Alvaro-Garcia JM, Maki R, Alvaro-Garcia JM. Quantitative analysis of cytokine gene expression in rheumatoid arthritis. J Immunol 1990;144:3347-3353.

Fletcher DS, Widmer WR, Luell S, Christen A, Orevillo C, Shah S *et al.* Therapeutic administration of a selective inhibitor of nitric oxide synthase does not ameliorate the chronic inflammation and tissue damage associated with adjuvant-induced arthritis in rats. J Pharmacol Exp Ther 1998;284:714-721.

Förstermann U, Closs EI, Pollok JS, Nakane M, Schwarz P, Gath I *et al.* Nitric oxide synthase isozymes. Characterization, purification, molecular cloning, and functions. Hypertension 1994;23:1121-1131.

Förstermann U, Dun N. Immunohistochemical localization of nitric oxide synthases. Methods Enzymol 1996;268:510-515.

Franze T, Weller MG, Niessner R, Poschl U. Comparison of nitrotyrosine antibodies and development of immunoassays for the detection of nitrated proteins. Analyst 2004;129:589-596.

Frederiks WM, Bosch KS. Localization of superoxide dismutase activity in rat tissues. Free Radic Biol Med 1997;22:241-248.

Frederiks WM, Bosch KS, Kooij A. Quantitative in situ analysis of xanthine oxidoreductase activity in rat liver. J Histochem Cytochem 1995;43:723-726.

Freemont AJ. Histopathology of the rheumatoid joint. In: Henderson, B., Edwards, J. C. W., and Pettipher, E. R.eds.Mechanisms and models of arthritis. London :Academic Press, 1995:83-113.

Freudenberger RS, Schwarz JPJ, Brown J, Moore A, Mann D, Givertz MM *et al.* Rationale, design and organisation of an efficacy and safety study of oxypurinol added to standard therapy in patients with NYHA class III - IV congestive heart failure. Expert Opin Investig Drugs 2004;13:1509-1516.

Fridovich I, Hansert B. Xanthine oxidase.V. Differential inhibition of the reduction of various electron acceptors. J Biol Chem 1962;237:916-921.

Frost MT, Halliwell B, Moore KP. Analysis of free and protein-bound nitrotyrosine in human plasma by a gas chromatography/ mass spectrometry method that avoids nitration artifacts. Biochem J 2000;345:453-458.

Fujii K, Tsuji M, Tajima M. Rheumatoid arthritis: a synovial disease? Ann Rheum Dis 1999;58:727-730.

Gaston B. Nitric oxide and thiol groups. Biochim Biophys Acta 1999;1411:323-333.

Gaut JP, Byun J, Tran HD, Lauber WM, Carroll JA, Hotchkiss RS *et al.* Myeloperoxidase produces nitrating oxidants in vivo. J Clin Invest 2002;109:1311-1319.

Gilroy DW, Colville-Nash PR, Willis D, Chivers J, Paul-Clark MJ, Willoughby DA. Inducible cyclooxygenase may have anti-inflammatory properties. Nat Med 1999;5:698-701.

Godber BJL, Doel JJ, Sapkota GP, Blake DR, Stevens CR, Eisenthal R *et al.* Reduction of nitrite to nitric oxide catalyzed by xanthine oxidoreductase. J Biol Chem 2000;275:7757-7763.

Goldstein S, Czapski G, Lind J, Merenyi G. Tyrosine nitration by simultaneous generation of (.)NO and O-(2) under physiological conditions. How the radicals do the job. J Biol Chem 2000;275:3031-3036.

Gow AJ, Duran D, Malcolm S, Ischiropoulos H. Effects of peroxynitrite-induced protein modifications on tyrosine phophorylation and degradation. FEBS Lett 1996;385:63-66.

Grabowski PS, Macpherson H, Ralston SH. Nitric oxide production in cells derived from the human joint. Br J Rheumatol 1996;35:207-212.

Grabowski PS, Wright PK, Van't Hof RJ, Helfrich MH, Oshima H, Ralston SH. Immunolocalization of inducible nitric oxide synthase in synovium and cartilage in rheumatoid arthritis and osteoarthritis. Br J Rheumatol 1997;36:651-655.

Greenacre SA, Ischiropoulos H. Tyrosine nitration: localisation, quantification, consequences for protein function and signal transduction. Free Radic Res 2001;34:541-581.

Griendling KK, Minieri CA, Ollerenshaw JD, Alexander RW. Angiotensin II stimulates NADH and NADPH oxidase activity in cultures vascular smooth muscle cells. Circ Res 1994;74:1141-1148.

Griffiths RJ. Characterisation and pharmacological sensitivity of antigen arthritis induced by methylated bovine serum albumin in the rat. Agents Actions 1992;35:88-95.

Grisham MB, Jourd'heuil D, Wink DA. Nitric oxide I. Physiological chemistry of nitric oxide and its metabolites: implications in inflammation. Am J Physiol 1999;276:G315-G321.

Groves JT. Peroxynitrite: reactive, invasive and enigmatic. Curr Opin Chem Biol 1999;3:226-235.

Grune T, Blasig IE, Sitte N, Roloff B, Haseloff R, Davies KJ. Peroxynitrite Increases the Degradation of Aconitase and Other Cellular Proteins by Proteasome. J Biol Chem 1998;273:10857-10862.

Gunther MR, Hsi LC, Curtis JF, Gierse JK, Marnett LJ, Eling TE *et al.* Nitric Oxide Trapping of the Tyrosyl Radical of Prostaglandin H Synthase-2 Leads to Tyrosine Iminoxyl Radical and Nitrotyrosine Formation. J Biol Chem 1997;272:17086-17090.

Halliwell B. Oxygen radicals, nitric oxide and human inflammatory joint disease. Ann Rheum Dis 1995;54:505-510.

Halliwell B. What nitrates tyrosine? Is nitrotyrosine specific as a biomarker of peroxynitrite in vivo? FEBS Lett 1997;411:157-160.

Halliwell B, Gutteridge JMC. Free radicals in biology and medicine.3rd edtion, Oxford University Press, UK. 1999;

Hardingham T. Articular cartilage. In: Maddison, P. J., Isenberg, D. A., Woo, P., and Glass, D. N.eds.Oxford Textbook of Rheumatology. OUP, 1998:405-420.

Hashimoto S, Takahashi K, Amiel D, Coutts RD, Lotz M. Chondrocyte apoptosis and nitric oxide production during experimentall induced osteoarthritis. Arthritis Rheum 1998;41:1266-1274.

Hasselbacher P. Joint physiology. In: Hochberg, M. C., Silman, A. J., Smolen, J. S., Weinblatt, M. E. *et al.*eds.Rheumatology. Mosby, 2003:69-74.

Hayashi T, Abe E, Yamate T, Taguchi Y, Jasin HE. Nitric oxide production by superficial and deep articular chondrocytes. Arthritis Rheum 1997;40:261-269.

Hellsten-Westing Y. Immunohistochemical localisation of xanthine oxidase in human cardiac and skeletal muscle. Histochemistry 1993;100:215-222.

Henrotin YE, Zheng SX, Deby GP, Labasse AH, Crielaard JM, Reginster JY. Nitric oxide downregulates interleukin 1beta (IL-1beta) stimulated IL-6, IL-8, and prostaglandin E2 production by human chondrocytes. J Rheumatol 1998;25:1595-1601.

Herce-Pagliai C, Kotecha S, Shuker DEG. Analytical methods for 3-nitrotyrosine as a marker of exposure to reactive nitrogen species: a review. Nitric Oxide 1998;2:324-336.

Hibbs JBJ, Taintor RR, Vavrin Z. Macrophage cytotoxicity: role for L-arginine deiminase and imino nitrogen oxidation to nitrite. Science 1987;235:473-476.

Hille R, Nishino T. Flavoprotein structure and mechanism. 4. Xanthine oxidase and xanthine dehydrogenase. FASEB J 1995;9:995-1003.

Hochberg MC, Rheumatology. In: Hochberg, M. C., Silman, A. J., Smolen, J. S., Weinblatt, M. E. *et al.*eds.Mosby, 2003.

Honda S, Migita K, Hirai Y, Ueki Y, Yamasaki S, Urayama S *et al.* Induction of COX-2 expression by nitric oxide in rheumatoid synovial cells. Biochem Biophys Res Commun 2000;268:928-931.

Hooper DC, Spitsin S, Kean RB, Champion JM, Dickson GM, Chaudhry I *et al.* Uric acid, a natural scavenger of peroxynitrite, in experimental allergic encephalomyelitis and multiple sclerosis. Proc Natl Acad Sci U S A 1998;95:675-680.

Huang FP, Dawson TM, Bredt DS, Snyder SH, Fishman MC. Targeted disruption of the neuronal nitric oxide synthase gene. Cell 1993;75:1273-1286.

Huang PL, Huang Z, Mashimo H, Bloch KD, Moskowitz MA, Bevan JA *et al.* Hypertension in mice lacking the gene for endothelial nitric oxide synthase. Nature 1995;377:239-242.

Huber A, Suar D, Kurjak M, Schusdziarra V, Allescher HD. Characterization and splice variants of neuronal nitric oxide synthase in rat small intestine. Am J Physiol 1998;275:G1146-G-1156.

Ichida K, Amaya Y, Kamatani N, Nishino T, Hosoya T, Sakai O. Identification of two mutations in human xanthine dehydrogenase gene responsible for classical type I xanthinuria. J Clin Invest 1997;99:2391-2397.

Ichida K, Amaya Y, Noda K, Minoshima S, Hosoya T, Sakai O *et al.* Cloning of the cDNA encoding human xanthine dehydrogenase (oxidase): structural analysis of the protein and chromosomal location of the gene. Gene 1993;133:279-284.

Ignarro LJ. Signal transduction mechanisms involving nitric oxide. Biochem Pharmacol 1991;41:485-490.

Ischiropoulos H. Biological tyrosine nitration: a pathophysiological function of nitric oxide and reactive oxygen species. Arch Biochem Biophys 1998;356:1-11.

Ischiropoulos H. Biological selectivity and functional aspects of protein tyrosine nitration. Biochem Biophys Res Commun 2003;305:776-783.

Ischiropoulos H, Zhu L, Beckman JS. Peroxynitrite formation from macrophage-derived nitric oxide. Arch Biochem Biophys 1992a;298:446-451.

Ischiropoulos H, Zhu L, Chen J, Tsai M, Martin JC, Smith CD *et al.* Peroxynitrite-mediated tyrosine nitration catalyzed by superoxide dismutase. Arch Biochem Biophys 1992b;298:431-437.

Jarasch ED, Bruder G, Heid HW. Significance of xanthine oxidase in capillary endothelial cells. Acta Physiol Scand Suppl 1986;548:39-46.

Johnson JL, Rajagopalan KV, Cohen HJ. Molecular basis of the biological function of molybdenum. Effect of tungsten on xanthine oxidase and sulphite oxidase in the rat. J Biol Chem 1974;249:859-866.

Jones OTG and Hancock JT, The NADPH oxidase of neutrophils and other cells. In: Winyard, P. G., Blake, D. R., and Evans, C. H.eds.Free radicals and inflammation. Basel :Birkhäuser, 2000.

Kamisaki Y, Wada K, Bian K, Balabanli B, Davis K, Martin E *et al.* An activity in rat tissues that modifies nitrotyrosine-containing proteins. Proc Natl Acad Sci U S A 1998;95:11584-11589.

Kanczler JM, Millar TM, Bodamyali T, Blake DR, Stevens CR. Xanthine oxidase mediates cytokine-induced, but not hormone-induced bone resorption. Free Radic Res 2003;37:179-187.

Kanski J, Behring A, Pelling J, Schöneich C. Proteomic identification of 3-nitrotyrosine-containing rat cardiac proteins: effect of biological aging. Am J Physiol Heart Circ Physiol 2004;288:H371-H381.

Kaur H, Halliwell B. Evidence for nitric oxide-mediated oxidative damage in chronic inflammation. Nitrotyrosine in serum and synovial fluid from rheumatoid patients. FEBS Lett 1994;350:9-12.

Kelm M. Nitric oxide metabolism and breakdown. Biochim Biophys Acta 1999;1411:273-289.

Khan J, Brennand DM, Bradley N, Gao B, Bruckdorfer R, Jacobs M. 3-Nitrotyrosine in the proteins of human plasma determined by an ELISA method. Biochem J 1998;330:795-801.

Kissner R, Nause T, Bugnon P, Lye PG, Koppenol WH. Formation and properties of peroxynitrite as studied by laser flash photolysis, high-pressure stopped-flow technique, and pulse radiolysis. Chem Res Toxicol 1998;10:1285-1292.

Koeck T, Fu X, Hazen SL, Crabb JW, Stuehr DJ, Aulak KS. Rapid and selective oxygen-regulated protein tyrosine denitration and nitration in mitochondria. J Biol Chem 2004;279:27257-27262.

Kooij A, Bosch KS, Frederiks WM, van Noorden CJ. High levels of xanthine oxidoreductase in rat endothelial , epithelial and connective tissue cells. A relation

between localization and function? Virchows Arch B Cell Pathol Incl Mol Pathol 1992a;62:143-150.

Kooij A, Frederiks WM, Gossrau R, van Noorden CJF. Localisation of xanthine oxidoreductase activity using the tissue protectant polyvinyl alcohol and final electron acceptor tetranitro BT. J Histochem Cytochem 1991;39:87-93.

Kooij A, Schijns M, Frederiks WM, van Noorden CJ, James J. Distribution of xanthine oxidoreductase activity in human tissues - a histochemical and biochemical study. Virchows Arch B Cell Pathol Incl Mol Pathol 1992b;63:17-23.

Kooy NW, Royall JA. Agonist-induced peroxynitrite production from endothelial cells. Arch Biochem Biophys 1994;310:352-359.

Kooy NW, Royall JA, Ischiropoulos H, Beckman JS. Peroxynitrite-mediated oxidation of dihydrorhodamine 123. Free Radic Biol Med 1994;16:149-156.

Koppenol WH. The basic chemistry of nitrogen monoxide and peroxynitrite. Free Radic Biol Med 1998;25:385-391.

Kruijsen MWM, van den Berg WB, van de Putte LBA. Sequential alterations of periarticular structures in antigen-induced arthritis in mice. Histological observations on fibrous capsule, ligaments, bone and muscles, using whole joint sections. Br J Exp Path 1983;64:298-305.

Kuhn DM, Sadidi M, Liu X, Kreipke C, Geddes T, Borges C *et al.* Peroxynitrite-induced Nitration of Tyrosine Hydroxylase. Identification of tyrosines 423, 428, and 432 as sites of modification by matrix-assisted laser desorption ionization time-of-flight mass spectrometry and tyrosine scanning mutagenesis. J Biol Chem 2002;277:14336-14342.

Kuo WN, Kanadia RN, Shanbhag WP, Toro R. Denitration of peroxynitrite-treated proteins by 'protein nitratases' from rat brain and heart. Mol Cell Biochem 1999;201:11-16.

Laude K, Thuillez C, Richard V. Peroxynitrite triggers a delayed resistance of coronary endothelial cells against ischaemia-reperfusion injury. Am J Physiol Heart Circ Physiol 2002;283:H1418-H1423.

Lefer DJ, Scalia R, Campbell B, Nossuli T, Hayward R, Salamon M *et al.* Peroxynitrite inhibits leukocyte-endothelial cell interactions and protects against ischemia-reperfusion injury in rats. J Clin Invest 1997;99:684-691.

Levick JR. An investigation into the validity of subatmospheric pressure recordings from synovial fluid and their dependence on joint angle. J Physiol 1979;289:55-67.

Li H, Samouilov A, Liu X, Zweier JL. Characterization of the magnitude and kinetics of xanthine oxidase-catalyzed nitrite reduction. Evaluation of its role in nitric oxide generation in anoxic tissues. J Biol Chem 2001;276:24482-24489.

Linder N, Rapola J, Raivio KO. Cellular expression of xanthine oxidoreductase in normal human tissue. Lab Invest 1999;79:967-974.

Loeser RF, Carlson CS, Del Carlo M, Cole A. Detection of nitrotyrosine in aging and osteoarthritic cartilage: Correlation of oxidative damage with the presence of interleukin-1beta and with chondrocyte resistance to insulin-like growth factor 1. Arthritis Rheum 2002;46:2349-2357.

MacMillan-Crow LA, Crow JP, Kerby JD, Beckman JS, Thompson JA. Nitration and inactivation of manganese superoxide dismutase in chronic rejection of human renal allografts. Proc Natl Acad Sci U S A 1996;93:11853-11858.

Maier R, Bilbe G, Rediske J, Lotz M. Inducible nitric oxide synthase from human articular chondrocytes: cDNA cloning and analysis of mRNA expression. Biochim Biophys Acta 1994;1208:145-150.

Mallozzi C, Di Stasi AM, Minettio M. Nitrotyrosine mimics phophotyrosine binding to the SH2 domain of the src family of tyrosine kinase lyn. FEBS Lett 2001;503:189-195.

Mankin HJ. The reaction of articular cartilage to injury and osteoarthritis (2 parts). N Engl J Med 1974;291:1285, 1335-1292, 1340, respectively.

Mapp PI, Grootveld MC, Blake DR. Hypoxia, oxidative stress and rheumatoid arthritis. Br Med Bull 1995;51:419-436.

Mapp PI, Klocke R, Walsh DA, Chana JK, Stevens CR, Gallagher PJ *et al.* Localization of 3-nitrotyrosine to rheumatoid and normal synovium. Arthritis Rheum 2001;44:1534-1539.

Mapp PI, Terenghi G, Walsh DA, Chen ST, Cruwys SC, Garrett N *et al.* Monoarthritis in the rat knee induces bilateral and time-dependent changes in substance P and calcitonin gene-related peptide immunoreactivity in the spinal cord. Neuroscience 1993;57:1091-1096.

Massey V, Komai H, Palmer G, Elion GB. On the mechanism of inactivation of xanthine oxidase by allopurinol and other pyrazolo[3,4-d]pyrimidines. J Biol Chem 1970;245:2837-2844.

Matsuo M, Nishida K, Yoshida A, Murakami T, Inoue H. Expression of caspase-3 and -9 relevant to cartilage destruction and chondrocyte apoptosis in human osteoarthritic cartilage. Acta Med Okayama 2001;55:333-340.

Mayer B, Schrammel A, Klatt P, Koesling D, Schmidt K. Peroxynitrite-induced accumulation of cyclic GMP in endothelial cells and stimulation of purified soluble guanylyl cyclase. Dependence on glutathione and possible role of S-nitrosation. J Biol Chem 1995;270:17355-17360.

McCartney-Francis N, Allen JB, Mizel DE, Albina JE, Xie QW, Nathan CF *et al.* Suppression of arthritis by an inhibitor of nitric oxide synthase. J Exp Med 1993;178:749-754.

McCartney-Francis NL, Song XY, Mizel DE, Wahl SM. Selective inhibition of inducible nitric oxide synthase exacerbates erosive joint disease. J Immunol 2001;166:2734-2740.

McCord JM. Oxygen-derived free radicals in postischemic tissue injury. N Engl J Med 1985;312:159-163.

McInnes IB, Leung B, Wei XQ, Gemmell CC, Liew FY. Septic arthritis following staphylococcus aureus infection in mice lacking inducible nitric oxide synthase. J Immunol 1998;160:308-315.

McInnes IB, Leung BP, Field M, Wei XQ, Huang FPSRD, Kinninmonth A *et al.* Production of nitric oxide in the synovial membrane of rheumatoid and osteoarthritis patients. J Exp Med 1996;184:1519-1524.

McKusick VA. Molybdenum cofactor deficiency. 2004. http://www.ncbi.nlm.nih.gov/entrez/dispomim.cgi?id=252150 (29/Dec./2004).

McKusick VA. Nitric oxide synthase 1; NOS1. 2005a. http://www.ncbi.nlm.nih.gov/entrez/dispomim.cgi?id=163731 (31/July/2005a).

McKusick VA. Nitric oxide synthase 2a. 2005b. http://www.ncbi.nlm.nih.gov/entrez/dispomim.cgi?id=163730 (31/July/2005c).

McKusick VA. Nitric oxide synthase 3. 2005c. http://www.ncbi.nlm.nih.gov/entrez/dispomim.cgi?id=163729 (31/July/2005d).

McKusick VA. Xanthine dehydrogenase, XDH. 2005d. http://www.ncbi.nlm.nih.gov/entrez/dispomim.cgi?id=607633 (31/July/2005e).

McLean L. The pathogenesis of gout. In: Hochberg, M. C., Silman, A. J., Smolen, J. S., Weinblatt, M. E. *et al.*eds.Rheumatology. Mosby, 2003:1903-1918.

McQueen FM, Stewart N, Crabbe J, Robinson E, Yeoman S, Tan PL *et al.* Magnetic resonance imaging of the wrist in early rheumatoid arthritis reveals progression of erosions despite clinical improvement. Ann Rheum Dis 1999;58:156-163.

Melchiorri C, Meliconi R, Frizziero L, Silvestri T, Pulsatelli L, Mazzetti I *et al.* Enhanced and coordinated in vivo expression of inflammatory cytokines and nitric oxide synthase by chondrocytes from patients from osteoarthritis. Arthritis Rheum 1998;41:2165-2174.

Meng W, Ma J, Ayata C, Hara H, Huang PL, Fishman MC *et al.* ACh dilates pial arterioles in endothelial and neuronal NOS knockout mice by NO-dependent mechanisms. Am J Physiol 1996;271:H1145-H1150.

Miles AM, Bohle DS, Glassbrenner PA, Hansert B, Wink DA, Grisham MB. Modulation of superoxide-dependent oxidation and hydroxylation reactions by nitric oxide. J Biol Chem 1996;271:40-47.

Millar TM, Stevens CR, Benjamin N, Eisenthal R, Harrison R, Blake DR. Xanthine oxidoreductase catalyses the reduction of nitrates and nitrite to nitric oxide under hypoxic conditions. FEBS Lett 1998;427:225-228.

Miller ML. Pyogenic arthritis in adults. In: Maddison, P. J., Isenberg, D. A., Woo, P., and Glass, D. N.eds.Oxford Textbook of Rheumatology. Oxford University Press, 1998:849-860.

Miller RT, Martasek P, Roman LJ, Nishimura JS, Masters BS. Involvement of the reductase domain of neuronal nitric oxide synthase in superoxide anion production. Biochemistry 1997;36:15277-15284.

Mitchell HH, Shoule HA, Grindley HS. The origin of nitrates in the urine. J Biol Chem 1916;24:461-490.

Moriwaki Y, Yamamoto T, Higashino K. Distribution and pathophysiologic role of molybdenum-containing enzymes. Histol Histopathol 1997;12:513-524.

Moriwaki Y, Yamamoto T, Suda M, Nasako Y, Takahashi S, Agbedana OE *et al.* Purification and immunohistochemical tissue localisation of human xanthine oxidase. Biochim Biophys Acta 1993;1164:215-222.

Moriwaki Y, Yamamoto T, Yamaguchi K, Takahashi S, Higashino K. Immunohistochemical localization of aldehyde and xanthine oxidase in rat tissues using polyclonal antibodies. Histochem Cell Biol 1996;105:71-79.

Moriwaki Y, Yamamoto T, Yamakita JI, Takahashi S, Higashino K. Comparative localization of aldehyde oxidase and xanthine oxidoreductase activity in rat tissue. Histochem J 1998;30:69-74.

Mulherin D, Fitzgerald O, Bresnihan B. Synovial tissue macrophage populations and articular damage in rheumatoid arthritis. Arthritis Rheum 1996;39:115-124.

Murrell GA, Jang D, Williams RJ. Nitric oxide activates metalloprotease enzymes in articular cartilage. Biochem Biophys Res Commun 1995;206:15-21.

Nade S, Newbold PJ. Factors determining the level and changes in intra-articular pressure in the knee joint of the dog. J Physiol 1983;338:21-36.

Naseem KM, Low SY, Sabetkar M, Bradley NJ, Khan J, Jacobs M *et al.* The nitration of platelet cytosolic proteins during agonist-induced activation of platelets. FEBS Lett 2000;473:119-122.

Nathan C. Nitric oxide as a secretory product of mammalian cells. FASEB J 1992;6:3051-3064.

Nathan C, Xie QW. Regulation of synthesis of nitric oxide. J Biol Chem 1994;269:13725-13728.

Nossuli TO, Hayward R, Jensen D, Scalia R, Lefer AM. Mechanisms of cardioprotection by peroxynitrite in myocardial ischemia and reperfusion injury. Am J Physiol 1998;275:H509-H519.

Oldreive C, Zhao K, Paganga G, Halliwell B, Rice-Evans C. Inhibition of nitrous acid-dependent tyrosine nitration and DNA base deamination by flavonoids and other phenolic compounds. Chem Res Toxicol 1998;11:1574-1579.

Palacios FA, Novaes GS, Guzzo ML, Laurindo IM, de Mello SB. Interrelationship of the kinin system, nitric oxide and eicosanoids in the antigen-induced arthritis in rabbits. Mediators Inflamm 1999;8:245-251.

Palmer RJM, Hickery MS, Charles IG, Moncada S, Bayliss MT. Induction of nitric oxide synthase in human chondrocytes. Biochem Biophys Res Commun 1993;193:398-405.

Palmer RM, Ashton DS, Moncada S. Vascular endothelial cells synthesize nitric oxide from L-arginine. Nature 1988;333:664-666.

Pap T, Muller-Ladner U, Gay RE, Gay S. Fibroblast biology. Role of synovial fibroblasts in the pathogenesis of rheumatoid arthritis. Arthritis Res 2000;2:361-367.

Pearson CM, Wood FD. Studies of polyarthritis and other lesions induced in rats by injection of mycobacterial adjuvant. I. General clinical and pathological characteristics and some modifying factors. Arthritis Rheum 1959;2:440-459.

Pelletier JP, Jovanovic D, Fernandes JC, Manning P, Connor JR, Currie MG *et al.* Reduced progression of experimental osteoarthritis in vivo by selective inhibition of inducible nitric oxide synthase. Arthritis Rheum 1998;41:1275-1286.

Pelletier JP, Lascau-Coman V, Jovanovic D, Fernandes JC, Manning P, Connor JR *et al.* Selective inhibition of inducible nitric oxide synthase in experimental osteoarthritis is associated with reduction in tissue levels of catabolic factors. J Rheumatol 1999;26:2002-2014.

Pettipher ER and Blake S. Antigen-induced arthritis. In: Henderson, B. Edwards J. C. W. Pettipher E. R., ed.Mechanisms and models in rheumatoid arthritis. London :Academic Press, 1995:457-470.

Pfeiffer S, Mayer B. Lack of tyrosine nitration by peroxynitrite generated at physiological pH. Journal of Biological Chemistry 1998;273:27280-27285.

Pitt RM, McKelvey TG, Saenger JS, Shah AK, Jones HP, Manci EA *et al.* A tungsten-supplemented diet delivered by transplacental and breast-feeding routes lowers intestinal xanthine oxidase activity and affords cytoprotection in ischemia-reperfusion injury to the small intestine. J Pediatr Surg 1991;26:930-935.

Pryor WA, Squadrito GL. The chemistry of peroxynitrite: a product from the reaction of nitric oxide with superoxide. Am J Physiol 1995;268:L699-722.

Radi R. Nitric oxide, oxidants and protein tyrosine nitration. Proc Natl Acad Sci U S A 2004;101:4003-4008.

Reiter CD, Teng RJ, Beckman JS. Superoxide Reacts with Nitric Oxide to Nitrate Tyrosine at Physiological pH via Peroxynitrite. J Biol Chem 2000;275:32460-32466.

Rohn TT, Nelson LK, Sipes KM, Swain SD, Jutila KL, Quinn MT. Priming of human neutrophils by peroxynitrite: potential role in enhancement of the local inflammatory response. J Leucoc Biol 1999;65:59-70.

Roitt IM, Brostoff J, and Male DK. Hypersensitivity-Type IV. In: Immunology. Gower Medical Publishing, 1985:22.1-22.10.

Rubbo H, Radi R, Trujillo M, Telleri R, Kalyanaraman B, Barnes S *et al.* Nitric oxide regulation of superoxide and peroxynitrite-dependent lipid peroxidation. J Biol Chem 1994;269:26066-26075.

Sakurai H, Kohsaka H, Liu MF, Higashiyama H, Hirata Y, Kanno K *et al.* Nitric oxide production and inducible nitric oxide synthase expression in inflammatory arthritides. J Clin Invest 1995;96:2357-2363.

Samouilov A, Kuppusamy P, Zweier JL. Evaluation of the magnitude and rate of nitric oxide production from nitrite in biological systems. Arch Biochem Biophys 1998;357:1-7.

Sanders SA, Eisenthal R, Harrison R. NADH oxidase activity of human xanthine oxidoreductase--generation of superoxide anion. Eur J Biochem 1997;245:541-548.

Sandhu JK, Robertson S, Birnboim HC, Goldstein R. Distribution of protein nitrotyrosine in synovial tissues of patients with rheumatoid arthritis and osteoarthritis. J Rheumatol 2003;30:1173-1181.

Santos CX, Anjos EL, Augusto O. Uric acid oxidation by peroxynitrite: multiple reactions, free radical formation, and amplification of lipid oxidation. Arch Biochem Biophys 1999;372:285-294.

Sarnesto A, Linder N, Raivio KO. Organ distribution and molecular forms of human xanthine dehydrogenase/ xanthine oxidase protein. Lab Invest 1996;74:48-56.

Savvides SN, Scheiwein M, Bohme CC, Arteel GE, Karplus PA, Becker K *et al.* Crystal Structure of the Antioxidant Enzyme Glutathione Reductase Inactivated by Peroxynitrite. J Biol Chem 2002;277:2779-2784.

Sawa T, Akaike T, Maeda H. Tyrosine nitration by peroxynitrite formed from nitric oxide and superoxide generated by xanthine oxidase. J Biol Chem 2000;275:32467-32474.

Schardinger F. Über das Verhalten der Kuhmilch gegen Methylenblau und seine Verwendung zur Unterscheidung von ungekochter und gekochter Milch. Untersuch Nahrungs Genussmittel 1902;5:1113-1121.

Schmidt P, Youhnovski N, Daiber A, Balan A, Arsic M, Bachschmid M *et al.* Specific Nitration at Tyrosine 430 Revealed by High Resolution Mass Spectrometry as Basis for Redox Regulation of Bovine Prostacyclin Synthase. J Biol Chem 2003;278:12813-12819.

Schumacher HR, Arayssi T, Crane M, Lee J, Gerard H, Hudson AP *et al.* Chlamydia trachomatis nucleic acids can be found in the synovium of some asymptomatic subjects. Arthritis Rheum 1999;42:1281-1284.

Schwedhelm E, Tsikas D, Gutzki FM, Frölich JC. Gas chromatographic tandem mass spectrometric quantification of free 3-nitrotyrosine in human plasma at the basal state. Analyt Biochem 1999;276:195-203.

Silver IA. Measurement of pH and ionic composition of pericellular sites. Philos Trans R Soc Lond B Biol Sci 1975;271:261-272.

Smith MD, Triantafillou S, Parker A, Youssef PP, Coleman M. Synovial membrane inflammation and cytokine production in patients with early osteoarthritis. J Rheumatol 1997;24:365-371.

Speden DJ, Hewinson J, Mapp PI, Blake DR. Xanthine oxidase in inflammatory arthritis. Rheumatology 2002;41(Suppl 1):S34.

Stefanovic-Racic M, Meyers K, Meschter C, Coffey JW, Hoffman RA, Evans CH. N-monomethyl arginine, an inhibitor of nitric oxide synthase, suppresses the development of adjuvant arthritis in rats. Arthritis Rheum 1994;37:1062-1069.

Stefanovic-Racic M, Morales TI, Taskiran D, McIntyre LA, Evans CH. The role of nitric oxide in proteoglycan turnover by bovine articular cartilage organ cultures. J Immunol 1996;156:1213-1220.

Stevens CR, Benboubetra M, Harrison R, Sahinoglu T, Smith EC, Blake DR. Localisation of xanthine oxidase to synovial endothelium. Ann Rheum Dis 1991a;50:760-762.

Stevens CR, Blake DR, Merry P, Revell PA, Levick JR. A comparative study by morphometry of the microvasculature in normal and rheumatoid synovium. Arthritis Rheum 1991b;34:1508-1513.

Stevens CR, Millar TM, Clinch JG, Kanczler JM, Bodamyali T, Blake DR. Antibacterial properties of xanthine oxidase in human milk. Lancet 2000;356:829-830.

Stirpe F, Della Corte E. The regulation of rat liver xanthine oxidase. Conversion in vitro of the enzyme activity from dehydrogenase (type D) to oxidase (type O). J Biol Chem 1969;244:3855-3863.

Suzuki H, DeLano FA, Parks DA, Jamshidi N, Granger DN, Ishii H *et al.* Xanthine oxidase activity associated with arterial blood pressure in spontaneously hypertensive rats. Proc Natl Acad Sci U S A 1998;95:4754-4759.

Szabo C, Oshima H. DNA damage induced by peroxynitrite: subsequent biological effects. Nitric Oxide 1997;1:373-385.

Tak PP. Examination of the synovium and synovial fluid. In: Firestein, G. S., Panayi, G. S., and Wollheim, F. A.eds.Rheumatoid Arthritis. New frontiers in pathogenesis and treatment. Oxford University Press, 2000:55-67.

Tak PP, Smeets TJ, Daha MR, Kluin PM, Meijers KA, Brand R *et al.* Analysis of the synovial cell infiltrate in early rheumatoid synovial tissue in relation to local disease activity. Arthritis Rheum 1997;40:217-225.

Tarpey MM, Fridovich I. Methods of Detection of Vascular Reactive Species: Nitric Oxide, Superoxide, Hydrogen Peroxide, and Peroxynitrite. Circ Res 2001;89:224-236.

Taskiran D, Stefanovic-Racic M, Georgescu H, Evans C. Nitric oxide mediates suppression of cartilage proteoglycan synthesis by interleukin-1. Biochem Biophys Res Commun 1994;200:142-148.

Teng RJ, Ye YZ, Parks DA, Beckman JS. Urate produced during hypoxia protects heart proteins from peroxynitrite-mediated protein nitration. Free Radic Biol Med 2002;33:1243-1249.

Terada LS, Piermattei D, Shibao GN, McManaman JL, Wright RM. Hypoxia regulates xanthine dehydrogenase activity at pre- and posttranslational levels. Arch Biochem Biophys 1997;348:163-168.

Tomita M, Sato EF, Nishikawa M, Yamano Y, Inoue M. Nitric oxide regulates mitochondrial respiration and functions of articular chondrocytes. Arthritis Rheum 2001;44:96-104.

Trentham DE, Townes AS, Kang AH. Autoimmunity to type II collagen an experimental model of arthritis. J Exp Med 1977;146:857-868.

Turpaev KT, Amchenkova AM, Narovlansky AN. Two pathways of the nitric oxide-induced cytotoxycal action. Biochem Mol Biol Int 1997;41:1025-1033.

Ueki Y, Miyake S, Tominaga Y, Eguchi K. Increased nitric oxide levels in patients with rheumatoid arthritis. J Rheumatol 1996;23:230-236.

Umezawa K, Akaike T, Fujii S, Suga M, Setoguchi K, Ozawa A *et al.* Induction of nitric oxide synthesis and xanthine oxidase and their roles in the antimicrobial

mechanism against Salmonella typhimurium infection in mice. Infect Immun 1997;65:2932-2940.

Uppu RM, Squadrito GL, Cueto R, Pryor WA. Selecting the most appropriate synthesis of peroxynitrite. Methods Enzymol 1996;269:285-296.

van de Loo FA, Arntz OJ, van Enckevort FH, van Lent PL, van den Berg WB. Reduced cartilage proteoglycan loss during zymosan-induced gonarthritis in NOS2-deficient mice and in anti-interleukin-1-treated wild-type mice with unabated joint inflammation. Arthritis Rheum 1998;41:634-646.

van der Loo B, Labugger R, Skepper JN, Bachschmid M, Kilo J, Powell JM *et al.* Enhanced Peroxynitrite Formation Is Associated with Vascular Aging. J Exp Med 2000a;192:1731-1744.

van der Loo B, Labugger R, Skepper JN, Bachschmid M, Kilo J, Powell JM *et al.* Enhanced Peroxynitrite Formation Is Associated with Vascular Aging. J Exp Med 2000b;192:1731-1744.

van der Loo B, Labugger R, Skepper JN, Bachschmid M, Kilo J, Powell JM *et al.* Enhanced Peroxynitrite Formation Is Associated with Vascular Aging. J Exp Med 2000d;192:1731-1744.

van der Loo B, Labugger R, Skepper JN, Bachschmid M, Kilo J, Powell JM *et al.* Enhanced Peroxynitrite Formation Is Associated with Vascular Aging. J Exp Med 2000c;192:1731-1744.

van der Vliet A, Eiserich JP, Halliwell B, Cross CE. Formation of reactive nitrogen species during peroxidase-catalyzed oxidation of nitrite. J Biol Chem 1997;272:7617-7625.

van der Vliet A, Jason P, Eiserich JP, Kaur H, Cross CE, Halliwell B. Nitrotyrosine as biomarker for reactive nitrogen species. Methods Enzymol 1996;269:175-185.

Veihelmann A, Hofbauer A, Krombach F, Dorger M, Maier M, Refior HJ *et al.* Differential function of nitric oxide in murine antigen-induced arthritis. Rheumatology 2002;41:509-517.

Veihelmann A, Landes J, Hofbauer A, Dorger M, Refior HJ, Messmer K *et al.* Exacerbation of antigen-induced arthritis in inducible nitric oxide synthase-deficient mice. Arthritis Rheum 2001;44:1420-1427.

Viera L, Ye YZ, Estevez AG, Beckman JS. Immunohistochemical methods to detect nitrotyrosine. Methods Enzymol 1999;301:373-381.

Vorbach C, Scriven A, Capecchi MR. The housekeeping gene xanthine oxidoreductase is necessary for milk fat droplet enveloping and secretion: gene sharing in the lactating mammary gland. Genes Dev 2002;16:3233-3235.

Walker JM. Electrophoretic techniques. In: Wilson, K. and Walker, J. M.eds.Principles and techniques of practical biochemistry. Cambridge :Cambridge University Press, 1994:425-460.

Walsh DA. Angiogenesis and arthritis. Rheumatology 1999;38:103-112.

Wang P, Zweier JL. Measurement of Nitric Oxide and Peroxynitrite Generation in the Postischemic Heart. Evidence for peroxynitrite-mediated reperfusion injury. J Biol Chem 1996;271:29223-29230.

Waud WR, Rajagopalan KV. Purification and properties of the NAD+-dependent (type D) and O2-dependent (type O) forms of rat liver xanthine dehydrogenase. Arch Biochem Biophys 1976;172:354-364.

Wei XQ, Charles IG, Smith A, Ure J, Feng GJ, Huang FP *et al.* Altered immune responses in mice lacking inducible nitric oxide synthase. Nature 1995;375:408-411.

Weitzberg E, Lundberg JON. Nonenzymatic nitric oxide production in humans. Nitric Oxide 1998;2:1-7.

Whiteman M, Halliwell B. Protection against peroxynitrite-dependent tyrosine nitration and alpha 1-antiproteinase inactivation by ascorbic acid. A comparison with other biological antioxidants. Free Radic Res 1996;25:275-283.

Whiteman M, Ketsawatsakul U, Halliwell B. A reassessment of the peroxynitrite scavenging activity of uric acid. Ann N Y Acad Sci 2002;962:242-259.

Whiteman M, Rose P, Siau JL, Halliwell B. Nitrite-mediated protection against hypochlorous acid-induced chondrocyte toxicity: a novel cytoprotective role of nitric oxide in the inflamed joint? Arthritis Rheum 2003;48:3140-3150.

Wink DA, Cook JA, Kim SY, Vodovotz Y, Pacelli R, Krishna MC *et al.* Superoxide modulates the oxidation and nitrosation of thiols by nitric oxide-derived reactive intermediates. J Biol Chem 1997;272:11147-11151.

Wollheim FA. Pathogenesis of osteoarthritis. In: Hochberg, M. C., Silman, A. J., Smolen, J. S., Weinblatt, M. E. *et al.*eds.Rheumatology. Mosby, 2003:1801-1815.

Woolley DE. Cellular mechanisms of cartilage destruction. In: Henderson, B., Edwards, J. C. W., and Pettipher, E. R.eds.Mechanisms and models in rheumatoid arthritis. Academic Press, 1995:115-132.

Wu HH, Cork RJ, Mize RR. Normal development of the ipsilateral retinocollicular pathway and its disruption in double endothelial and neuronal nitric oxide synthase gene knockout mice. J Comp Neurol 2000;426:651-665.

Xia Y, Roman LJ, Masters BS, Zweier JL. Inducible nitric-oxide synthase generates superoxide from the reductase domain. J Biol Chem 1998a;273:22635-22639.

Xia Y, Tsai AL, Berka V, Zweier JL. Superoxide generation from endothelial nitric-oxide synthase. A Ca2+/calmodulin-dependent and tetrahydrobiopterin regulatory process. J Biol Chem 1998b;273:25804-25808.

Xu P, Huecksteadt TP, Harrison R, Hoidal JR. Molecular cloning, tissue expression of human xanthine dehydrogenase. Biochem Biophys Res Commun 1994;199:998-1004.

Xu P, Huecksteadt TP, Hoidal JR. Molecular cloning and characterization of the human xanthine dehydrogenase gene (XDH). Genomics 1996;34:173-180.

Xu P, LaVallee P, Hoidal JR. Repressed expression of the human xanthine oxidoreductase gene. E-Box and TATA-like elements restrict ground state transcriptional activity. J Biol Chem 2000;275:5918-5926.

Yermilov V, Rubio J, Becchi M, Friesen MD, Pignatelli B, Oshima H. Formation of 8-nitroguanine by the reaction of guanine with peroxynitrite in vitro. Carcinogenesis 1995;16:2045-2050.

Yermilov V, Yoshie Y, Rubio J, Oshima H. Effects of carbon dioxide/bicarbonate on induction of DNA single-strand breaks and formation of 8-nitroguanine, 8-oxoguanine and base-propenal mediated by peroxynitrite. FEBS Lett 1996;399:67-70.

Zhang Z, Naughton D, Winyard PG, Benjamin N, Blake DR, Symons MC. Generation of nitric oxide by a nitrite reductase activity of xanthine oxidase: a potential pathway for nitric oxide formation in the absence of nitric oxide synthase activity.Erratum in: Biochem Biophys Res Commun 1998,251:667. Biochem Biophys Res Commun 1998;249:767-772.

Zou MH, Leist M, Ullrich V. Selective Nitration of Prostacyclin Synthase and Defective Vasorelaxation in Atherosclerotic Bovine Coronary Arteries. Am J Pathol 1999;154:1359-1365.

Zweier JL, Wang P, Samouilov A, Kuppusamy P. Enzyme-independent formation of nitric oxide in biological tissues. Nat Med 1995;1:804-809.

Reprinted from ARTHRITIS & RHEUMATISM
John Wiley & Sons, Inc
Vol. 44, No. 7, July 2001

Localization of 3-Nitrotyrosine to Rheumatoid and Normal Synovium

Paul I. Mapp,[1] Rainer Klocke,[1] David A. Walsh,[2] Jasvinder K. Chana,[3] Clifford R. Stevens,[1] Patrick J. Gallagher,[4] and David R. Blake[1]

Objective. **To determine the localization of 3-nitrotyrosine (3-NT), a footprint marker of peroxynitrite ($ONOO^-$) and other reactive nitrogen species, to the inflamed human synovium and to compare this with normal synovial and nonsynovial tissue of human and animal origin.**

Methods. **Monoclonal and polyclonal antibodies were used to investigate for 3-NT, inducible nitric oxide synthase (iNOS), macrophage marker CD68, and the vascular smooth muscle marker α-actin by avidin–biotin immunocytochemistry.**

Results. **In the inflamed synovium, 3-NT was found in the vascular smooth muscle and macrophages. In normal human synovium, 3-NT was present in the vascular smooth muscle and some lining cells and was not associated with immunoreactivity for iNOS. Similarly, 3-NT could be demonstrated in the vascular smooth muscle cells of normal rats and iNOS knockout mice. It was not present in the vascular smooth muscle of healthy, nonsynovial tissue.**

Conclusion. **The synovial vasculature in histologically normal human and naive rodent synovium was alone among the normal tissues studied in exhibiting iNOS-independent immunoreactivity for 3-NT. These findings suggest a physiologic role for $ONOO^-$ in normal synovial vascular function.**

Presented by Rainer Klocke in partial fulfillment of the requirements for a PhD degree, University of Bath, Bath, UK.

Supported by the Arthritis Research Campaign, UK. Dr. Blake is a Glaxo Wellcome Professor of Rheumatology.

[1]Paul I. Mapp, PhD, Rainer Klocke, MRCP, Clifford R. Stevens, PhD, David R. Blake, FRCP: University of Bath, Bath, UK; [2]David A. Walsh, MRCP, PhD: University of Nottingham, Nottingham, UK; [3]Jasvinder K. Chana, BSc: Queen Mary and Westfield College, London, UK; [4]Patrick J. Gallagher, FRCP: Southampton General Hospital, Southampton, UK.

Address correspondence and reprint requests to Paul I. Mapp, PhD, Department of Medical Sciences, University of Bath, Claverton Down, Bath BA2 7AY, UK.

Submitted for publication May 31, 2000; accepted in revised form March 6, 2001.

The reaction of nitric oxide (NO) with superoxide ($O_2^{\cdot -}$) leads to the formation of the potent oxidant peroxynitrite ($ONOO^-$). The attack of $ONOO^-$, or its decomposition products, acts upon aromatic amino acids, leading to their nitration (1). One such reaction product, 3-nitrotyrosine (3-NT), is relatively stable, and its presence in tissues is strong evidence for the formation of $ONOO^-$ in vivo (2). Investigators at our laboratory have previously shown that there are increased concentrations of nitrite in the serum and synovial fluid of patients with rheumatoid arthritis (RA), and, to a lesser extent, osteoarthritis (OA), indicating that increased synthesis of NO is a feature of rheumatic diseases (3). Thus, localization of 3-NT to the synovium may give clues to the involvement of NO in the pathology of synovitis in RA.

Furthermore, 3-NT has also been found in the serum and synovial fluid of patients with RA; healthy subjects and patients with OA showed no detectable 3-NT (1). In this study, we investigated the RA synovium, by immunohistochemistry, for the presence of 3-NT residues and also the enzyme inducible NO synthase (iNOS), the macrophage marker CD68, and the vascular smooth muscle marker α-actin. The pathologic RA specimens were compared and contrasted with both histologically normal arthroscopic and postmortem synovium and normal tissues obtained from other sites in the body. Additionally, corresponding tissues from healthy rats and iNOS knockout and wild-type mice were examined.

MATERIALS AND METHODS

Tissue origin, collection, and preparation. Human synovium was obtained at the time of joint surgery from 13 patients (10 women and 3 men) satisfying the American College of Rheumatology (formerly, the American Rheumatism Association) revised criteria for RA (4). The mean age was 68 years (range 58–84 years), and the mean disease

duration was 21 years (range 3–43 years). Six of the patients were receiving disease-modifying antirheumatic therapy and/or prednisolone up to 7.5 mg/day. Control synovia were obtained postmortem from subjects with no previous clinical history of arthritis (n = 3; all women) and patients undergoing knee arthroscopy for traumatic symptoms (n = 7; 3 women). The causes of death in the postmortem group were opportunistic bronchopneumonia and human immunodeficiency virus nephropathy in a 45-year-old patient, cerebral infarction in a 48-year-old patient, and bronchopneumonia in an 87-year-old patient. The arthroscopy group had a mean age of 33 years (range 21–55 years). The arthroscopically biopsied knees were radiologically normal, and a tourniquet was not used in the operative procedure. Arthroscopic findings were as follows: meniscal lesions (4 subjects), ruptured posterior cruciate ligament (1 subject), and normal (2 subjects). At least 5 sections per specimen were examined.

Control normal human nonsynovial tissue was obtained from blocks held in the pathology department at the Royal London Hospital. The source of the normal specimens included skin, colon, small intestine, and kidney (5 specimens of each), heart (4 specimens), appendix, liver, spleen, striated muscle, tonsil, pituitary, and tongue (3 specimens of each), and adrenal and parotid glands (2 specimens of each).

Seven-week-old male Wistar rats (n = 5) and 10-week-old male 129SvEv, wild-type (n = 3), and $iNOS^{-}/iNOS^{-}$ mice (n = 2; Bantin & Kingman, Hull, UK) were killed by cervical dislocation, followed by dissection and fixation of knee synovium (total knee in the case of the mice), skin, small intestine, colon, and liver within 5 minutes of death. Twelve-week-old male Wistar rats (n = 3) were killed by ether overdose, and synovium was fixed by transcardiac perfusion with 500-ml formal saline.

Staining procedures. Paraffin-embedded 4-μm sections were dewaxed, rehydrated, and washed in phosphate buffered saline (PBS). Primary antibodies were then applied at predetermined optimal dilutions in PBS. In the case of the rabbit primary antibodies (anti–3-NT; TCS Biologicals, Buckingham, UK, and anti-iNOS; Alexis, Nottingham, UK), the incubation was carried out overnight at 4°C. Mouse primary antibodies (α-actin, clone 1A4; Sigma, Poole, UK, and CD68, clone PGM1; Dako, Ely, UK) were incubated for 1 hour at room temperature. The sections were then washed and a biotinylated secondary antibody at a dilution of 1:100 in PBS was applied. After washing in PBS, the sections were stained using avidin–biotin–peroxidase/alkaline phosphatase (Vector, Peterborough, UK) and Sigma Fast to yield a red reaction product.

Immunocytochemical controls. Negative controls were provided by omission of the primary antibody, incubation of the specimens in nonimmune rabbit serum, preincubation of the rabbit antibody in 10 m*M* 3-NT, and incubation of the positive control specimens in 100 m*M* sodium hydrosulfite prior to staining (5). Positive control samples (n = 4) were obtained from human coronary artery atheroma, as described by Beckman et al (2).

RESULTS

Findings in immunocytochemical controls. No staining was observed on any of the negative control slides. The staining obtained for 3-NT in the coronary artery atheroma, the positive immunocytochemical control, was concordant with that described by Beckman et al (2). Briefly, positive 3-NT immunoreactivity was observed in the vascular smooth muscle and diffusely in the fibrous material of the lesion (Figure 1A). Higher-power examination revealed that the foamy macrophages in the lesion showed strong 3-NT immunoreactivity (Figure 1B).

Specimens from patients with RA. *Intimal layer.* A varying proportion of the lining cells in the RA specimens showed 3-NT immunoreactivity (Figure 1C). Such cells were seen in all the specimens examined. The proportion of positive cells varied according to the morphologic appearance of the tissue. Those specimens with an active appearance contained ~50% positive lining cells, while those with a fibrotic, "burned out" appearance contained fewer positive cells (5–10%). The number of cells staining positively for the CD68 antigen paralleled those showing positive 3-NT immunoreactivity.

Subintimal layer. In infiltrating cells, 3-NT immunoreactivity was seen in the perivascular inflammatory infiltrates in the subintimal region (Figure 1D). These cells had the morphologic characteristics of macrophages and were also CD68+ and iNOS positive. Giant cells were positive for 3-NT immunoreactivity (Figure 1E). 3-NT immunoreactivity was also seen in blood vessels in the synovium (Figure 1F). The staining was restricted to vascular smooth muscle cells (VSMCs) and was not present in the endothelial cells (Figure 1G). Blood vessel 3-NT immunoreactivity was observed in all sections examined. In parallel sections, iNOS staining was seen in the vascular smooth muscle of those blood vessels showing 3-NT immunoreactivity.

Normal human synovial specimens. In both the postmortem and arthroscopic biopsy specimens (Figure 1H), 3-NT immunoreactivity was seen in the vascular smooth muscle of blood vessels and in some lining cells. The majority of blood vessels showed positive 3-NT immunoreactivity in VSMC. Inducible NOS protein antigen was not detected in these specimens. CD68 expression was very weak and limited to ~30–40% of the normal lining cells. The weakness of the staining meant that we were unable to determine, with conviction, if 3-NT immunoreactive lining cells were also CD68+.

Other normal human tissue specimens. In the other normal human specimens examined, staining was not seen in vascular smooth muscle. The presence of blood vessels was confirmed by positive staining for α-actin.

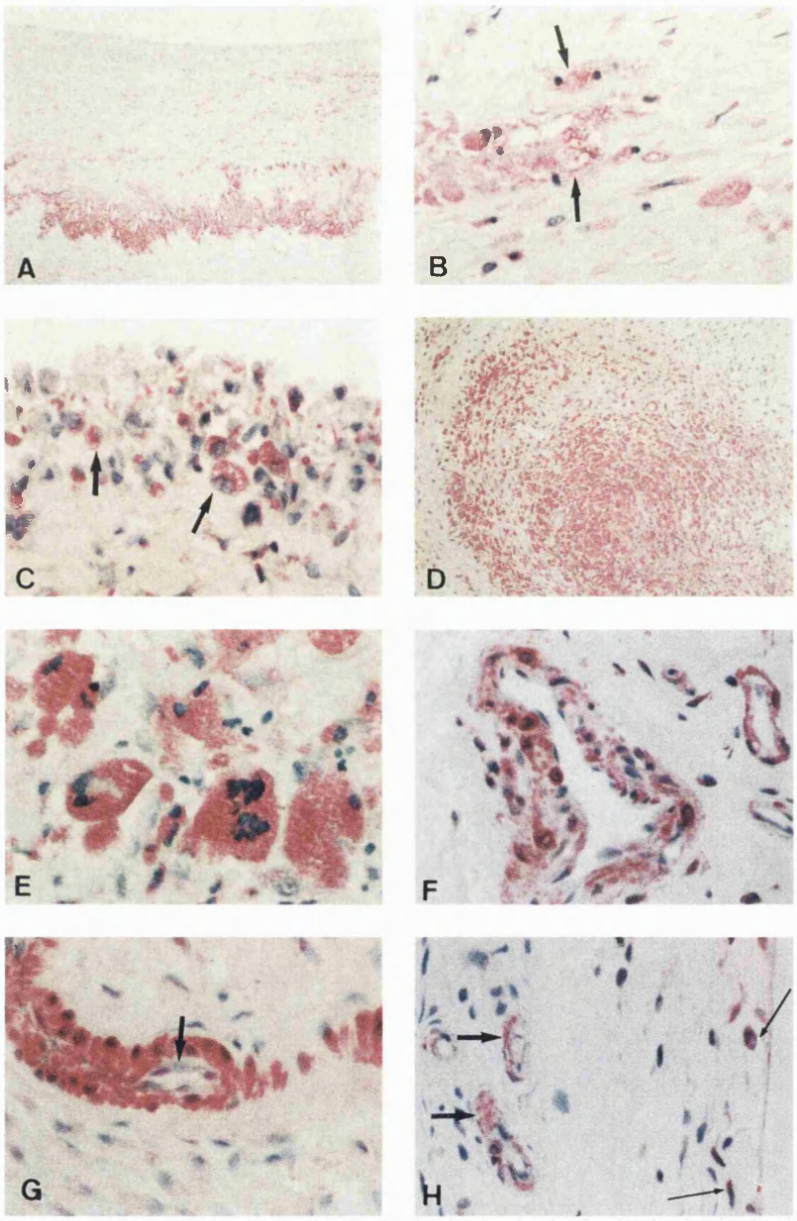

Figure 1. Immunohistochemical staining for 3-nitrotyrosine (3-NT) immunoreactivity in rheumatoid and normal human synovium, performed by the avidin–biotin technique with alkaline phosphatase as the signaling enzyme and fast red as the chromogen. A red reaction product indicates positive 3-NT immunoreactivity. The blue nuclear counterstain is Mayer's hematoxylin. **A,** Atherosclerotic plaque, showing positive 3-NT immunoreactivity (red). Needle-shaped gaps in the tissue show where cholesterol crystals have been removed by the tissue-processing procedure. **B,** Higher-power view of the same section illustrated in **A,** showing 3-NT immunoreactivity in the foamy macrophages associated with the lesion (**arrows**). **C,** Intimal lining layer from a patient with rheumatoid arthritis (RA). Positive 3-NT–immunoreactive cells (**arrows**) and negative cells are present in the same field of view. **D,** A perivascular accumulation of inflammatory cells, showing large numbers of 3-NT–immunoreactive cells. **E,** High-power view of multinucleated giant cells, showing positive 3-NT immunoreactivity. **F,** Blood vessels of different sizes from RA synovium; vascular smooth muscle shows 3-NT immunoreactivity. **G,** Positive 3-NT immunoreactivity in vascular smooth muscle cells of blood vessels in RA synovium. Note that the endothelial cells are not stained (**arrow**). **H,** Positive 3-NT immunoreactivity in a specimen of normal synovium. The 3-NT immunoreactivity is localized to the vascular smooth muscle of blood vessels (**arrows**) and to some intimal cells (**thin arrows**). (Original magnification × 150 in **A** and **D**; × 400 in **B, C, F,** and **H**; × 650 in **E** and **G**.)

Normal rat specimens. Both immersion- and perfusion-fixed rat synovium showed 3-NT immunoreactivity, confined to VSMCs (Figures 2A and B), which was not found in the vasculature of other rat tissues studied (i.e., skin, intestine, colon, liver, and [from rats with perfusion-fixed synovium only] meningeal vessels).

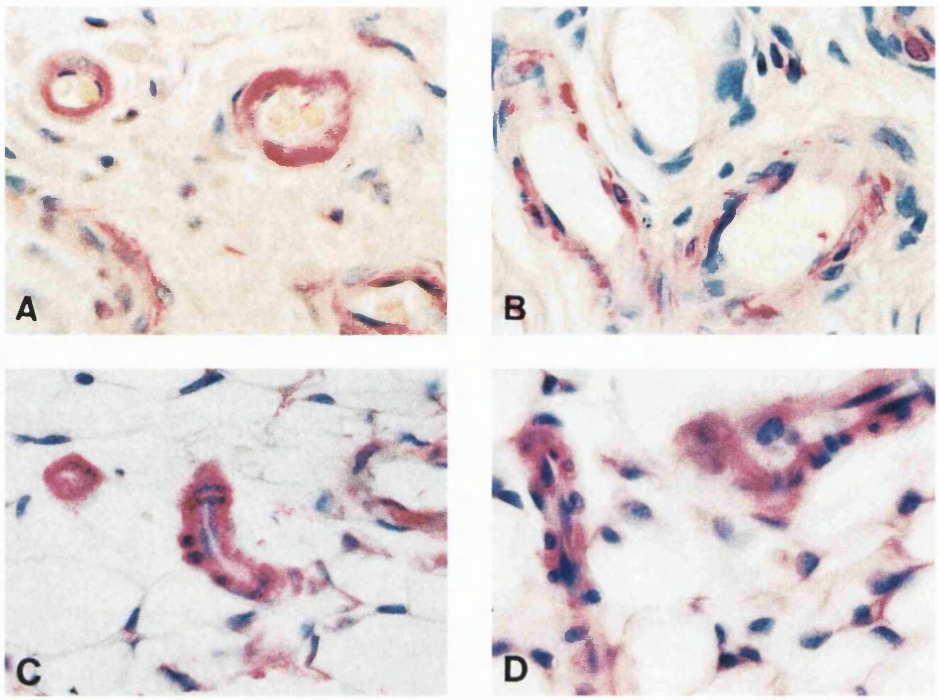

Figure 2. Immunohistochemical staining of 3-nitrotyrosine (3-NT) immunoreactivity in synovium from Wistar rats, 129SvEv wild-type mice, and inducible nitric oxide synthase–negative (iNOS$^-$)/iNOS$^-$ mice, performed by the avidin–biotin technique with alkaline phosphatase as the signaling enzyme and fast red as the chromogen. A red reaction product indicates positive 3-NT immunoreactivity. The blue nuclear counterstain is Mayer's hematoxylin. **A,** Positive 3-NT immunoreactivity in vascular smooth muscle cells (VSMC) in immersion-fixed knee synovium of a healthy Wistar rat. **B,** Positive 3-NT immunoreactivity in VSMC in perfusion-fixed knee synovium of a normal Wistar rat. Note the vessel free of 3-NT immunoreactivity between and adjacent to 2 other vessels showing strong 3-NT immunoreactivity. **C,** Positive 3-NT immunoreactivity in VSMC in synovium from a 129SvEv mouse. **D,** Positive 3-NT immunoreactivity in VSMC in synovium from a 129SvEv iNOS$^-$/iNOS$^-$ mouse. (Original magnification × 650.)

Vessels were differentially immunoreactive for 3-NT, i.e., adjacent blood vessels could show strong or no 3-NT immunoreactivity.

Wild-type and iNOS knockout mouse knee tissue. Both the wild-type and iNOS knockout mice demonstrated 3-NT immunoreactivity in VSMCs of the synovium (Figures 2C and D). In other tissues from wild-type mice (skin, liver, small intestine, colon, and heart), 3-NT immunoreactivity was not seen in VSMC.

DISCUSSION

In this report, we describe the distribution of 3-NT in the RA synovium and also its localization to histologically healthy human and naive animal synovium. The formation of 3-NT is widely believed to be a result of the attack on tyrosine by the strong oxidizing agent $ONOO^-$. However, while the $O_2^{\cdot -}$/NO interaction may be the dominant mechanism of 3-NT formation, other pathways have been proposed. Therefore, it is safer to conclude that the formation of 3-NT is a result of the generation of reactive nitrogen species rather than $ONOO^-$ specifically (6). In positive control coronary artery atheroma, the staining pattern seen was concordant with the findings of Beckman et al (2). In the synovial specimens from patients with RA, the staining for 3-NT was predominantly in macrophages, giant cells (including some with a foamy appearance), and in the vascular smooth muscle of the larger, noncapillary blood vessels.

As previously shown by Grabowski et al (7), macrophages stained positively for CD68 and iNOS. The presence of 3-NT in the macrophages of the RA synovium is consistent with previous reports that activated rat macrophages can produce $ONOO^-$ (8). Experimental in vitro studies show that more $O_2^{\cdot -}$ is detected when

iNOS is inhibited and, conversely, superoxide dismutase (SOD) increases the measurable NO release from macrophages. The generation of $ONOO^-$ in macrophages is thus probably via NO and $O_2^{\cdot -}$ production from iNOS and NADPH oxidases, respectively.

In the inflamed synovium, 3-NT was localized to the vascular smooth muscle but not to endothelial cells, and corresponded with iNOS immunoreactivity. Expression of iNOS in vascular smooth muscle under pathologic circumstances has previously been demonstrated in chronic inflammation and septic shock. Among the functional consequences of $ONOO^-$ on rodent vascular smooth muscle under experimental in vitro conditions are cellular energetic and contractile failure, apparently due to impaired mitochondrial respiration (9). While chronically inflamed rat joints display much-reduced vasomotor responses (10), this has yet to be confirmed in human arthritis, and the relation to $ONOO^-$ remains to be established. The formation of 3-NT in the RA joint may be enhanced by the prevailing acidotic and hypercapnic conditions, both of which have been shown to favor the formation of 3-NT in vitro (11).

The finding of 3-NT immunoreactivity in VSMC of apparently normal human synovium was surprising. To our knowledge, NT immunoreactivity in nondiseased tissue has been previously identified only in human intestinal and bladder epithelium (5). We have considered the possibility that this is due to pathologic or postmortem changes. Past synovial microtrauma in the arthroscopic synovial specimens may account for our findings, but the absence of such lesions found on microscopic examination would provide evidence against this. Furthermore, care was taken to keep ischemic/hypoxic stress to a minimum before and during arthroscopic synovial sampling by not using a tourniquet for the procedure.

Due to obvious problems in obtaining synovial tissue from healthy human subjects, we further investigated 3-NT immunoreactivity in naive rodents. In the rats, we compared tissue obtained by perfusion with that obtained by immersion fixation, the mode used on human specimens. We observed the same tissue distribution of 3-NT immunoreactivity by both fixation techniques, and this was identical to the findings in normal human tissue specimens. Furthermore, as in human specimens, 3-NT immunoreactivity was absent in rat VSMC of nonsynovial origin (e.g., vessels in the intestine, colon, and meninges), irrespective of fixation method. In the absence of iNOS protein, 3-NT immunoreactivity could still be demonstrated in the normal human synovial specimens. To exclude the possibility of previous iNOS expression as the source of 3-NT in synovial vessels, we examined tissue from immersion-fixed wild-type and iNOS knockout mice and found 3-NT present in the synovial vascular smooth muscle in both strains. Taken together, these findings indicate that pathologic and/or early postmortem changes are unlikely causes for our findings.

We further considered the possibility of tyrosine nitration, resulting from endogenous peroxidase activity in the presence of nitrite (6). However, in animal as well as normal human synovium, we observed no specific histochemical peroxidase activity, except in erythrocytes (results not shown). Taken together with the low amount of nitrite expected to be present in normal synovium (3), this points once more to an $ONOO^-$ mediated mechanism of tyrosine nitration.

In the absence of iNOS protein in normal synovium, an alternative to NO (to explain the production of $ONOO^-$) is required. Obvious candidates are the constitutive forms of NOS, but it is unclear whether their lower magnitude of NO production is sufficient to lead to $ONOO^-$ formation. We have previously described that xanthine oxidase (XOD) produces not only $O_2^{\cdot -}$, but also NO via reduction of nitrite in vitro under hypoxic conditions (12,13). Recently, we have shown that XOD is also capable of producing NO under physiologic oxygen tension in the presence of SOD (14), implying the formation of $ONOO^-$ in the absence of enhanced dismutation of $O_2^{\cdot -}$. Whether XOD or a constitutive NOS is the source of $ONOO^-$ in normal synovium requires further investigation.

We are unaware of a physiologic role for $ONOO^-$, with the possible exception of an antimicrobial function in human breast milk, as we have recently illustrated (15). A similar host defense role of $ONOO^-$ may underlie its presence in normal human synovium. The exclusiveness of 3-NT in vascular smooth muscle of the synovium, compared with various other tissues, suggests a tissue-specific, physiologic role of $ONOO^-$ that requires further elucidation.

In conclusion, 3-NT has been localized to macrophages and giant cells in the rheumatoid synovium, an observation in common with other inflammatory conditions. In addition, we have demonstrated the presence of iNOS-independent 3-NT in the inflamed and normal vasculature of human and rodent synovium. The synovial vascular smooth muscle 3-NT immunoreactivity is peculiar to this tissue and we did not see it in other normal tissues examined. Therefore, we propose a physiologic role for $ONOO^-$ in modifying synovial vascular function.

REFERENCES

1. Kaur H, Halliwell B. Evidence for nitric oxide-mediated oxidative damage in chronic inflammation: nitrotyrosine in serum and synovial fluid from rheumatoid patients. FEBS Lett 1994;350: 9–12.
2. Beckmann JS, Ye YZ, Anderson PG, Chen J, Accavitti MA, Tarpey MM, et al. Extensive nitration of protein tyrosines in human atherosclerosis detected by immunohistochemistry. Biol Chem Hoppe Seyler 1994;375:81–8.
3. Farrell AJ, Blake DR, Palmer RM, Moncada S. Increased concentrations of nitrite in synovial fluid and serum samples suggest increased nitric oxide synthesis in rheumatic diseases. Ann Rheum Dis 1992;51:1219–22.
4. Arnett FC, Edworthy SM, Bloch DA, McShane DJ, Fries JF, Cooper NS, et al. The American Rheumatism Association 1987 revised criteria for the classification of rheumatoid arthritis. Arthritis Rheum 1988;31:315–24.
5. Viera L, Ye YZ, Estevez AG, Beckman JS. Immunohistochemical methods to detect nitrotyrosine. Methods Enzymol 1999;301: 373–81.
6. Halliwell B. What nitrates tyrosine? Is nitrotyrosine specific as a biomarker of peroxynitrite formation in vivo? FEBS Lett 1997; 411:157–60.
7. Grabowski PS, Wright PK, Van't Hof RJ, Helfrich MH, Ohshima H, Ralston SH. Immunolocalization of inducible nitric oxide synthase in synovium and cartilage in rheumatoid arthritis and osteoarthritis. Br J Rheumatol 1997;36:651–5.
8. Beckman JS, Crow JP. Pathological implications of nitric oxide, superoxide and peroxynitrite formation. Biochem Soc Trans 1993; 21:330–4.
9. Zingarelli B, Day BJ, Crapo JD, Salzman AL, Szabo C. The potential role of peroxynitrite in the vascular contractile and cellular energetic failure in endotoxic shock. Br J Pharmacol 1997;120:259–67.
10. McDougall JJ, Karimian SM, Ferrell WR. Prolonged alteration of vasoconstrictor and vasodilator responses in rat knee joints by adjuvant monoarthritis. Exp Physiol 1995;80:349–57.
11. Lymar SV, Jiang Q, Hurst JK. Mechanism of carbon dioxide-catalyzed oxidation of tyrosine by peroxynitrite. Biochemistry 1996;35:7855–61.
12. Millar TM, Stevens CR, Benjamin N, Eisenthal R, Harrison R, Blake DR. Xanthine oxidoreductase catalyses the reduction of nitrates and nitrite to nitric oxide under hypoxic conditions. FEBS Lett 1998;427:225–8.
13. Zhang Z, Naughton D, Winyard PG, Benjamin N, Blake DR, Symons MC. Generation of nitric oxide by a nitrite reductase activity of xanthine oxidase: a potential pathway for nitric oxide formation in the absence of nitric oxide synthase activity. Biochem Biophys Res Commun 1998;249:767–72.
14. Godber BLJ, Doel JJ, Sapkota GP, Blake DR, Stevens CR, Eisenthal R, et al. Reduction of nitrite to nitric oxide catalyzed by xanthine oxidoreductase. J Biol Chem 2000;275:7757–63.
15. Stevens CR, Millar TM, Clinch JG, Kanczler JM, Bodamyali T, Blake DR. Antibacterial properties of xanthine oxidase in human milk. Lancet 2000;356:829–30.

Inactivation of xanthine oxidoreductase is associated with increased joint swelling and nitrotyrosine formation in acute antigen-induced arthritis

R. Klocke[1,2], A.R. Mani[3], K.P. Moore[3], C.J. Morris[1], D.R. Blake[1,2], P.I. Mapp[1]

[1]Department of Pharmacy & Pharmacology/School for Health, University of Bath; [2]Royal National Hospital for Rheumatic Diseases, Bath; [3]Centre for Hepatology, Department of Medicine, Royal Free & University College Medical School, UCL, London, UK.

Abstract

Objective

Arthritis is associated with increased articular formation of nitrotyrosine, which may contribute to injury. Nitrotyrosine is formed by nitration of tyrosine by reactive nitrogen species such as peroxynitrite, the formation of which may be enhanced by xanthine oxidoreductase (XOR), since it can generate nitric oxide from nitrite/nitrate, and superoxide during xanthine metabolism. We hypothesized that inactivation of XOR would protect against antigen-induced arthritis (AIA) and decrease nitrotyrosine formation.

Methods

AIA was induced with methylated bovine serum albumin (mBSA) in three groups of Wistar rats: animals fed on (1) tungsten-enriched chow (0.7 g/kg) (TG), which inactivates XOR, (2) standard chow (SG), and (3) rats treated with allopurinol (50 mg/kg/day; p.o.*) (AG). Nitrotyrosine in patella-synovium was quantified by mass spectrometry three weeks after intra-articular (*i.a.*) antigen injection.*

Results

Treatment with tungsten, but not allopurinol, suppressed plasma and articular XOR activity at ≤ 0.9% of normal levels. XOR inactivation was associated with increased knee swelling 24-48 hrs post i.a. *mBSA, compared with controls (mean increase ± SEM of knee diameter from baseline of 3.3 ± 0.5, 2.0 ± 0.3 and 1.9 ± 0.2 mm in TG, SG and AG (n = 14 each group), respectively; $p < 0.05$, TG vs SG, ANOVA). Mean ratio of articular nitrotyrosine-tyrosine (± SEM) was increased in the XOR-inactivated group, compared with controls: 12.3 ± 0.7, 9.6 ± 0.8 and 10.4 ± 0.5 pg/μg in TG, SG and AG, respectively; $p < 0.05$, TG vs SG.*

Conclusion

Contrary to expectation, XOR inactivation was associated with increased joint swelling and articular tyrosine nitration in acute AIA, suggesting a novel, protective role for XOR in inflammatory arthritis.

Key words

Xanthine oxidoreductase, arthritis, reactive nitrogen species, nitrotyrosine, tungsten, allopurinol.

Rainer Klocke; Ali R. Mani, MD; Kevin P. Moore, PhD; Chris J. Morris, PhD; D.R. Blake; Paul I. Mapp, PhD.

This work was supported by the Arthritis Research Campaign and the Wellcome Trust, UK.

Please address correspondence to: Rainer Klocke, The Guest Hospital, Tipton Road, Dudley, West Midlands DY1 4SE, United Kingdom. E-mail: Rainer.Klocke@dgoh.nhs.uk.

Received on August 3, 2004; accepted in revised form on March 31, 2005.

Introduction

Both nitric oxide (NO) and superoxide ($O_2^{\bullet -}$) are generated in increased amounts in inflamed joints (1-3), but their precise role in pathogenesis remains unclear. NO and $O_2^{\bullet -}$ react rapidly with each other *in vitro* to form peroxynitrite ($ONOO^-$) (4), a highly reactive nitrating and oxidizing agent. $ONOO^-$ induced modification of proteins, DNA and other biomolecules can lead to altered cell function, cell necrosis and apoptosis (5). The nitration of tyrosine to the relatively stable 3-nitrotyrosine (3-NT) is one consequence of $ONOO^-$ exposure *in vitro* (6-8). Other reactive nitrogen species (RNS) can also cause nitration of tyrosine in a peroxidase-dependent manner (9-11), but which of these pathways predominate *in vivo* is unknown. 3-NT is therefore best considered a marker of RNS formation in general (12). $ONOO^-$ can induce expression of cyclooxygenase 2 (COX2) in rheumatoid synoviocytes *in vitro* (13). We and others described the immunolocalisation of 3-NT in the rheumatoid synovium (14,15), suggesting that these reactions occur *in vivo* and contribute to disease pathology.

3-NT formation originates from endogenous NO, generated from arginine by one of the three isoforms of NO synthase (NOS). However, we and others have previously shown that xanthine oxidoreductase (XOR) can also generate NO (16,17) *in vitro*. XOR is expressed in the synovium (18) and best known for its house-keeping role in xanthine oxidation to yield uric acid and $O_2^{\bullet -}$. During xanthine oxidation XOR can also reduce nitrite to NO, suggesting that XOR may be a peroxynitrite synthase (19, 20).

We aimed to test the hypothesis that suppression of XOR activity in inflamed joints decreases nitration of proteins and joint inflammation. This has potentially important implications, since if true, XOR inhibitors, such as allopurinol, may be useful therapeutically in inflammatory arthritis *per se*. In contrast to our expectation we observed that XOR inactivation enhances acute experimental arthritis and nitration of articular proteins.

Materials and methods

Chemicals were obtained from Sigma, Poole, UK, unless stated otherwise and all concentrations are final.

Animals

Male out-bred Wistar rats of weaning age (Charles River, UK) were housed under standard conditions for one week before experimental interventions began. Procedures complied with the Animals (Scientific Procedures) Act 1986, UK. All invasive interventions animals were performed under 4% isoflurane/oxygen (2 l/min) anaesthesia.

Pharmacological inhibition of XOR and induction of antigen-induced arthritis (AIA)

Three groups of animals were studied (Fig. 1): (1) rats treated with tungsten-enriched chow to inactivate XOR by replacing active-centre molybdenum with tungsten (21) ('Tungsten Diet'; TG); (2) animals maintained on standard diet ('Standard Diet'; SG) and (3) mBSA-immunised animals on standard chow, treated with the XOR-inhibitor allopurinol ('+Allopurinol'; AG). AIA was induced as previously described (22). Briefly, from experimental Day 0 (Fig. 1) animals (mean weight ± SEM 132±2 gm) were fed for three weeks on tungsten-enriched (sodium tungstate 0.7 g/kg chow; ICN, Basingstoke, UK) or standard chow (SG; SDS, Witham, UK) before subcutaneous (s.c.) immunisation with 500 µg mBSA [as 100 µl of 10 mg mBSA/ml 0.9% saline, mixed 1:1(v/v) with complete Freund's adjuvant (CFA)] on Day 21. Three control animals in each diet group were injected with saline/CFA. This immunisation was repeated one week later (Day 28). One day before intra-articular (i.a.) antigen challenge, a subgroup of the standard diet group was started on allopurinol (50 mg/kg/day, p.o., by gavage). The following day (Day 42), all animals were injected with 500 µg mBSA (as 100 µl of 5mg/ml sterile 0.9% saline) and vehicle via i.a. injection into the right and left knee, respectively. Three weeks later (Day 63) [when a previous study had shown destructive arthritis to be present (22)] all animals

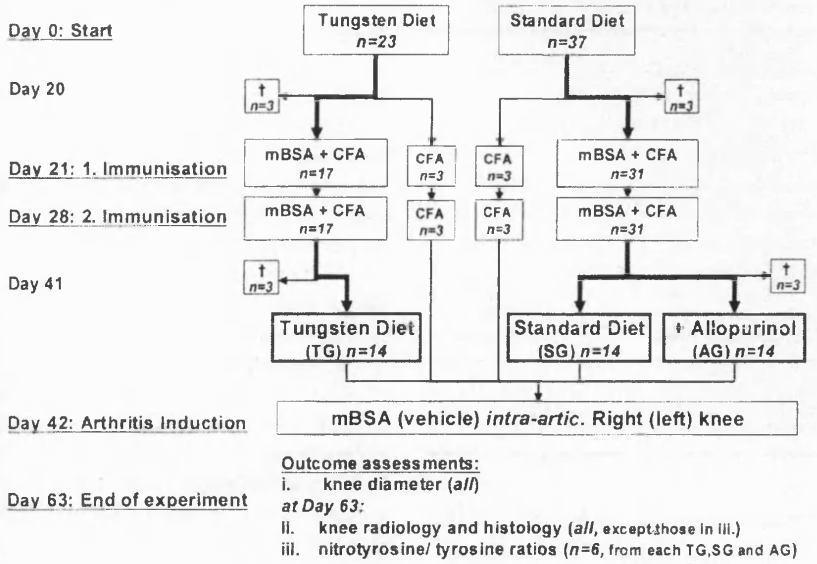

Fig. 1. Experimental design of the antigen-induced arthritis. †, animals sacrificed for measurement of XO activity; mBSA, methylated bovine serum albumin; CFA, complete Freund's adjuvant.

were killed and blood, knee joints or dissected patella with adjacent synovium taken for further analysis.

Clinical assessment

Animals were weighed weekly. Mediolateral knee diameters were measured on non-anaesthetised animals with digital callipers (Mitutoyo, Andover, UK) before, 24, 48 hours, 5, 7 and 14 days after i.a. mBSA/vehicle injection. Measurements were undertaken blinded to the intervention group, and recorded to the nearest 0.1 mm.

Delayed-type hypersensitivity (DTH) testing

One week after the second mBSA immunisation (Day 35) , a subgroup of animals (n = 5, from each diet group) were injected intra-dermally into the right and left ear with 2.5 µg mBSA (as 50 µl of 0.5 mg/ml 0.9% saline) and vehicle, respectively. Local skin reaction was assessed 48 hours later for redness and induration.

XOR activity assay

XOR activity was measured in citrated plasma and mechanical homogenates of snap-frozen patella-synovium (in phosphate-buffered saline (PBS) with 10 µg/ml aprotinin and 0.5 nM phenylmethylsulfonylfluoride). The analysis used a sensitive fluorospectrometric method (23), based on the XOR-mediated oxidation of pterin to isoxanthopterin. Briefly, pterin (20 µM) was added to sample of pre-determined optimum dilution in PBS and increase of fluorescence (λ excitation/ emission = 345/390 nm) measured (F4500, Hitachi, UK). Addition of allopurinol (10 µM) verified the enzymatic specificity of the reaction and isoxanthopterin (200 nM) provided a fluorescent standard. Samples were measured in triplicate and XOR activity was calculated and expressed as nmol per min per g sample tissue protein, with protein concentration determined according to Bradford (24).

Quantification of nitrotyrosine

Nitrotyrosine and tyrosine content was measured in patella-synovium by gas chromatography/mass spectrometry (GCMS), as previously described (25). Briefly, snap-frozen tissues were mechanically homogenised in PBS and chloroform-methanol (2:1) on ice. Centrifugation at 9000 g for 15 min yielded a protein precipitate middle layer, which was lyophilized. To avoid artefactual tyrosine nitration associated with the commonly employed acidic hydrolysis, 1-1.5 mg of protein was then hydrolyzed in 4 M sodium hydroxide at 120°C for 16 hrs containing 20 ng $^{13}C_9$-nitrotyrosine and 10 µg D_4-tyrosine as stable isotopic interval standards. Following solid phase extraction, nitrotyrosine and tyrosine was quantified by gas chromatography/negative ion chemical ionization mass spectrometry. Results were expressed as nitrotyrosine/tyrosine [pg/µg].

Radiographic and histological analysis

Knee joints were x-rayed in two planes (Faxitron, Field Emission Ltd., London, UK) and coded radiographs evaluated independently by two experienced investigators (26). Knees were then decalcified, dehydrated and embedded in paraffin. Sagittal sections, stained with haematoxylin-eosin, were examined for inflammatory and destructive changes (27).

Statistical methods

Where appropriate, mean values were analysed by unpaired t-test, or one-way analysis of variance (ANOVA) with Dunnett's *post*-test.

Results

Animals of all three groups thrived well and there were no abnormal macroscopic findings at *post mortem* examination. Three of 5 animals in each diet group demonstrated a positive DTH reaction to mBSA.

Xanthine oxidase activity

The activity of xanthine oxidase in plasma and joint homogenates are shown in Table I. Mean XO activity in plasma or joint homogenates of tungsten-treated (TG) animals was ≤ 0.9% of that of the control group (SG). In the allopurinol-treated (AG) animals mean XO activity in plasma was decreased to 7%, but XOR activity was not significantly different in the patella-synovium compared to controls.

Joint swelling

Mean baseline diameters ± SEM of mBSA-injected knee joints were comparable in the TG, SG and AG groups at 12.3 ± 0.2, 12.5 ± 0.2 and 12.5 ± 0.1 mm, respectively. Twenty-four and 48 hours after *i.a.* mBSA-injection, knee diameters showed a greater increase

Table I. XO activity in rat plasma, and patella-synovium homogenates.

	Tungsten Diet	Standard Diet	Allopurinol
Plasma			
Day 20	0.3 ± 0.4	172 ± 16 *	NA
Day 41	ND	219 ± 5	NA
Day 63	ND	162 ± 11 †	12 ± 2
Patella-Synovium			
Day 63	1.1 ± 3.1	127 ± 22 β	160 ±17

Values are mean XO activity (± SEM), as nmol x min-1 x g tissue protein-1, measured by spectro-fluorimetric pterin assay. Sample sizes were n = 3 animals for each group, except for plasma of day 21 (n = 6). Left and right patella-synovium samples were analysed separately. Each sample was measured in triplicate. Experimental days were: Day 20, after 3 weeks on experimental diet and prior to s.c. mBSA immunisation: Day 41, prior to *i.a.* mBSA injection; Day 63, three weeks after *i.a.* injection. ND, not detectable; NA, not applicable. * $p < 0.001$ vs Tungsten Diet (unpaired t-test); † $p < 0.001$ vs Allopurinol (unpaired t-test) and β $p < 0.001$ vs Tungsten Diet (ANOVA with Dunnett's *post*-test).

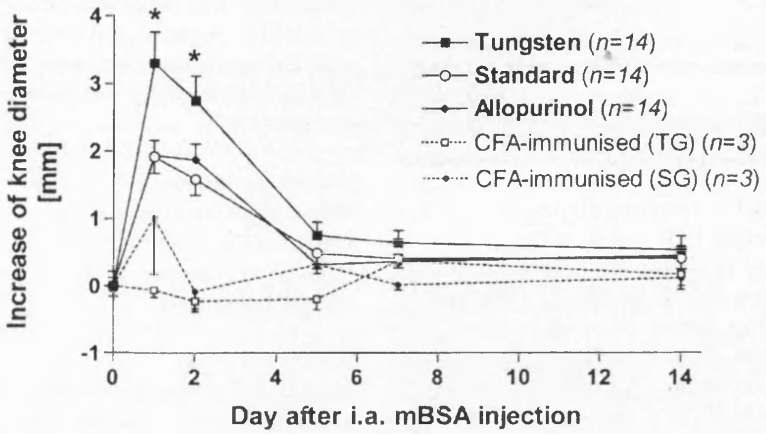

Fig. 2. Mean change of transverse diameter of mBSA-injected knees from baseline (*i.e.* prior to *i.a.* mBSA) over time. Bars represent SEM. * $p < 0.05$ vs . standard diet group (ANOVA with Dunnett's post-test).

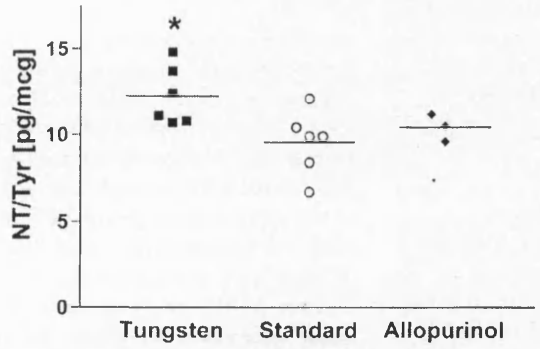

Fig. 3. Nitrotyrosine-tyrosine ratios of patella-synovium homogenates (3 weeks post *i.a.* mBSA injection). Bars represent mean values. * $p < 0.05$ for difference of means between tungsten- vs. standard-diet group (ANOVA with Dunnett's post-test).

from baseline in the tungsten- compared with the standard-diet group (n = 14, each group): mean difference (95%-confidence interval) were 1.3 (0.3, 2.4) mm and 1.2 (0.2, 2.1) mm, respectively ($p<0.05$; ANOVA with Dunnett's post-test) (Fig. 2). There was no significant increase in knee diameter in the CFA-immunised animals.

Nitrotyrosine/tyrosine content

Mean nitrotyrosine-tyrosine ratios (± SEM) of right patella-synovium homogenates of day 21 were significantly higher at 12.3 ± 0.7 pg/µg in the tungsten group (n = 6) compared with controls (9.6 ± 0.8 pg/µg) (n = 6), and were unchanged at 10.4 ± 0.5 pg/µg in the allopurinol group (n = 3) ($p < 0.05$, TG vs SG; ANOVA with Dunnett's *post*-test) (Fig. 3).

Radiographic and histological analysis

Radiological and histological analysis did not show chronic inflammatory and/or destructive joint disease in any group (n = 8, for each TG, SG and AG).

Discussion

We hypothesized that XOR contributes to the formation of RNS and nitration of articular proteins and that inhibition of XOR would ameliorate the course of experimental arthritis. In contrast, inactivation of articular XOR activity by tungsten was associated with a greater increase of mean knee swelling during acute antigen-induced arthritis (AIA) compared to standard-fed controls. Furthermore, tungsten-treated animals showed increased nitrotyrosine formation in arthritic joints compared with controls, as measured by a highly sensitive gas chromatographic-mass spectrometric method. This suggests that XOR inactivation enhanced joint inflammation early during the course of AIA. Although the effect is relatively modest, this is the first study to indicate that XOR may have a protective effect in immune complex-mediated disease, and supplements our previous observation that suggests a beneficial role for XOR in innate immune responses (19). We are unaware of other published studies of tungsten-induced XOR inactivation in AIA. Using dietary tungsten in adjuvant arthritis in Lewis rats, our group has previously observed a reduction in radiographic erosion and bone demineralization scores in tungsten-treated animals compared to controls, suggesting that XOR contributes to joint damage (28). Pathogenetic differences between animal models may account for these contrasting results. Acute AIA is a localised, non-destructive, immune complex disease of a few days duration (29). T-cell hypersensitivity and intra-articular antigen-retention are required for a chronic, destructive arthritis to develop. In contrast, adjuvant arthritis is a destructive, T-cell mediated disease from the outset (30). XOR could thus have divergent effects

on acute synovial inflammation and chronic destructive arthritis. Indeed, distinct anti-inflammatory activity is increasingly recognised as an integral part of classical pro-inflammatory enzymes, such as iNOS (31, 32) and COX2 (33) and may hold clues to explain the progression of joint damage despite inactive synovial inflammation seen in rheumatoid arthritis (RA) (34, 35). Our findings may also partly explain why acute gout arthritis is exacerbated by XOR inhibition with allopurinol.

How may XOR limit protein nitration and acute joint inflammation ? Uric acid, the final oxidation product of XOR-mediated purine metabolism, is a potent inhibitor of peroxynitrite-induced tyrosine nitration under physiological conditions *in vitro* (36). Endogenous uric acid inhibits protein tyrosine nitration in rat heart homogenates (37). Administration of uric acid reduced tissue damage in experimental autoimmune encephalitis, an animal model of multiple sclerosis, (38) and zymosan-induced rat knee arthritis (39). Since oxidative effects of $ONOO^-$ seem unaffected (36) or even enhanced by uric acid (40), it is suggested that protein tyrosine nitration itself is an important mediator of tissue inflammation and damage (41).

This study has limitations. Although increased 3-NT concentration is good indirect evidence that increased inflammation occurred, we lack histological data of enhanced acute inflammation in the XOR-inactivated animals. This is due to the fact that study design and power considerations were aimed at the detection of a difference in the development of chronic destructive arthritis, as the outcome most relevant in comparison to RA. Although the majority of animals developed delayed-type hypersensitivity to mBSA, they failed to progress to a chronic destructive arthritis, contrasting our earlier experience with the same AIA induction protocol (22). Subtle strain variation in our outbred Wistar rats may account for this observation. Secondly, tungsten is not a specific XOR inhibitor, but will also inhibit the two other molybdenum-enzymes known to exist in rat and man, *i.e.* sulfite oxidase (SO) and aldehyde oxidase (AO) (42). To our knowledge SO and AO have no reported relevance to inflammatory arthritis. Finally, sample sizes, especially for 3-NT measurements in the allopurinol group, were small. This was partly due to sample size limits of the GCMS assay and, based on the better XOR inactivation by tungsten, samples were prioritized accordingly.

In conclusion, we have shown that inactivation of XOR by dietary tungsten was associated with increased acute joint swelling and increased nitration of articular proteins, indicating increased joint inflammation during acute antigen-induced arthritis. This suggests that XOR may have a novel protective role in immune complex-mediated arthritis. Further studies are required to confirm these findings histologically and clarify the relevance of uric acid and allopurinol in this model.

References

1. FARRELL AJ, BLAKE DR, PALMER RM, MONCADA S: Increased concentrations of nitrite in synovial fluid and serum samples suggest increased nitric oxide synthesis in rheumatic diseases. *Ann Rheum Dis* 1992; 51: 1219-22.
2. MCINNES IB, LEUNG BP, FIELD M *et al.*: Production of nitric oxide in the synovial membrane of rheumatoid and osteoarthritis patients. *J Exp Med* 1996; 184: 1519-24.
3. HALLIWELL B: Oxygen radicals, nitric oxide and human inflammatory joint disease. *Ann Rheum Dis* 1995; 54: 505-10.
4. ISCHIROPOULOS H, ZHU L, BECKMAN JS: Peroxynitrite formation from macrophage-derived nitric oxide. *Arch Biochem Biophys* 1992; 298: 446-51.
5. SZABO C: Multiple pathways of peroxynitrite cytotoxicity. *Toxicol Lett* 2003; 140-141: 105-12.
6. GOLDSTEIN S, CZAPSKI G, LIND J, MERENYI G: Tyrosine nitration by simultaneous generation of (•)NO and $O^-_{(2)}$ under physiological conditions. How the radicals do the job. *J Biol Chem* 2000; 275: 3031-6.
7. REITER CD, TENG RJ, BECKMAN JS: Superoxide reacts with nitric oxide to nitrate tyrosine at physiological pH via peroxynitrite. *J Biol Chem* 2000; 275: 32460-6.
8. SAWA T, AKAIKE T, MAEDA H: Tyrosine nitration by peroxynitrite formed from nitric oxide and superoxide generated by xanthine oxidase. *J Biol Chem* 2000; 275: 32467-74.
9. EISERICH JP, CROSS CE, JONES AD, HALLIWELL B, VAN DER VLIET A: Formation of nitrating and chlorinating species by reaction of nitrite and hypochlorous acid. *J Biol Chem* 1996; 32: 19199-208.
10. VAN DER VLIET A, EISERICH JP, HALLIWELL B, CROSS CE: Formation of reactive nitrogen species during peroxidase-catalyzed oxidation of nitrite. *J Biol Chem* 1997; 272: 7617-25.
11. ESPEY MG, XAVIER S, THOMAS DD, MIRANDA KM, WINK DA: Direct real-time evaluation of nitration with green fluorescent protein in solution and within human cells reveals the impact of nitrogen dioxide vs. peroxynitrite mechanisms. *Proc Natl Acad Sci USA* 2002; 99: 3481-6.
12. HALLIWELL B: What nitrates tyrosine ? Is nitrotyrosine specific as a biomarker of peroxynitrite *in vivo* ? *FEBS Lett* 1997; 411: 157-60.
13. MIGITA K, YAMASAKI S, IDA H *et al.*: The role of peroxynitrite in cyclooxygenase-2 expression of rheumatoid synovium. *Clin Exp Rheumatol* 2002; 20: 59-62.
14. MAPP PI, KLOCKE R, WALSH DA *et al.*: Localization of 3-nitrotyrosine to rheumatoid and normal synovium. *Arthritis Rheum* 2001; 44: 1534-9.
15. SANDHU JK, ROBERTSON S, BIRNBOIM HC, GOLDSTEIN R: Distribution of protein nitrotyrosine in synovial tissues of patients with rheumatoid arthritis and osteoarthritis. *J Rheumatol* 2003; 30: 1173-81.
16. GODBER BJL, DOEL JJ, SAPKOTA GP *et al.*: Reduction of nitrite to nitric oxide catalyzed by xanthine oxidoreductase. *J Biol Chem* 2000; 275: 7757-63.
17. LI H, SAMOUILOV A, LIU X, ZWEIER JL: Characterization of the magnitude and kinetics of xanthine oxidase-catalyzed nitrite reduction. Evaluation of its role in nitric oxide generation in anoxic tissues. *J Biol Chem* 2001; 276: 24482-9.
18. STEVENS CR, BENBOUBETRA M, HARRISON R, SAHINOGLU T, SMITH EC, BLAKE DR: Localisation of xanthine oxidase to synovial endothelium. *Ann Rheum Dis* 1991; 50: 760-2.
19. STEVENS CR, MILLAR TM, CLINCH JG, KANCZLER JM, BODAMYALI T, BLAKE DR: Antibacterial properties of xanthine oxidase in human milk. *Lancet* 2000; 356: 829-30.
20. MILLAR TM, KANCZLER JM, BODAMYALI T, BLAKE DR, STEVENS CR: Xanthine oxidase is a peroxynitrite synthase: newly identified roles for a very old enzyme. *Redox Rep* 2002; 7: 65-70.
21. JOHNSON JL, RAJAGOPALAN KV, COHEN HJ: Molecular basis of the biological function of molybdenum. Effect of tungsten on xanthine oxidase and sulphite oxidase in the rat. *J Biol Chem* 1974; 249: 859-66.
22. MAPP PI, TERENGHI G, WALSH DA *et al.*: Monoarthritis in the rat knee induces bilateral and time-dependent changes in substance P and calcitonin gene-related peptide immunoreactivity in the spinal cord. *Neuroscience* 1993; 57: 1091-6.
23. BECKMAN JS, PARKS DA, PEARSON JD, MARSHALL PA, FREEMAN PA: A sensitive fluorometric assay for measuring xanthine dehydrogenase and oxidase in tissues. *Free Radic Biol Med* 1989; 6: 607-15.
24. BRADFORD MM: A rapid and sensitive method for the quantitation of microgram quantities of protein utilizing the principle of protein-dye binding. *Anal Biochem* 1976; 72:

248-54.

25. FROST MT, HALLIWELL B, MOORE KP: Analysis of free and protein-bound nitrotyrosine in human plasma by a gas chromatography/mass spectrometry method that avoids nitration artifacts. *Biochem J* 2000; 345: 453-8.
26. CLARK RL, CUTTINO JTJ, ANDERLE SK, CROMARTIE WJ, SCHWAB JH: Radiologic analysis of arthritis in rats after systemic injection of streptococcal cell walls. *Arthritis Rheum* 1979; 22: 25-35.
27. KRUIJSEN MWM, VAN DEN BERG WB, VAN DE PUTTE LBA: Sequential alterations of periarticular structures in antigen-induced arthritis in mice. Histological observations on fibrous capsule, ligaments, bone and muscles, using whole joint sections. *Br J Exp Path* 1983; 64: 298-305.
28. SPEDEN DJ, HEWINSON J, MAPP PI, BLAKE DR: Xanthine oxidase in inflammatory arthritis. *Rheumatology* 2002; 41 (Suppl. 1): 34.
29. GRIFFITHS RJ: Characterisation and pharmacological sensitivity of antigen arthritis induced by methylated bovine serum albumin in the rat. *Agents Actions* 1992; 35: 88-95.
30. PEARSON CM, WOOD FD: Studies of polyarthritis and other lesions induced in rats by injection of mycobacterial adjuvant. I. General clinical and pathological characteristics and some modifying factors. *Arthritis Rheum* 1959; 2: 440-59.
31. MCCARTNEY-FRANCIS NL, SONG XY, MIZEL DE, WAHL SM: Selective inhibition of inducible nitric oxide synthase execerbates erosive joint disease. *J Immunol* 2001; 166: 2734-40.
32. VEIHELMANN A, LANDES J, HOFBAUER A *et al.*: Exacerbation of antigen-induced arthritis in inducible nitric oxide synthase-deficient mice. *Arthritis Rheum* 2001; 44: 1420-7.
33. GILROY DW, COLVILLE-NASH PR, WILLIS D, CHIVERS J, PAUL-CLARK MJ, WILLOUGHBY DA: Inducible cyclooxygenase may have anti-inflammatory properties. *Nat Med* 1999; 5: 698-701.
34. MULHERIN D, FITZGERALD O, BRESNIHAN B: Synovial tissue macrophage populations and articular damage in rheumatoid arthritis. *Arthritis Rheum* 1996; 39: 115-24.
35. MCQUEEN FM, STEWART N, CRABBE J *et al.*: Magnetic resonance imaging of the wrist in early rheumatoid arthritis reveals progression of erosions despite clinical improvement. *Ann Rheum Dis* 1999; 58: 156-63.
36. WHITEMAN M, HALLIWELL B: Protection against peroxynitrite-dependent tyrosine nitration and alpha 1-antiproteinase inactivation by ascorbic acid. A comparison with other biological antioxidants. *Free Radic Res* 1996; 25: 275-83.
37. TENG RJ, YE YZ, PARKS DA, BECKMAN JS: Urate produced during hypoxia protects heart proteins from peroxynitrite-mediated protein nitration. *Free Radic Biol Med* 2002; 33: 1243-9.
38. HOOPER DC, SPITSIN S, KEAN RB *et al.*: Uric acid, a natural scavenger of peroxynitrite, in experimental allergic encephalomyelitis and multiple sclerosis. *Proc Natl Acad Sci USA* 1998; 95: 675-80.
39. BEZERRA MM, BRAIN SD, GREENACRE S *et al.*: Reactive nitrogen species scavenging, rather than nitric oxide inhibition, protects from articular cartilage damage in rat zymosan-induced arthritis. *Br J Pharmacol* 2004; 141: 172-82.
40. SANTOS CX, ANJOS EL, AUGUSTO O: Uric acid oxidation by peroxynitrite: multiple reactions, free radical formation, and amplification of lipid oxidation. *Arch Biochem Biophys* 1999; 372: 285-94.
41. ISCHIROPOULOS H: Biological selectivity and functional aspects of protein tyrosine nitration. *Biochem Biophys Res Commun* 2003; 305: 776-83.
42. MORIWAKI Y, YAMAMOTO T, HIGASHINO K: Distribution and pathophysiologic role of molybdenum-containing enzymes. *Histol Histopathol* 1997; 12: 513-24.